KU LEUVEN

ARENBERG DOCTORAL SCHOOL
Faculty of Engineering Science

The interprosthetic gap as a risk factor for interprosthetic fractures of the femur

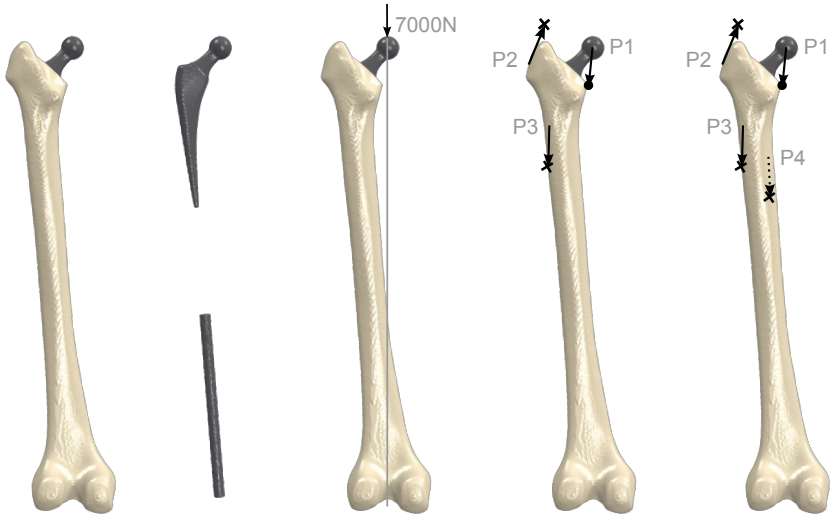

Thomas Quirynen

Supervisor:
Prof. dr. ir. G.H. van Lenthe
Prof. dr. ir. J. Vander Sloten

Dissertation presented in partial fulfillment of the requirements for the degree of Doctor of Engineering Science (PhD): Mechanical Engineering

June 2016

The interprosthetic gap as a risk factor for interprosthetic fractures of the femur

Thomas QUIRYNEN

Examination committee:
Prof. dr. ir. A. Bultheel, chair
Prof. dr. ir. G.H. van Lenthe, supervisor
Prof. dr. ir. J. Vander Sloten, supervisor
Prof. dr. ir. B. Innocenti
Prof. dr. ir. J. Van Humbeeck
Prof. dr. med. J-P. Simon
Prof. dr. med. M. Mulier
Prof. dr. ir. D. Ruffoni
(ULG - University of Liège)

Dissertation presented in partial fulfillment of the requirements for the degree of Doctor of Engineering Science (PhD): Mechanical Engineering

June 2016

Uitgegeven in eigen beheer, Thomas Quirynen, Celestijnenlaan 300C - bus 2419, B-3001 Heverlee (Belgium)

Dankwoord

Het is soms moeilijk om te definiëren hoe een interesse tot stand is gekomen. Van thuis uit is mijn interesse in het medische (tandheelkundige) beetje bij beetje gegroeid. Er was dan ook weinig twijfel toen ik zag dat ik tijdens mijn masteropleiding het medische kon combineren met de ingenieurswetenschappen. Een toevallige uitnodiging van Prof. Simon om een paar operaties bij te wonen deed mijn interesse in dit vakgebied alleen maar toenemen. Dit dankwoord kondigt dan ook jammer genoeg het einde aan van een uiterst boeiende periode aan de KU Leuven, maar ook het begin van een hopelijk even interdisciplinaire carrière. Het was een iets hobbeliger parcours dan ik in de zomer van 2010 in gedachten had, maar met hulp van familie, vrienden en collega's (hopelijk vergeet ik hieronder niemand!) ben ik erin geslaagd deze calvarietocht tot een goed einde te brengen.

Mijn eerste woord van dank gaat natuurlijk naar mijn promotoren, Professor G. Harry van Lenthe en Professor Jos Vander Sloten. Een chronologische aanpak lijkt mij het best geschikt:

Jos, bedankt voor de eerste contacten binnen UZ Pellenberg te leggen die uiteindelijk hebben geleid tot dit doctoraat. Jouw aanwezigheid op de soms moeilijke discussies in Pellenberg en het vertrouwen dat je mij gaf apprecieer ik nog steeds ten zeerste. Het vertrek van Prof. Bellemans en Dr. Corten heeft mijn doctoraat wat in de war gestuurd, maar leidde uiteindelijke wel tot een concreet onderzoeksproject. Bedankt om mij tijdens deze periode te blijven steunen.

Harry, bedankt om de rol van promotor over te nemen toen ik met mijn nieuwe project (en uiteindelijke doctoraatsonderwerp) in jouw kennisgebied terecht kwam. Bedankt om ondanks je drukke agenda toch steeds tijd voor mij vrij te maken, om me op het juiste pad te zetten als ik door de bomen het bos niet meer zag. Onze vergaderingen leverden vaak nieuwe inzichten

op wat de presentatie van mijn onderzoeksresultaten alleen maar ten goede is gekomen. Je grondige verbeteringen aan mijn artikels hebben me ook op vlak van wetenschappelijk schrijven veel bijgebracht.

I would like to express my gratitude to the members of the Jury: Prof. MD. Jean-Paul Simon, Prof. Bernardo Innocenti, Prof. Jan Van Humbeeck, Prof. MD. Michiel Mulier en Prof. Davide Ruffoni for your willingness to review my manuscript and for your comments and helpful suggestions. Your presence in the jury truly strengthens the inter-disciplinary nature of this thesis.

Rita, bedankt voor de enorme helpende hand bij het inplannen van meetings en nog zo veel meer administratieve taken. Dat alles vlot loopt op de afdeling is zeker ook aan jou te danken. Stefan, bedankt voor de hulp bij bestellingen en allerhande ICT-problemen. Ivo, geen technisch probleem was te groot voor jou. Je hulp bij het bouwen van testopstellingen wordt nog steeds ten zeerste gewaardeerd.

To all BMe colleagues: thank you for contributing to an amazing working atmosphere. It is amazing to see that the line between colleague and friend becomes blurry. The social events (Christmas parties, dinners, boardgame nights,...) organised by Zhaoyin, Marija and Tiago certainly helped in achieving this, as did the most random discussions imaginable during lunch-time. The fact that newcomers are rapidly included in one of the two lunch groups enhances the friendliness of the department and quickly made me feel at home. Thank you, Zhaoyin, Marija, Gabrijel, Tiago, Tassos, Julie, Heleen, Vulé, Tommy, Markos, Toan, Wouter, Dries, Hannelore, Nele, Alex, Michel and Karen. Special thanks to Pim and Sanne, not only for sharing the same office, but also for the laughs we shared. Even my *slight* coffee addiction due to Greek frappé and the Nespresso machine will be cherished.

Aan alle vrienden (studie-, fitness-, fiets-, klim-, bordspel-, kookavond-, reis-vrienden, enz), bedankt voor de steun en om me op te vrolijken op de momenten dat het, om welke redenen dan ook, wat moeilijker ging. Bedankt Laurent, Jeroen, Tim, Steven, Dries, Maarten, Bart, David, Johan, Tine, Nathalie, David, Carolina, Steven, Alex, Leen, Bram, Kiki en Vincent. Veel van jullie maken deel uit van meer dan één hierboven vermelde 'groep', wat tot mijn vreugde toch duidt op meer dan een gemeenschappelijke interesse. Bedankt om me niet alleen te motiveren om mijn doctoraat af te werken, maar ook om me uit te dagen op zowel sportief als culinair vlak. De momenten, reizen en avonden die we samen hebben doorgebracht zal ik nog lang blijven koesteren. Hopelijk kan ik die draad na het lichte PhD-afwerk-isolement terug oppikken.

Papa, mama, bedankt om mij de voorbije 28 jaar-en-half altijd te blijven steunen en motiveren, ongeacht welke uitdaging ik wou aangaan. Al die tijd werd ik op weg geholpen en geïnspireerd. Jullie hebben me geleerd dat het geoorloofd is om, zolang ik er moeite aan besteed, dingen te proberen, zelfs al lopen ze niet altijd even goed af. Bedankt om er altijd voor mij te zijn. Mijn koppigheid om er steeds weer volop voor te willen gaan heb ik dan ook aan jullie te danken.

Aan de rest van de familie, we zien elkaar niet vaak, maar het hartelijke welkom tijdens verjaardagen en andere festiviteiten zou ik niet willen missen. Merci oma, opa, ome Ruddi, tante Carla, Michiel, Zoë en Liam alsook ome Dirk, tante Miet, Guy en Jo. Tenslotte zijn er nog Bianca en Jeroen. Bedankt voor de entertainende discussies tijdens het avondeten, en om me de mogelijkheid te geven om 's avonds wat te vertellen over mijn dag.

Lien, liefje, bedankt voor het 'zachte' duwtje in de rug dat de laatste fase van m'n doctoraat heeft ingezet. Jouw heldere kijk op en raad bij alles wat tijdens de laatste stresserende maanden moest uitgewerkt en gepland worden heeft me zeker vooruitgeholpen. Je stond en staat altijd klaar om me te motiveren en om me tot rust te laten komen. Dit maakt het leven nog aangenamer met z'n tweeën!

Thank you all for this amazing experience!

Leuven, 3 Juni 2016

Abstract

An interprosthetic (IP) gap is created when an arthroplasty is performed on both joints of the same bone to replace deteriorated joints. Specifically in this thesis, placement of a hip and knee prosthesis in the femur was examined. Such an ipsilateral placement of stemmed prostheses into the same bone creates a gap of varying size and location depending on the prosthesis stem lengths. The IP gap is measured in between the tips of the prosthesis stems. Nowadays, the occurrence of the IP gap and IP fracture is infrequent (around 1.25% of patients with an IP gap) and predominantly found in patients with advanced age. As life expectancy is increasing and prosthesis placement in younger patients is rapidly rising, an exponential increase in the occurrence of the IP gap in both young and old patients can be expected, as well as an increase in prosthesis revisions. These prosthesis revisions feature longer stems and lead to smaller gaps. Since the clinical hypothesis is that the creation of an IP gap acts as a stress riser and that small IP gaps further increase the fracture risk of the femur, the IP gap might become a serious clinical concern in the near future. Still, the influence of the IP gap on femoral fracture risk has not yet been studied in detail and even though IP fracture reconstruction is a challenging treatment, a treatment protocol has not yet been defined. This thesis thus aims to offer a deeper insight (1) in the properties of the IP gap (size & location), (2) in other clinical relevant parameters that could influence femoral fracture risk (cortical thickness, bone E-modulus and prosthesis shape such as neck and stem length), (3) in the fracture morphology and (4) in the options for fracture treatment.

Two different approaches were utilized to fulfil these research aims. Firstly, an experimental test set-up was build to investigate the effect of creation of the IP gap and the effect of several IP gap sizes on femoral fracture load. This was achieved by loading synthetic bone specimens with implanted prostheses, along the mechanical axis of the specimen until failure occurred. Subsequently, fracture morphology was recorded and the specimens were reconstructed following different treatment protocols. These reconstructed specimens were again loaded

to failure to define the optimal fracture reconstruction. Secondly, finite element models were created to compare strains on the femoral cortex for models with different IP gaps. The simplified cylindrical and parametric model was loaded along the mechanical axis of the femur mimicking stance on one leg. The anatomically relevant model was based upon a CT scan of a synthetic femur combined with laser-scanned prostheses as used in the experimental tests. This model was loaded along the mechanical axis of the femur and by two even more physiologically relevant loads representing walking and stair climbing. Both models allowed for variation of the IP gap size, gap location and bone E-modulus. The simplified model was also used to investigate the effect of cortical thickness alteration. Likewise, the anatomical model was used to study the impact of the prosthesis shape.

Experimental tests and finite element analyses reached similar conclusions. An IP gap did not act as a stress riser, but models with such a gap had, on the contrary, a higher fracture load and lower strains than a model with a hip prosthesis only. Based on fracture load and femoral strains, small IP gaps and more distal gaps were proven to be favourable. Hence, this thesis rejected both clinical hypotheses. Furthermore, smaller cortical thickness and longer prosthesis neck lengths had a noticeably increased femoral fracture risk. As for fracture reconstruction, fractures with a medial butterfly fragment were the most common fracture morphology. An optimal reduction of the fragments was a prerequisite for construct stability. Such a reduction, held in place with a long locking plate and fixed to the bone with screws proved to be the most beneficial treatment, both mechanically and biologically. Results showed that addition of an anterior strut was only advisable when the plate construct failed to achieve sufficient initial stability.

In conclusion, this thesis investigates the effect of several clinically relevant parameters on the immediate post-op characteristics of the IP gap. Influence of IP gap size, IP gap location, bone mechanical properties and hip prosthesis neck and stem length on femoral fracture load and femoral strains, for an immediate post-surgery situation, were quantified. Interprosthetic fracture morphology and fracture reconstruction were studied as well. Addition of bone remodelling simulations to the finite element model could offer insights in the long-term behaviour of the IP gap size and location. This could be investigated in a future study.

Beknopte samenvatting

Een interprothetische (IP) afstand ontstaat wanneer een artroplastie wordt uitgevoerd op beide gewrichten van hetzelfde bot met als doel de gedegenereerde gewrichten te vervangen. Deze thesis onderzoekt specifiek de plaatsing van een heup- en knie-prothese in de femur. Zo een ipsilaterale plaatsing van protheses met een prothesesteel in hetzelfde bot creert een IP afstand met een bepaalde grootte en locatie afhankelijk van de lengte van de prothesestelen. De IP afstand wordt gemeten tussen de uiteindes van de prothesestelen. Vandaag de dag zijn patiënten met een IP afstand en IP breuk zeldzaam (ongeveer 1.25% van de patiënten met een IP afstand), en zijn deze patiënten voornamelijk van gevorderde leeftijd. Aangezien de algemene levensverwachting alsook de plaatsing van protheses in jongere patiënten toeneemt, kan een exponentiële toename van zowel jonge als oudere patiënten met een IP afstand worden verwacht. Bovendien wordt ook een stijging in het aantal prothese-revisies voorspeld. Deze prothese-revisies gebruiken protheses met langere stelen en leiden dus tot kleinere IP afstanden. In de nabije toekomst kan de IP afstand een ernstige klinische bezorgdheid worden, gezien de klinische hypothese is dat de IP afstand leidt tot een toename van rekken en dat kleine IP afstanden het breukrisico van de femur verder doen toenemen. Toch is de invloed van de IP afstand op het breukrisico van de femur nog niet in detail bestudeerd, en hoewel de reconstructie van een IP breuk een uitdagende en moeilijke behandeling is, is er nog geen behandelingsprotocol gedefinieerd. Deze thesis stelt dan ook als doel om een dieper inzicht te creëren (1) in de eigenschappen van de IP afstand (grootte & locatie), (2) in andere klinische parameters die het breukrisico van de femur zouden kunnen beïnvloeden (dikte van de cortex, E-modulus van het bot en vorm van de prothese zoals lengte van de nek en steel), (3) in de breukmorfologie en (4) in de mogelijke behandelingen voor breukreconstructie.

Twee verschillende technieken werden gebruikt om de doelstellingen van deze thesis te bereiken. Vooreerst werd een experimentele opstelling gebouwd om de invloed van de IP afstand en van verschillende groottes van IP afstand na te gaan op de breukbelasting van de femur. Deze doelstelling werd bereikt

door synthetische bot-specimens, geïmplanteerd met protheses, te belasten volgens de mechanische as van het bot totdat breuk optrad. Daaropvolgend werd breukmorfologie gedefinieerd en werden de breuken hersteld volgens verschillende behandelingsprotocols. Deze gereconstrueerde specimens werden vervolgens opnieuw belast totdat de constructie faalde. Ten tweede werden eindige elementen modellen ontworpen om rekken in de femorale cortex te vergelijken voor modellen met verschillende IP afstanden. Het vereenvoudigde cilindrische en parametrische model werd belast volgens de mechanische as van de femur om stand op één been na te bootsen. Het anatomisch relevant model was gebaseerd op een CT-scan van een synthetisch bot gecombineerd met laser-ingescande protheses zoals degene gebruikt tijdens de experimentele testen. Op dit model werd een last aangelegd volgens de mechanische as van het bot, en werden twee meer anatomisch relevante belastingen aangelegd die wandelen en trappen lopen imiteerden. Beide modellen lieten toe om de E-modulus van het bot en de grootte en locatie van de IP afstand aan te passen. Het vereenvoudigd model werd ook gebruikt om het effect van een veranderende corticale dikte na te gaan. Op een gelijkaardige manier werd het anatomisch relevant model gebruikt om de invloed van de vorm van de prothese te bestuderen.

Conclusies waren gelijkaardig voor zowel de experimentele testen als voor de eindige elementen modellen. Een IP afstand zorgde niet voor een toename van rekken, maar modellen met een IP afstand hadden een hogere breukbelasting en lagere rekken dan modellen met enkel een heupprothese. Gebaseerd op breukbelasting en femorale rekken werd aangetoond dat kleine en meer distale IP afstanden gunstig waren. Deze thesis verwerpt dus beide klinische hypotheses. Daarenboven blijkt dat een dunnere cortex en een langere prothesenek het breukrisico van de femur gevoelig doen toenemen. Wat betreft breukreconstructies was de meest voorkomende breukmorfologie een breuk met een mediaal vlinder fragment. Een optimale reductie van de fragmenten is een eerste vereiste voor stabiliteit van de reconstructie. We hebben aangetoond dat zo een reductie, gefixeerd met een lange *locking* plaat die aan het bot is bevestigd met schroeven, de meest gunstige behandeling vormde, zowel mechanisch als biologisch. De resultaten toonden aan dat toevoegen van een anterieure bot-*strut* enkel aan te raden was als de plaat niet voldoende stabiliteit kon leveren.

Samengevat benadrukt deze thesis de invloed van verschillende klinisch relevante parameters op de onmiddellijk post-operatieve eigenschappen van de IP afstand. De invloed van grootte en locatie van IP afstand, mechanische eigenschappen van het bot en nek- en steel-lengte van de heupprothese op femorale breukbelasting en rekken werd gekwantificeerd. IP breuk-morfologie en reconstructie werden eveneens bestudeerd. Aangezien de toevoeging van bot-hermodellering aan het eindige elementen model een zicht kan bieden op het lange termijn gedrag van de IP gap, kan dit in de toekomst verder bestudeerd worden.

List of abbreviations

δ**max**	Deflection at failure (Chapter 3)
ϵ_{95}	Mean 5% highest strains in the femoral cortex (Chapter 6)
FE	Finite element
FEA	Finite element analysis
Fmax	Load at fracture (Chapter 3)
IP	Interprosthetic
MAL	Loading along the mechanical axis
THA	Total hip arthroplasty
THR	Total hip replacement
TKA	Total knee arthroplasty
TKR	Total knee replacement
SC	Load protocol mimicking stair climbing
StrainH	Maximal strain in the gap region (Chapter 5)
StrainL	Minimal strain in the gap region (Chapter 5)
W	Load protocol mimicking walking

Clinical terminology

Anterior
: Towards the front of the body

Arthritis
: Deterioration of articulating surface of the joint
See figure 2.3b on page 8

Arthroplasty
: Replacement of (the articulating surfaces of) a joint with a prosthesis

Bone strut
: Long bone plate, controversially used to improve fracture reconstruction stability

Coronal plane
: Plane that divides the body into front and back

Cortical bone
: Dense, outer layer of the bone

Diaphysis
: Shaft of a long bone

Distal
: Located towards the feet of the body

Dorsal
: Located towards the back of the body

Femur
: Thigh bone

Interprosthetic
: Between the tips of two prostheses placed in the same bone

Intercondylar fossa
: Deep notch between the articular surfaces of the femur, at the side of the knee. See figure 2.2 on page 7

Intramedullary canal
: Central cavity of the bone shaft. See figure 2.2 on page 7

Ipsilateral
: Placed at both sides (of the bone)
E.g. a hip and knee prosthesis in a femur

Knee condyle
: Articular surfaces of the femur, at the side of the knee

Lateral
: Towards the side of the body

Medial
: Towards the middle of the body

Periosteal
: Sleeve of connective tissue around e.g. the femoral shaft

Peri-prosthetic
: Located in the region of the prosthesis stem

Posterior
: Towards the back of the body

Proximal
: Located towards the head of the body

Reduction
: Restoration of the normal alignment of a fractured bone

Sagittal plane
: Plane that divides the body into left and right

Trabecular bone
: Spongy bone, located at the ends of long bones

Trochanter minor/major
: Protrusion on the femur, to which several muscles attach
See figure 2.2 on page 7

Valgus
: Angulation away from the middle

Ventral
: Located towards the front of the body

Version
: Orientation of the femoral neck in relation to the femoral condyles (knee level)

Contents

List of Figures

List of Tables

Chapter 1

Thesis aims and outline

An interprosthetic gap arises when prostheses are placed ipsilateral or at both sides of the same bone to replace deteriorated joints. Specifically for this thesis, arthroplasty of both the hip and knee joint of the femur (bone of the upper leg) will be investigated. Most prostheses, especially in revision surgeries, feature long stems that are placed into the shaft of the bone to provide prosthesis fixation and stability. The interprosthetic gap is accordingly measured between the tip of the hip and knee prosthesis stem.
Up to date, ipsilateral prosthesis placement is primarily performed in elderly patients and its occurrence is rare. However, an exponential increase is expected since a growing amount of younger patients opt for early prosthesis placement and indications for hip and knee arthroplasties are broadening. Furthermore, the population is steadily growing older, while still expecting to maintain their mobility. As prosthesis lifetime is limited, these trends will lead to an increase of revision surgeries where prostheses with longer stems are commonly used. This increase in prosthesis (re-)placements will undoubtedly lead to an increase in pluri-prosthetisized femurs, resulting in smaller interprosthetic gaps.
Current knowledge concerning the impact of the interprosthetic gap is lacking, even though fracture treatment in ipsilateral implanted femurs is challenging. As such, fracture should be avoided and the clinical relevant parameters that could influence fracture risk (e.g. mechanical properties of the bone, gap size, gap location, ...) should be examined in detail.
This Ph.D. thesis aims to offer a better insight in the influence of the interprosthetic gap on femoral fracture load, femoral strains, fracture morphology and fracture reconstructions. This work focusses on avoiding post-op fracture risk, and not on long term bone remodelling. This will be achieved through both *in vitro* experimental tests and *in silico* simulations by finite element modelling.

1.1 Research aims

- A first aim of this thesis is to investigate the clinical hypothesis that 'small **interprosthetic gap sizes** increase femoral fracture risk'.
- As a second aim, the hypothesis that 'not only interprosthetic gap size but also **interprosthetic gap location** might influence femoral biomechanics' is examined.
- A third aim is to examine whether or not there are **other parameters**, besides IP gap size and location, that may influence femoral biomechanics. Several variables such as prosthesis shape, prosthesis stem and neck length and mechanical properties of the bone (cortical thickness and E-modulus) will be varied.
- Morphology of the fracture plays an important role in fracture reconstruction. As such, a fourth aim of this thesis is to define the **fracture morphology** that arises in specimens with ipsilateral implanted prostheses.
- A fifth, and last aim is to examine whether the interprosthetic gap influences the biomechanical outcome of **fracture reconstruction** with a fracture fixation plate.

1.2 Thesis outline

This thesis can be split into two major parts. A first part uses experimental load-to-failure tests while the second part focuses on finite element analysis. The content of this thesis is organized as follows:

- **Chapter 2** contains the general introduction to this thesis. This chapter introduces the concept of the interprosthetic gap and the concept of fixation plate-based fracture reconstructions and explains its clinical relevance. It further summarizes the state of the art by discussing the literature concerning the IP gap.
- **Chapter 3** summarizes the first part of the experimental tests. Synthetic bone specimen (Sawbones) are loaded to failure to investigate the influence of the distance between the tips of ipsilateral placed hip and knee prosthesis (IP gap) on femoral biomechanics. Fracture morphology as well as failure load, energy to failure and deflection during loading are measured and compared for several clinically relevant IP gaps.
- Using the fractured specimen from chapter 3, **Chapter 4** discusses the fixation and reduction of these fractures with three different types of reconstruction plates. The influence of the interprosthetic gap on the failure load of the plate constructs is also investigated experimentally. After selection of the best performing plate, the additional benefit of adding a anterior synthetic bone strut to the plate construct is explored.
- In **Chapter 5**, a simplified parametric finite element (FE) model of a femur with IP gap demonstrates the capabilities of finite element analysis. In this simplified model, bone and prostheses are modelled as cylinders, and the applied load and boundary conditions are identical to the experimental test set-up. The parametric nature of the model allows for variation of IP gap size and position, and results in 132 different FE specimens. Two other relevant clinical parameters, bone E-modulus and cortical thickness, are also varied. Femoral strains of all specimens are analysed and linked to failure load.
- **Chapter 6** continues on the previous chapter and utilizes FEA to create an anatomical relevant FE model, based upon a CT-scan of a synthetic bone specimen. 3D-models of the prostheses used in the experimental tests further contribute to the creation of a more accurate model. Using 5 hip prosthesis models, commonly implanted in clinical practice, prosthesis size, interprosthetic gap size and gap location are altered. Three loading conditions are applied; the load protocol used during experimental testing,

a load mimicking walking and a load mimicking stair running. Femoral strains of all specimens are analysed and linked to failure load.

- **Chapter 7** concludes this thesis by discussing the previous chapters, presenting an overall conclusion and recommending potential future work.

Chapter 2

General introduction

Life expectancy is rapidly increasing. Populations around the world are ageing and due to improvements in longevity and falls in birth rates, people older than 65 years old will become a proportionally larger group in society (Fig 2.1). On a global level, the 85-and-over population is projected to increase 351% between 2010 and 2050, compared to a 188% increase for the population aged 65 or older and a 22% increase for the population under age 65 (World Health Organization 2011). The amount of patients with associated chronic diseases, leading to joint deterioration and resulting in (partial) mobility impairment will thereby increase considerably.

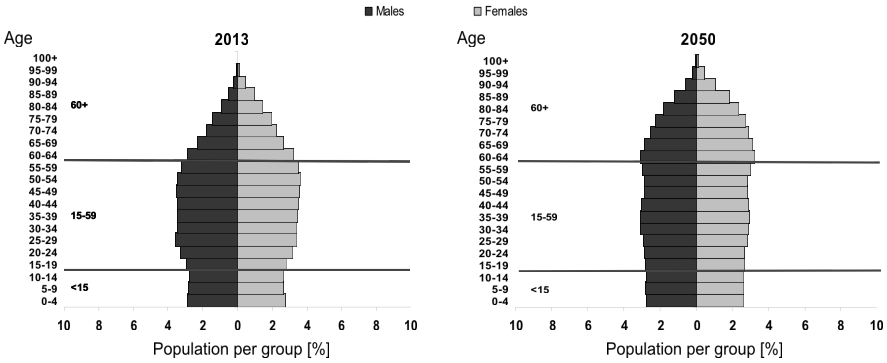

Figure 2.1: Population pyramids for the more developed regions: 2013 and 2050. Populations around the world are ageing and birth rates are decreasing, resulting in a increasing proportion of people above the age of 60 years old. From *World Population Ageing* (United Nations 2013).

Along with an increase in their age, patients with deteriorated joints more and more wish to maintain their functional mobility, retain their independent lifestyle and continue their participation in society (Fiedler & Fenton 2011, World Health Organization 2015). In addition, they are advocated to stay mobile since physical exercise can slow down the progress of bone loss, and intense exercise may even serve to increase the bone density in an elderly patient (Savela et al. 2015). Amongst older patients, an overall increase in joint replacement surgeries, or arthroplasties, utilizing prostheses is thus expected.
Next to this trend, prosthesis placement in younger patients is increasing as well. It is shown that nowadays, the demography of patients awaiting hip replacement surgery is changing from solely elderly arthritic patients to a varied patient group with young as well as old patients. These young patients hope to regain their former mobility consisting of often physically demanding activities (Learmonth et al. 2007) and, due to their younger age and the limited lifetime of prostheses, will most certainly need to undergo prosthesis revision surgery. Patient longevity and changing patient expectations already today caused a significant rise in the total amount of hip arthroplasties: e.g. a 23% rise was noted between 2005 and 2011 in the OECD (*Organisation for Economic Co-operation and Development*) countries, while population grew by only 4%. This was mainly due to a major increase in arthroplasty amongst younger patients (35% increase) (Pabinger & Geissler 2014). A similar increase is noted for knee arthroplasties: 38% increase between 2005 and 2011 (Pabinger et al. 2015).
The fact that younger patients, demanding higher functional ability, opt for earlier (albeit initially resurfacing) hip surgery and the broader indications for hip arthroplasty placement does not only cause an increase in primary prosthesis placement (Skyttä et al. 2011, Ravi et al. 2012, Sing et al. 2015), but will cause an exponential increase in revision surgeries in the near future as well, especially since placement of both hip and knee arthroplasty is predicted to continue to rise (Culliford et al. 2015, Pivec et al. 2012, Kurtz et al. 2007).
These trends for both young and old patients will thus result in a noticeable increase in patients with at least one implanted prosthesis. Also, in more and more patients, both joints of the same bone might require implant surgery, leading to an ipsilateral placement of prostheses and creation of an interprosthetic gap between the tips of the two prostheses. I.e. for this thesis, a hip and knee prosthesis in the femur (Fig. 2.2). At last, prosthesis lifetime is limited warranting revision surgery and prosthesis replacement, often applying longer stem, which will lead to smaller interprosthetic gaps (see section 2.1).
As such, multiple challenges arise, of which several are of orthopaedic nature. These challenges should thus be handled with care. E.g. initial treatment with less invasive prostheses enhances the possibilities for revision surgeries, the influence of the interprosthetic gap on biomechanics of the femur should be identified thoroughly to prevent femoral fracture and, if fracture does happen,

fracture management should be optimized.

2.1 Pathology & prosthesis types

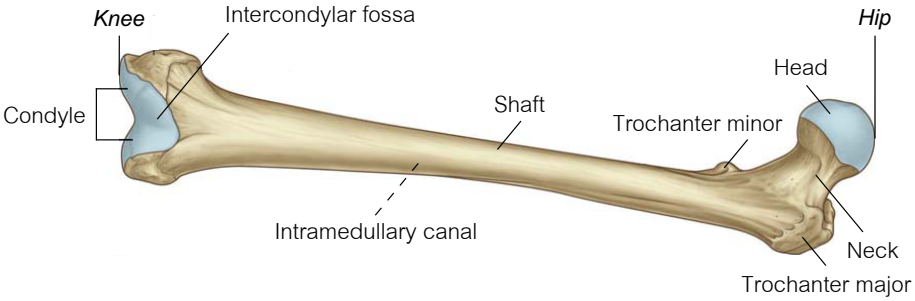

Figure 2.2: Anatomy of the femur. Cartilage is represented by the blue area. Adapted from *Gray's anatomy for students third ed.* (Drake et al. 2015).

The thigh bone, or femur, connects two load bearing joints, the hip and knee joint. One of the reasons to place a hip or knee implant is to treat arthritis, a disease that damages and accelerates wear-and-tear of the joint cartilage of the hip and/or the knee (Fig. 2.2). A common form is osteoarthritis, which often arises in people after they reach middle age and which is caused by wear and tear of the articular cartilage. Inflammatory arthritis on the other hand affects people of all ages. This disease can affect both the hip and knee joint, compromising patient mobility and causing stiffness, pain and difficulty in walking (Bartel et al. 2006) (Fig. 2.3a & 2.3b). Conservative options to restore the deteriorated hip or knee joint in younger patients focus on replacement of the joint cartilage with minimal impact on the surrounding bone structure (Learmonth et al. 2007). These techniques offer an initial treatment option which postpones the replacement or arthroplasty of the entire joint. E.g. hemiarthroplasty (partial hip replacement of only the femoral head) or hip resurfacing uses a prosthesis that covers the cartilage of the femoral head and is fixated with a short stem in the femoral neck.
Arthroplasty of the entire hip joint (THA) on the other hand removes the femoral head and neck by cutting the bone along a line that runs from the trochanter minor to the trochanter major (Fig. 2.2). In a next step, a prosthesis with three basic components is implanted: a stem that is inserted into the femoral shaft (A), a ball that attaches to the top of the prosthesis (B) and a cup that attaches to the acetabulum of the pelvis (C, Fig. 2.3c).

The lifetime of both (cemented) hip and knee prostheses is unfortunately limited to around 15-20 years (Kane et al. 2003, Mäkelä et al. 2008). Once past it's lifetime, when the prosthesis is worn out, loosens or when other complications occur a revision prosthesis will replace the initial prosthesis (Fig. 2.3). To ensure sufficient fixation in the bone, revision prostheses are often larger and have longer prosthesis stems. These longer stemmed revision prostheses, used in hip and knee prosthesis revisions, will accordingly reduce the interprosthetic gap size. This might be of great concern, as the clinical hypothesis is that small interprosthetic gaps increase femoral fracture risk.

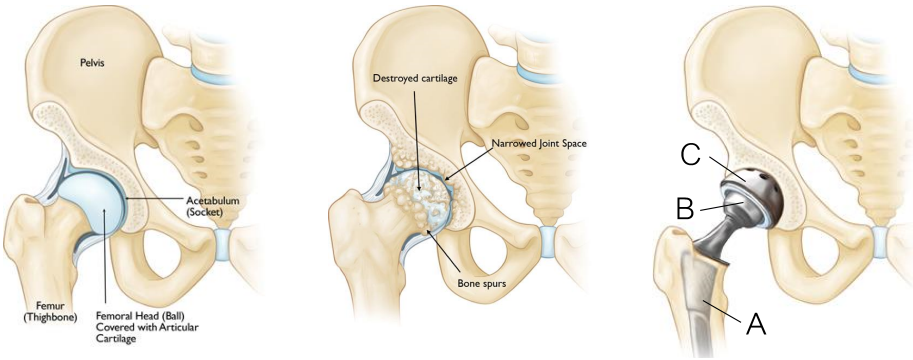

(a) Healthy hip (b) Damaged hip (c) Hip prosthesis

Figure 2.3: Prosthesis placement in the hip to replace the arthritic hip joint. From (AAOS - American academy of orthopaedic surgeons 2016).

If a patient with an interprosthetic gap does suffer fracture, fracture management and treatment should be optimized. The morphology of femoral shaft fractures can vary greatly, depending on the force applied on the bone and the presence and location of a prosthesis (Fig. 2.4a). Femoral shaft fractures in a femur are preferably treated with intramedullary nailing. During this technique a metal rod, extending beyond the fracture to keep it into position, is inserted in the intramedullary canal of both parts of the fractured femur (Bartel et al. 2006). Due to lack of access to the intramedullary canal in femurs with ipsilateral prosthesis, interprosthetic fractures are commonly treated with a fracture fixation plate (Fig. 2.4b). This treatment places a plate overlapping the region of the fracture and repositions (reduces) the bone fragments to their initial alignment.

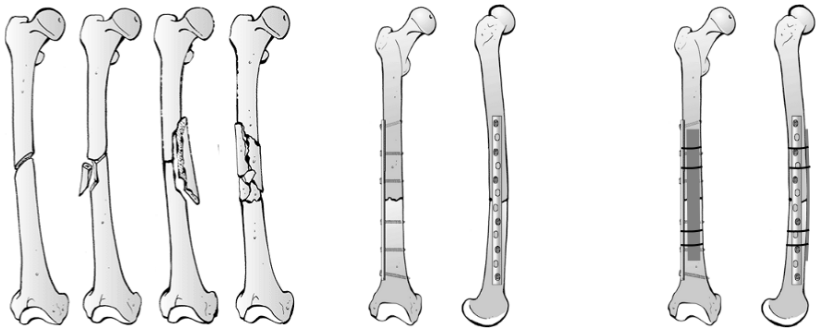

(a) Fracture classification (b) Fixation plate (c) Fixation plate & strut

Figure 2.4: (a) Classification of fractures commonly encountered in clinical practice. From left to right: oblique fracture, lateral butterfly, medial butterfly and multi-fragment fracture. (b) Fracture treatment with a fixation plate. (c) Fracture treatment with a fixation plate and anterior strut. Adapted from *Rockwood & Green's Fractures in Adults* (Nork 2006).

A variety of both plate length and plate fixation types (cable-fixation, screw-fixation or both) exists in clinical practice:

- 20 cm Accord plate (cable retained, Smith & Nephew, Fig. 2.5a)
- 39 cm LCP plate (cable & screw retained, Synthes, Fig. 2.5b)
- 43 cm NCB plate (screw retained, Zimmer, Fig. 2.5c)

The use of bone plates to reconstruct interprosthetic fractures is, even today, challenging, and there is no defined treatment algorithm (Ebraheim et al. 2014, Ehlinger et al. 2013, Solarino et al. 2014). As a guideline, interprosthetic fracture treatment is thought to show similarities with the reconstruction of peri-prosthetic fractures (Hou et al. 2011). The ultimate goal of a plate reconstruction is to fixate the fracture and to restore the fractured femur to provide adequate initial stability and stiffness to allow the fracture to heal.
A point of controversy in peri-prosthetic and inter-prosthetic fracture treatment is whether or not a bone strut should be added to the plate construct (Bryant et al. 2009, Hou et al. 2011). This long piece of grafted cortical bone is placed alongside the plate construct on the anterior side of the bone (Fig. 2.4c). Addition of a strut is, by some, thought to be a prerequisite for construct stability.
An overview of relevant literature concerning plate and fixation type can be found in section 2.2.2, table 2.1 and table 2.2.

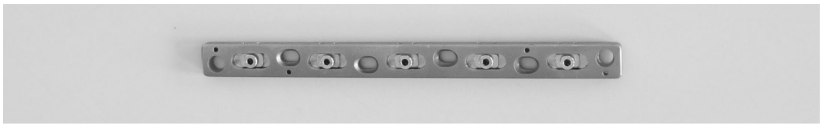

(a) Accord plate

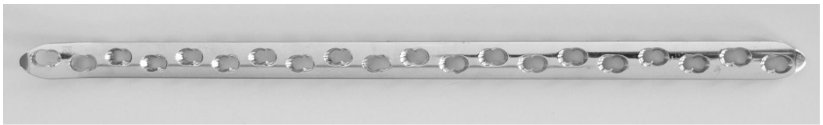

(b) LCP plate

(c) NCB plate

Figure 2.5: Three different types of fracture fixation plates which are commonly used in clinical practice.

2.2 The IP gap: State of the art in biomechanical testing

Currently, ipsilateral implant placement is mainly performed in patients of advanced age. These patients, often with additional co-morbidities, impede *in vivo* clinical follow-up studies to investigate the effect of the interprosthetic gap on fracture risk and fracture reconstruction of the femur. Opposed to clinical studies on fracture reconstruction in femurs with an interprosthetic gap (section 2.2.2, table 2.2), no clinical studies on the risk factors of femoral fracture in ipsilateral implanted femurs exist. Furthermore, the inter-patient variability of femoral shape, length and bone quality might have an impact on femoral strains as well, which could make it difficult to reach clear conclusions based on a clinical follow-up study. Also, strain measurement *in vivo* is not possible. As such, experimental or finite element analysis seems to be better suited to investigate the influence of the interprosthetic gap on femoral biomechanics.

2.2.1 Experimental - IP gap

Experimental research eliminates some unwanted variables that exist in clinical follow-up studies: A specified loading condition can be imposed on all specimens and loading can be controlled in detail. Cadaver femurs are often used during experimental tests, but they still have some suboptimal inherent variables such as variability in specimen shape, length, bone mechanical properties, bone quality and pre-existing damage in the bone (Moazen et al. 2011). These variables make it virtually impossible to reproduce experimental experiments (Papini et al. 2007). Synthetic bone analogues (Fig. 2.6) on the contrary are comparable to healthy bone, based on the similar stiffness and strain curves (Cristofolini et al. 2010, Gardner et al. 2010, Heiner 2008, Zdero et al. 2008). Moreover, the cortical shell of the bone analogue matches toughness and tensile strength of human cortical bone (Chong et al. 2007). Bone analogues have very small variability and hence can be used as a relevant model for human bone, particularly in comparative studies (Papini et al. 2007).

Figure 2.6: Example of a validated synthetic bone specimen (Fourth generation Sawbones #3403, Pacific Research Laboratories, Mälmo, Sweden). Cross-section on the right shows cortical bone (fibre filled epoxy, dark grey outer shell) and trabecular bone (polyurethane foam, light grey interior volume).

Some experimental studies focusing on the interprosthetic gap have already been performed, but within certain limitations. A first study used a 250 mm hollow cylinder with material properties of a synthetic femur analogue (Iesaka et al. 2005). A 100 mm cylindrical stem was implanted in the cylinder in combination with a ipsilateral stem of varying length to create IP gaps of 1, 5, 35 and 85 mm. The construct was loaded under cantilever bending, and strains at one of the prosthesis tips were measured (Fig. 2.7a). Strain values for all stem sizes fell within 5% of the strain of a model with only one implanted stem. As such, addition of a second stem, or creation of a interprosthetic gap did not act as a stress riser, even not for small IP gaps. Even though this study is the first to investigate the influence of the IP gap, it is subjected to several

limitations. Only a small range of gap sizes was simulated while gap location remained fixed, so no variation of gap location was taken into account.

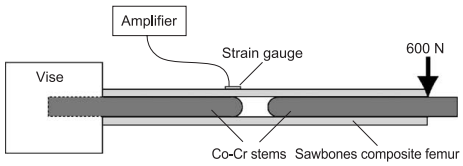

(a) Setup of cantilever bending

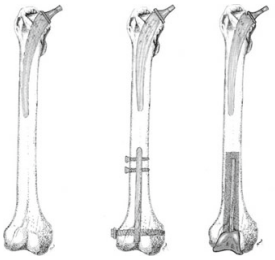

(b) Relevant specimens with IP gaps

Figure 2.7: IP gap: State of art in biomechanical testing by Iesaka et al. 2005 (2.7a) and Lehmann et al. 2012 (2.7b).

Also, shape influence of both femur and prosthesis were not modelled and cantilever bending does not fully mimic anatomical loading. Lastly, strains were measured at one specific point of the IP gap, and as such no insight was gained concerning strain patterns or strain of the entire IP gap.
Two other studies investigated the influence of the interprosthetic gap on specimen fracture strength (Lehmann et al. 2010, Lehmann et al. 2012). Cadaver femurs were loaded under four-point bending to compare fracture strength of a specimen with (1) a hip prosthesis, (2) a hip prosthesis with ipsilateral femoral nail and (3) a hip prosthesis with ipsilateral knee prosthesis (Fig. 2.7b). The specimen with ipsilateral hip an knee prosthesis had the highest fracture load of all three specimens. This indicated that the presence of an IP gap had no negative influence on femoral strength, but was even preferable over a specimen with THA only. However, no gap size variation was modelled. Also, the clinical relevance of applying four-point bending may be limited.
A last study investigated the influence of two clinically relevant parameters on femoral fracture strength. Cadaver femurs were implanted with a hip and a knee prosthesis. IP gap size (35, 80 and 160 mm) was varied and the femurs were randomized into three groups by cortical thickness (Weiser et al. 2014). Specimens were loaded under four-point bending. Results showed no significant difference between mean fracture strength of the different gap sizes. Fracture resistance did however increase with increasing cortical thickness. As a downside, only a limited variation of gap sizes was tested, and as discussed above, the use of four-point bending is not ideal.

2.2.2 Experimental - fracture reconstruction

Interprosthetic fractures where no prosthesis loosening occurs are commonly reconstructed using fixation plates. No studies examining the influence of the interprosthetic gap size on plate reconstructions exist up to date. The treatment of peri-prosthetic fractures can be used as a guideline for interprosthetic fracture treatment (Hou et al. 2011). Experimental studies on peri-prosthetic fractures do exist (Table 2.1), but all studies use 'hand-made' fractures, not taking into account the variability of fractures that occur in clinic (Fig. 2.4a). These studies almost all use the same loading protocol (Fig. 2.8).

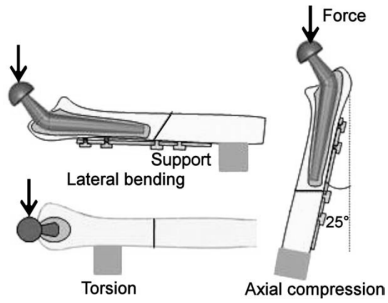

Figure 2.8: Loading protocol from (Zdero et al. 2008) used to load specimens with fractures represented by a 45° saw osteotomy. From (Moazen et al. 2011).

Guidelines from biomechanical studies investigating peri-prosthetic fracture treatment (Table 2.1), combined with the findings within small patient groups in clinical follow-up studies on interprosthetic fracture treatment (Table 2.2) (Solarino et al. 2014), lead to the following advice concerning plate length and fixation type. Long screw-retained locking plates (Fig. 2.9) have been proven to be biomechanically superior compared to other types of fracture fixation, provided there is no loosening of the prostheses (Solarino et al. 2014, Dennis et al. 2000, Dennis et al. 2001, Fulkerson et al. 2007, Choi et al. 2010, Lever et al. 2010, Ochs et al. 2013, Stoffel et al. 2016). These locking plates have several advantages:

- Reduced interference to blood supply due to absence of bone-plate contact or friction (Fig. 2.9a v.s. 2.9b, forces are transferred from bone to plate solely through the screws, and not through screw and bone-plate friction as in non-locking plates)
- There is no need for plate-bone contact to ensure a stable fixation and the plate does not need to be precisely adapted to the bone (Fig. 2.9c)
- Fixation of the screw in both bone and plate increases stability and decreases reduction loss (Fig. 2.9d)

Authors	Specimen type	Fracture representation	Loading (Fig. 2.8)	Preferred reconstruction
(Dennis et al. 2000)	Synthetic	45° oblique, THA tip	All 3 modes	Screw fixation > cable
(Dennis et al. 2001)	Cadaver	45° oblique, THA tip	All 3 modes	Plate > strut
(Wilson et al. 2005)	Cadaver	Transverse, THA tip	Gait	Cable plate (short!) with strut
(Fulkerson et al. 2006)	Cadaver	45° oblique, THA tip	All 3 modes	Screw fixation > cable
(Talbot et al. 2008)	Synthetic	Transverse, THA tip	All 3 modes	Screw plate (short!) with strut
(Zdero et al. 2008)	Synthetic	45° oblique, 5 mm gap	All 3 modes	Plate (short!) with strut
(Choi et al. 2010)	Synthetic	Transverse, 2 cm gap	All 3 modes	Plate (short!) with strut
(Lever et al. 2010)	Cadaver	45° oblique, THA tip	All 3 modes	Screw fixation > cable
(Graham et al. 2015)	Synthetic	Transverse, below THA	Axial load	Screw fixation > cable

Table 2.1: Overview of relevant literature: Experimental tests on peri-prosthetic fracture reconstruction using bone plates.

Authors	# Fractures	Reconstruction methods	Preferred reconstruction	Addition of a strut?
(Mamczak et al. 2010)	20	Plate fixation screws and/or cables	Span entire IP zone	No, aim to preserve soft tissue
(Michla et al. 2010)	8	Variation of techniques	Overlap fracture with 2 femur widths	Yes, due to poor bone quality
(Sah et al. 2010)	22	Single locking plate screws and cables	Anatomical reduction, large plate span no cables in fracture area	No, aim to preserve soft tissue
(Soenen et al. 2011)	14	Variation of techniques	Long locking plate, overlap IP gap by 2 femoral diameters	-
(Platzer et al. 2011)	19	Plate fixation screws and cables	Locking plates with sufficient overlap only use wires if needed for stability	-
(Hou et al. 2011)	12	Locking plate screws and cables	2 femoral diameters overlap	-
(Ochs et al. 2013)	*Literature review*		Locking plate, bypass fracture by 2 femoral diameters	-
(Ehlinger et al. 2013)	8	Locking plate screws and cables	Femur spanning plate	-
(Ebraheim et al. 2014)	15	Locking plates, screws optional cables & strut	Consider individual fracture type & bone quality to determine plate length and strut use	
(Pires et al. 2014)	6	Variation of techniques	Consider individual fracture type	If needed
(Stoffel et al. 2016)	*Systematic review*		Locking plates are preferred	-
(Hoffmann et al. 2016)	27	Polyaxial locked plate with additional cables	Long NCB-locked plating & anatomical reduction	Depending on fracture type avoid excessive tissue stripping

Table 2.2: Relevant clinical studies on interprosthetic fracture reconstruction using bone plates.

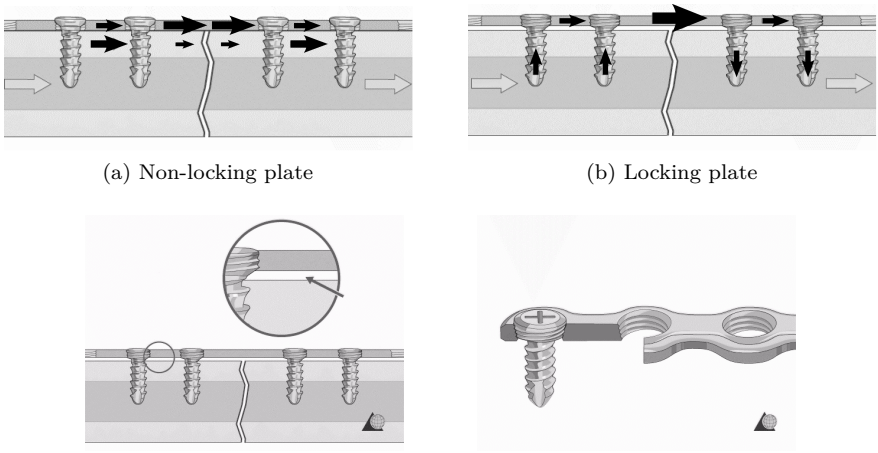

(a) Non-locking plate

(b) Locking plate

(c) No bone-plate contact

(d) Locking screw

Figure 2.9: Benefits of locking screw and plate. No friction is needed between plate and bone and force transmission happens solely through screws (Fig. 2.9a vs 2.9b). (AO Foundation 2016).

Another benefit of screw retained plates is that they have previously showed higher fixation efficiency over screw-and-cable retained plates. Fracture fragment migration has been observed to a lesser extent in screw fixations (Dennis et al. 2001, Sah et al. 2010, Graham et al. 2015, Platzer et al. 2011). The disadvantage of cable-retained plates is that cable loosening and slippage (e.g. during loading) can in fact lead to fracture fragment migration and consequential reduction loss. If cables are used, e.g. due to insufficient bone for screw placement (Ebraheim et al. 2014), it is advised that the cables should not be placed in the fracture area (Sah et al. 2010). Also, from a biological point of view, cable placement requires more soft tissue damage and periosteal stripping than screw placement, impacting fracture healing and damaging the already limited blood supply (Fulkerson et al. 2007, Hoffmann et al. 2016).
The length of the plate has likewise been defined as essential in achieving a stable fracture reconstruction. Literature agrees that the plate should overlap the fracture area by at least two femoral diameters at both the distal and proximal side (Sah et al. 2010, Hou et al. 2011, Michla et al. 2010, Mamczak et al. 2010, Platzer et al. 2011, Soenen et al. 2011, Ehlinger et al. 2013, Ochs et al. 2013, Hoffmann et al. 2016). Other studies even advice to span the entire interprosthetic zone to eliminate stress risers (Mamczak et al. 2010) or to span the full extent of the femur (Ehlinger et al. 2013).

Last but not least, achieving a (near) anatomical reduction has been indicated as a prerequisite for an optimal reconstruction (Mamczak et al. 2010, Sah et al. 2010, Hoffmann et al. 2016). Another, albeit controversial, approach in fracture management is the addition of a bone strut (Fig. 2.10) to the plate construct. Most papers advocating addition of a strut use a short bone fixation plate to treat interprosthetic or peri-prosthetic fractures. Since these plates do not offer sufficient support (Wilson et al. 2005, Talbot et al. 2008, Zdero et al. 2008, Choi et al. 2010), the outcome of these studies is that struts are needed to reach adequate stiffness. Likewise, struts are sometimes used in cases of poor bone quality (Michla et al. 2010). However, strut placement requires additional biological tissue stripping which may delay fracture healing (Mamczak et al. 2010, Sah et al. 2010, Hoffmann et al. 2016). From a biological point of view, struts should thus only be used in cases of severe bone loss or reduction instability (Solarino et al. 2014).

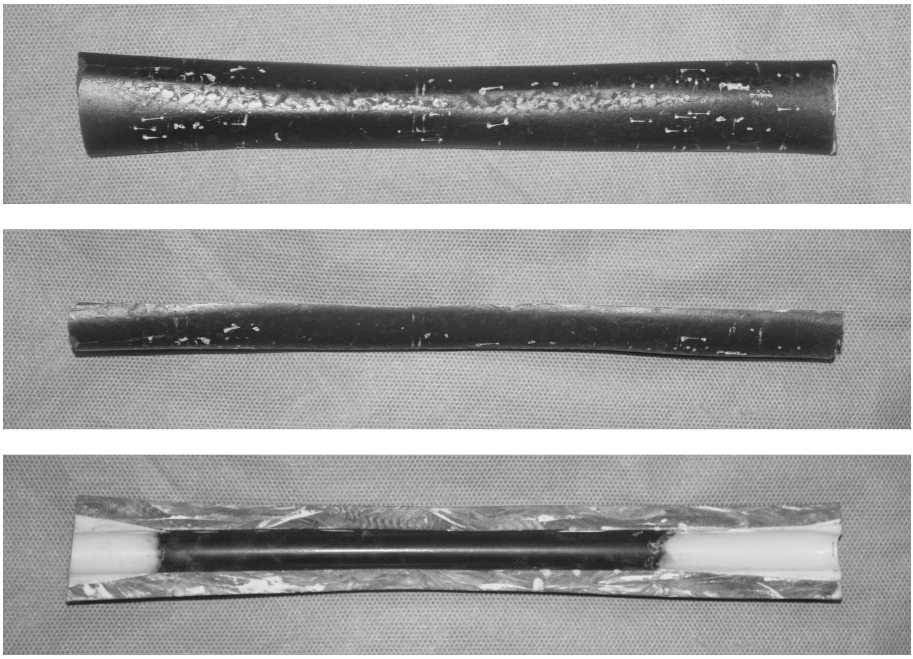

Figure 2.10: Example of a strut grafted from the diaphysis of a synthetic bone specimen (Fourth generation Sawbones #3403, Pacific Research Laboratories, Mälmo, Sweden). Displayed strut has a length of 23 cm and is grafted by cutting the femoral shaft in half.

2.2.3 Finite elements & IP gap

Finite element (FE) modelling in biomechanical engineering is an accepted computer-based simulation tool (Papini et al. 2007, Taylor & Prendergast 2015). Opposed to experimental testing, it offers cost-efficient testing, high reproducibility of experiments and detailed insight in stresses and strains of a 3D model. Especially strain patterns and strain maxima can be used to correctly identify failure risk and fracture onset location based on ultimate strain values (Schileo et al. 2008, Schileo et al. 2014, Bayraktar et al. 2004). Higher strains indicate a increased fracture risk. Furthermore, reproducibility of simulations is high and a variety of conditions with different loads and movement restrictions (boundary conditions) can be applied and controlled in great detail (Taylor & Prendergast 2015). Due to the adaptability of both shape and material properties (Young's modulus) of this 3D finite element model, FE modelling can also simulate bones of varying quality (Fig. 2.11).

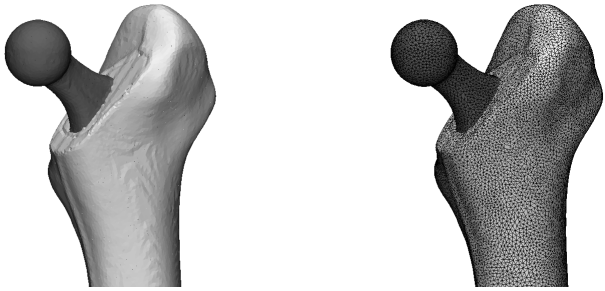

Figure 2.11: Example of a FE model of a femur with a hip prosthesis. Figure on the right shows the model with visualized mesh (see appendix C).

Two finite element studies focusing on the interprosthetic gap have already been performed, within certain limitations. A first study modelled the femur as a cylinder with isotropic material properties (Iesaka et al. 2005). Only cortical bone was modelled. Gap size was varied (1, 5, 35 and 85 mm) but gap location, another clinically relevant parameter, was fixed. The effect of cortical wall thickness was investigated as well. The model was loaded under cantilever bending and stress rather than strain was measured in the femoral shaft. They concluded that the size of the IP gap did not influence maximal tensile stresses, nor did the stem tips act as stress risers. Stresses were always lower or identical to stresses in the control model, represented by a femur without prostheses. Stresses did vary inversely with cortical thickness. Limitations were that only isotropic cortical bone was modelled, only a bending moment was simulated, shape of bone and prosthesis was neglected, gap location was fixed and big gaps were not included.

The second study solved part of these limitations (Soenen et al. 2013). A 3D model of a bone was created, consisting of cortical bone, trabecular bone and intramedullary canal. Cortical bone was modelled transverse isotropic, similar to its physiological appearance. A 3D model of a primary total hip and total knee arthroplasty (THA and TKA) were added to the bone model, and TKA length was varied to create gaps of 50, 70, 90, 110, 130 and 150 mm. A strain based 'fracture risk' criterion was created and, amongst others, a physiologically relevant load protocol mimicking gait was applied. The gap size did not influence fracture risk for gait loading, and a femur without prosthesis displayed higher strains than a femur with ipsilateral prostheses when subjected to the same loads. As such, neither prostheses insertion nor IP gap creation acted as a stress riser. Limitations of this study were that the THA length (thus gap location) was fixed excluding a representation of a patient with a revision hip prosthesis, and no small gaps were modelled.

2.2.4 Concluding remarks

Even though the interprosthetic gap is destined to become a serious clinical concern in the near future, it has not yet been studied in detail. Some aspects of the influence of the interprosthetic gap on femoral fracture risk have already been investigated, but within certain limitations. E.g.: The full range of gap sizes, representing both small and large gaps, has not yet been modelled in one and the same model neither has the location of the IP gap been varied. Other clinical relevant parameters such as the shape of the hip prosthesis, neck and stem length, have been ignored up to date. Furthermore, the clinical relevance of the loads, such as four-point-bending, applied in literature is questionable. Additionally, the influence of the interprosthetic gap size on the reconstruction of fractures has not yet been investigated.
Finally, the influence of the IP gap on fracture risk is not straightforward. Based on statements in literature the fracture risk of a femur increases with ipsilateral placement (Lehmann et al. 2012), surgeons intuitively fear that the distance between the stem tips may correlate with the femoral fracture risk (Soenen et al. 2013) and that a short distance between the tips of two stemmed implants in the same femur may predispose to fracture (Weiser et al. 2014). Notwithstanding the fact that all three studies rejected these hypotheses mentioned above, there is still a instinctive fear amongst surgeons towards (short) interprosthetic gaps.

Summarized, the currently available literature does not succeed in reaching clear conclusions on the role of the IP gap. This thesis intends to resolve these shortcomings by modelling several clinically relevant parameters that could influence femoral strains and fracture risk. Physiologically relevant loads will be

applied to the model. Influence of IP gap size, IP gap location, bone mechanical properties (cortical thickness and bone Young's modulus) and THA neck and stem length on femoral fracture load and femoral strains will be quantified. Interprosthetic fracture morphology and fracture reconstruction will be studied as well.

Chapter 3

Small interprosthetic gaps do not increase femoral peri-prosthetic fracture risk. An in vitro biomechanical analysis.

Thomas Quirynen[1], Kristoff Corten[3], Olivier Segal[2], Jean-Pierre Simon[2], Jos Vander Sloten[1], G. Harry van Lenthe[1]

[1] Biomechanics Section, Mechanical Engineering Department, KU Leuven, 3001 Heverlee, Belgium

[2] Orthopaedic Surgery Department, University Hospital Leuven, 3212 Pellenberg, Belgium

[3] Hip Unit, Orthopaedic Surgery Department, Hospital Oost-Limburg, 3600 Genk, Belgium

As adapted from Quirynen, T., Corten, K., Segal, O., Bellemans, J., Vander Sloten, J., Simon, J.-P. & van Lenthe, G. H. (2017). Small interprosthetic gaps do not increase femoral peri-prosthetic fracture risk. An in vitro biomechanical analysis, *Acta Orthopaedica Belgica*, **83**(2), 2017

Abstract

Objectives
It has been hypothesized that the interprosthetic gap between ipsilateral hip and knee replacements acts as a stress riser affecting bone fracture behaviour. The aim of this study was to quantify femoral strength and fracture morphology for a wide range of interprosthetic gaps.
Methods
Seven interprosthetic gaps (0-20 cm) were created in artificial femora (N=6-9/group). All specimens were loaded to failure following a compressive loading protocol. Fracture load and fracture morphology were recorded. Outcomes were compared to femora with a hip implant only (N=6; reference group).
Results
Fracture load was highest for 0 cm gaps. All other interprosthetic gaps had fracture loads similar to that of the reference group. Fracture occurred most frequently with a medial butterfly fragment located at the tip of the hip stem.
Conclusions
We conclude that small gaps do not act as stress risers. The specific fracture morphology may benefit from different treatment than peri-prosthetic hip fractures.

Keywords

Femur, interprosthetic fracture, biomechanics, implants

3.1 Introduction

The growing number of THA and TKA placements and revisions combined with a greater susceptibility to falls in the aging population cause a rise in the incidence of peri-prosthetic and inter-prosthetic fractures (Iorio et al. 2008, Kurtz et al. 2005, Berry 1999, Lewallen & Berry 1998, Haddad et al. 1999, Lindahl et al. 2005, Kinsella & Velkoff 2001, Werner 2011). Incidence of these peri-prosthetic femoral fractures is estimated between 0.3 to 5.5% after TKA placement (Rorabeck et al. 1998) while peri-prosthetic fractures after THA placement vary between 0.1-3.2% for primary and 2.1-24% for revision arthroplasty respectively (Berry 1999, Lindahl et al. 2005, Tsiridis et al. 2003, Ochs et al. 2013, Hou et al. 2011, Solarino et al. 2014, Della Rocca et al. 2011, Abendschein 2003).
The number of patients with a total hip arthroplasty (THA) and ipsilateral total knee arthroplasty (TKA) is increasing as well. THA and TKA revision surgery for various reasons often requires the use of long stems (Hou et al. 2011, Iorio et al. 2008). As a consequence, the inter-prosthetic (IP) gap between the tip of both components may become substantially small.
It has been hypothesized that small inter-prosthetic gaps induce higher stresses in the bone, hence, will lead to failure of the femoral bone at lower loads (Soenen et al. 2011, Weiser et al. 2014). Furthermore, considering the deterioration of bone quality that is associated with the aging population in combination with osteolysis due to aseptic loosening, elderly people may experience an even higher susceptibility for peri-prosthetic fractures. Indeed, patients with severe osteoporosis are more prone to inter-prosthetic fractures of the femur (Kenny et al. 1998, Franklin & Malchau 2007). The incidence of inter-prosthetic fractures in patients with ipsilateral prosthesis placement is 1.25% (Kenny et al. 1998). Treatment of an inter-prosthetic fracture of the femur, especially in the presence of an IP gap, remains a challenge. Due to the presence of the two rigid prostheses the remaining bone volume, needed for fracture fixation, is limited and obtaining a stable construct after osteosynthesis may become a serious challenge (Hou et al. 2011, Soenen et al. 2011).
However, it is not well understood how IP gaps affect local bone stresses and strains (Iesaka et al. 2005, Lehmann et al. 2010, Lehmann et al. 2012, Soenen et al. 2013) and little is known about fracture morphology and the resulting specific fracture management and reconstruction strategies (Solarino et al. 2014, Soenen et al. 2011, Platzer et al. 2011, Mamczak et al. 2010, Sah et al. 2010, Ehlinger et al. 2013). Better understanding the alterations in fracture strength of the femur with an inter-prosthetic gap will help the surgeon minimize the risk of jeopardizing the fracture strength of the femur.
Therefore, the aims of this study were (1) to evaluate the effect of the inter-prosthetic gap distance on the fracture strength of the femur and (2) to describe the inter-prosthetic fracture morphology.

3.2 Materials and methods

Six primary THA stems of 14 cm length (C-stem, Depuy J&J, Warsaw, Indiana) and six revision THA stems of 20 cm length (Exeter, Stryker, Kalamazoo, Michigan) were cemented into 12 medium sized (45.5 cm length) 4th generation artificial femora (Sawbones, Pacific Research Laboratories, Malmö, Sweden). Both prosthesis types have a tapered design and were placed with a fixed depth of 1 cm from the shoulder of the stem to the tip of the greater trochanter. Prosthesis placement was performed by trained surgeons (O.S. and H.F.) and based upon prosthesis markings. The Sawbones were mounted into a 250 kN mechanical testing machine (Instron, Norwood, Massachusetts) and loaded along the mechanical axis of the femur (Cherian et al. 2014). This axis has 7° of valgus inclination and a neutral position in the sagittal plane to simulate loading along the mechanical axis, which resulted in a combined compression and bending (Figure 3.1).

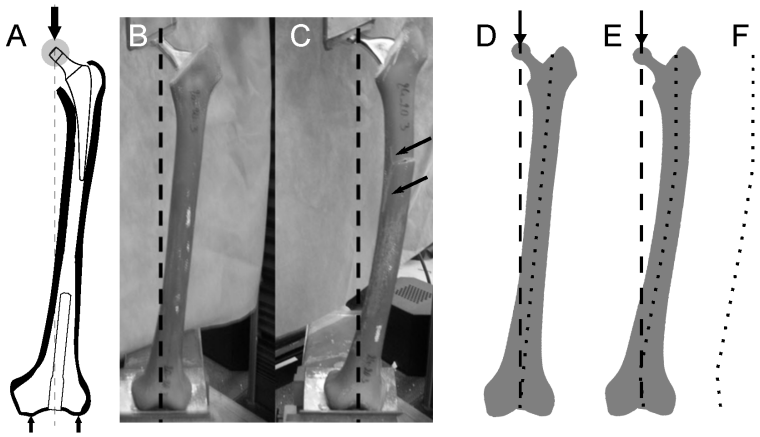

Figure 3.1: (A) Schematic and (B) actual representation of the set-up with indicated load axis (dashed line) representing the mechanical axis of the femur. Arrows on the image on the right indicate the fracture lines during medial butterfly fracture. Deflection (δ_{max}) is measured along the loading axis (dashed line). (C) Specimens were loaded until failure. (D) Schematic representation of the s-shaped bending. The line from the trochanteric region to the intercondylar region on the figure on the right is deformed into an s-shape under load (E & F).

Distally, the specimens were placed in a V-shaped holder constraining the movement in the sagittal plane. Proximally, forces were applied to the femoral stem through a polyethylene socket that was potted in the Instron testing

machine with neutral version relative to the stem. A compressive pre-load of 100N was applied, followed by progressive compression displacement of 8 mm/minute until failure. Failure was defined as a 10% decrease in the measured force (Zdero et al. 2008). The fracture pattern was documented with a high definition camera (Sony HDR-CX560VE) to allow for evaluation of the failure morphology. The measured parameters were fracture load (F_{max}), the deflection of the specimens at failure (δ_{max}), measured in the direction of the applied force, and the work to failure calculated as the area under the force-deflection curve.
In 51 additional femora, seven inter-prosthetic gap distances were created by combining either primary or revision total hip replacements with revision total knee replacements (Profix, Smith&Nephew, Memphis, Tennessee) (Figure 3.1). Stem length for the hip prostheses varied from 14 to 26 cm, whereas the stem length for the knee prostheses varied from 10 to 20 cm, leading to interprosthetic gaps ranging from 0 cm to 20 cm (Table 3.1). As to create the inter-prosthetic gap distances of 1.5 cm and 5 cm, the TKA stems were not placed flush with the intercondylar fossa. The small part of the TKA stem that protruded from the intercondylar fossa did not impact the testing set-up. The IP gap specimens were tested in an identical way as described above.

	THA Only		IP Gaps						
	THA Primary	THA Revision	Gap 20	Gap 15	Gap 10	Gap 5	Gap 3	Gap 1.5	Gap 0
Specimens per group	6	6	6	9	9	9	6	6	6
Primary THA stem (cm)	14	/	14	14	14	/	/	/	/
Revision THA stem (cm)	/	20	/	/	/	20	26	22	24
Revision TKA stem (cm)	/	/	10	15	20	20	15	20	20
Interprosthetic Gap (cm)	/	/	20	15	10	5	3	1.5	0

Table 3.1: Overview of all specimens used in this study. The different combinations of total hip arthroplasty (THA) and total knee arthroplasty (TKA) lengths are shown, together with the resulting gap distance. The name of the groups reflects the gap size.[1]

The Mann-Whitney-U test was used to analyse the difference between primary and revision hip prosthesis regarding fracture load, work to failure and ultimate deflection in the primary THA vs revision THA group, when no TKA was present. One-way ANOVA was used to evaluate the effect of gap size on

[1]Opposed to the other gap sizes, nine specimens were fractured for gaps of 5, 10 and 15 cm since these specimens were used in chapter 4.

fracture load, work at failure and ultimate deflection. In case of a significant effect, the gap size was compared to all other gap sizes in a pair-wise fashion using the Tukey-Kramer test. Correction for multiple testing was applied; all significance levels were set to 5%. All analyses were performed using Matlab 2014b's Statistics toolbox for Windows.

3.3 Results

For the reference measurements consisting of THA prostheses only, the fracture load (F_{max}) was 8407 +/- 463 N and 8435 +/- 459 N, for the primary and revision THA respectively (p=0.937; Figure 3.2). The femur with only a cemented THA revision stem demonstrated similar work to failure (calculated as the area under the force-deflection curve) to the femur with only a primary THA stem, 49.0 +/- 12 J versus 43.1 +/- 11.9 J respectively (p=0.394; Figure 3.2). Mean ultimate deflection (δ_{max}) was 8.852 +/- 1.785 mm and 9.698 +/- 1.357 mm for the primary and revision THA respectively (p=0.240). For these specimens with a THA only, 9 of 12 fractures occurred with a lateral butterfly fragment. A sawbone without prosthesis was not included since this would lead to fracture of the specimen in the area of the femoral neck (Schileo et al. 2014).

The fracture load after the insertion of a TKA revision stem was 8155 N (range 6759 N to 9796 N). The lowest fracture load (7346 +/- 519 N) was found with a 15 cm gap size. The highest fracture load (9415 +/- 206 N) was found with a gap size of 0 cm. The fracture load increased with decreasing gap size when the distance between both stems was smaller than 5 cm (Figure 3.2). Gap size had a significant influence of fracture load ($p<0.001$). The fracture load of the 0 cm gap was significantly higher than all other gap sizes ($p<0.05$). The fracture load of the 15 cm gap was lower than the 0.5 and 3 cm gap sizes ($p<0.05$). The mean ultimate deflection (δ_{max}) was 9.1 mm (range 7.3 to 16 mm). The highest deflection (11.1 +/- 2.6 mm) was found with the 20 cm gaps. The lowest deflection (8.6 +/- 1.2 mm) was found for the 3 cm gaps. No significant correlation between the gap size and δ_{max} was found (p=0.056). Work to failure was smaller with gap sizes between 5 cm to 15 cm than with 0 or 20 cm gaps. Gaps smaller than 5 cm required more work to failure (Figure 3.2). There was a trend of higher work to failure with gap sizes of 0 cm and 20 cm when compared to other gap sizes. A 0 cm gap required significantly higher work to failure compared to the 10 and 15 cm gaps ($p<0.05$) respectively. The 20 cm gaps required significantly higher work to failure compared to the 15 cm gaps (p=0.049).

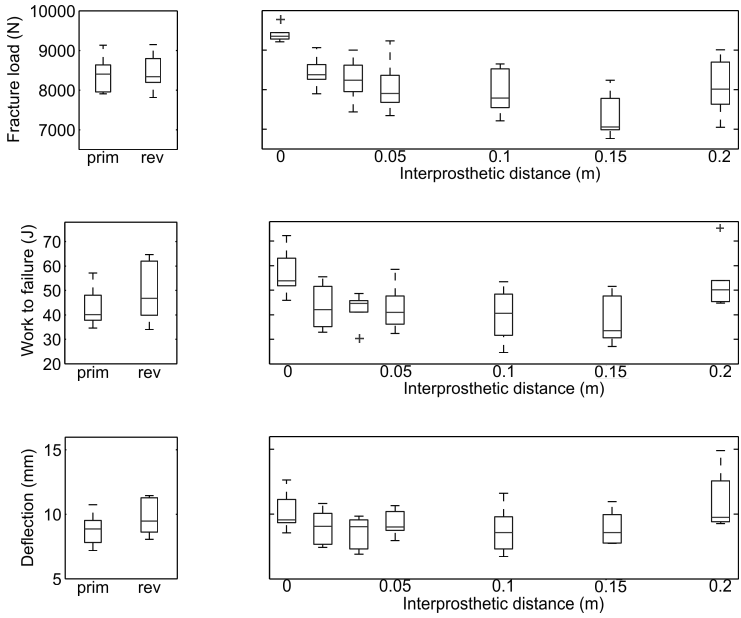

Figure 3.2: Results of primary (prim) and revision (rev) THA tests and IP gap variation are shown in boxplot format. Fracture load, work to failure and deflection at failure are shown. 0 cm gaps had a significantly higher F_{max} than all other gap sizes ($p<0.05$). F_{max} of 15 cm gaps was significantly lower ($p<0.001$), than 1.5 and 3 cm gaps. 0 cm gap required significantly higher work to failure than the 10 and 15 cm gaps ($p<0.05$). 20 cm gaps required significantly higher work at failure than 15 cm gaps ($p=0.049$).

Both the THA and TKA stems remained well fixed to the bone in all cases. All femurs failed at the level of the interprosthetic gap, close to the tip of the hip prosthesis (Figure 3.3). Gap fractures had a typical medial butterfly fragment in 34 of 51 specimens (67%). A lateral butterfly fragment was present in 12 specimens (23.5%): none of the 0 cm gaps, 17% of the 1.5 cm gaps and the 3 cm gaps, 55% of the 5 cm gaps, 11% of the 10cm gaps, 33% of the 15 cm gaps and 17% of the 20 cm gaps. An oblique fracture occurred in 3 cases (6%) (1 of the 3 cm, 10 cm and 15 cm gaps) and a multi-fragment fracture occurred in 1 case (5 cm gap). One specimen (10 cm gap) had an antero-medial butterfly.

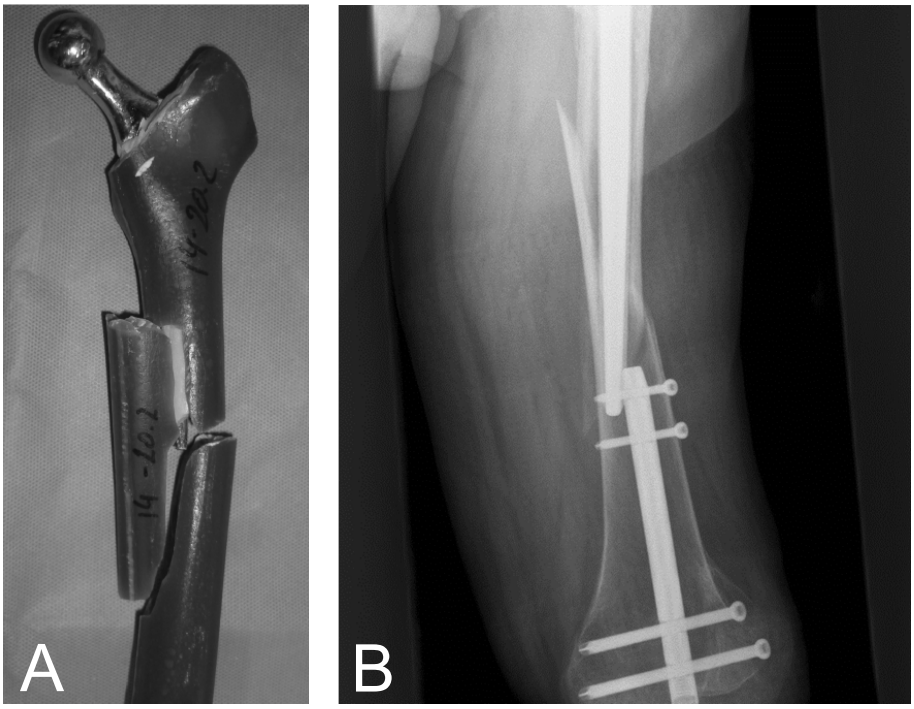

Figure 3.3: (A) Typical medial butterfly fracture at location of the interprosthetic gap, at the tip of the THA prosthesis. (B) As correlation to the clinical situation, an X-ray showing a similar fracture between a long revision THA and an intramedullary nail is shown as well.

Images from the high-definition video showed that, for the THA-only specimens, loading along the mechanical axis of the femur combined with fixed knee condyles caused an s-shaped bending. This bending shape is characterized by a lateral outward bending in the proximal part of the femur, followed by an inward bending in the femoral shaft starting just above the knee condyle. Insertion of the distal TKA stem led to a less pronounced s-shaped bending (Figure 3.1) which influenced the bending deformation as well.

3.4 Discussion

The aims of this study were (1) to evaluate the effect of the inter-prosthetic gap distance on the fracture strength of the femur and (2) to describe the inter-prosthetic fracture morphology. These aims of this study have been

achieved. We demonstrated that small inter-prosthetic gaps do not hamper the load-bearing capacity of the femur. Furthermore, we found that most femora fractured with a medial butterfly fragment.

Multiple sizes of THA were used, but these did not influence the maximal force at fracture. Inter-prosthetic gaps smaller than 5 cm were associated with an increased fracture load and work to failure compared to gaps larger than 5 cm. Even more, when the inter-prosthetic gap is decreased to a gap size of 0 cm, the fracture load and work to failure increased significantly when compared to larger gap sizes, for the loading conditions used in this study. Loading along the mechanical axis of the femur, or so-called isometric loading (Moazen et al. 2011) was applied since it is a well-accepted testing protocol which represents the major compressive loading at the hip joint (Soenen et al. 2013, Zdero et al. 2008, Lever et al. 2010, Cristofolini et al. 2010, Schileo et al. 2014, Ali et al. 2014). In our study, both the distal and proximal ends were free to rotate in the V-shaped holder and acetabular cup, respectively. As such, a more physiologically relevant loading was obtained.

Previous experimental studies investigating the IP gap used cantilever bending (Iesaka et al. 2005) or four-point bending (Lehmann et al. 2012). Cantilever bending only simulates the bending forces, whereas four-point bending leads to a constant moment over the specimen between the two supports. Neither of these represents an anatomical loading condition. Furthermore, in both the cantilever bending and four-point bending studies the specimen ends were embedded in steel pots (Lehmann et al. 2012, Iesaka et al. 2005), which limits the deformation of the specimen. Some studies have emphasized that the abductor force should be modelled (Stolk et al. 2001). We do acknowledge that addition of the abductor force can change the bending moment at the interprosthetic gap. Yet, the boundary conditions in our study (movement along the mechanical axis only (Speirs et al. 2007)) applied on the femoral head countered the excessive bending due to the lack of the abductor force and resulted in a physiological bending as well. Hence, we believe that including the abductor force would not change the outcome of this comparative study.

In this study we tested a wide range of gap sizes. The effect of IP gap size has been tested before on cylindrical, idealized, prosthetic stems through cantilever bending in Sawbone femora by Iesaka et al. (Iesaka et al. 2005). They found that when stems remained fixed to the bone, gap length variation did not influence the peak tensile stress on the femur, nor did stem tips act as stress risers, which is similar to the results of our study. The smallest gap of 1 mm showed a lower stress than all other larger gaps, which concurs with our findings of a significant higher fracture load for 0 cm gaps. Another study evaluated the impact of adding a stemmed TKA prosthesis or a distal retrograde nail to hip stem placed in a human cadaveric femur (Lehmann et al. 2012); yet, only one IP gap size was evaluated. They found that adding the stemmed

knee prosthesis did not increase the risk for fracture. Our study showed similar results, where TKA implantation did not lower the fracture load compared to THA-only specimens. The role of IP gap size has been evaluated in more detail in a finite element study where the femora were loaded under gait conditions (Soenen et al. 2013). Gap size did not influence the risk for fracture, nor did stem tips act as stress risers, similar to the results of our study. Yet, the THA stem length was fixed, and the smallest gap was 5 cm only.

Another strength of this study is that it is the first study on inter-prosthetic gaps where fracture location and fragment type were investigated. We found that 67% of the specimens failed with a diaphyseal medial butterfly fragment, as this is the location where the highest stresses and strains are located. This may be surprising at first sight, because several clinical studies reported supra-condylar inter-prosthetic fractures, located proximal to the TKA component (Soenen et al. 2011, Mamczak et al. 2010). Yet, this discrepancy can be explained by the fact that we used a stemmed TKA component, while previous reports referred to non-stemmed TKA components. In more detail, due to the presence of a THA and TKA stems the rigidity and resistance to fracture of the proximal and distal region of the femur are higher than in the native case. The diaphyseal bone at the location of the gap will absorb most of the energy during loading. Due to the nature of the mechanical-axis loading protocol, the bending component of the load decreases from proximal to distal (Figure 3.1a). As such, the largest bending in the bone is located at the tip of the THA stem. As a consequence, the fracture will originate at the lateral side of the IP gap, where high tensile stresses will occur that co-locate with the lowest strength (tensile strength lower than compressive strength (Tencer 2006)). When the crack grows in the transverse direction, the failure mode will switch to compressive failure, causing an oblique (shear) fracture line. As a consequence, a butterfly-shaped bone fragment is created. We attribute the variability of fracture morphology in one gap group to slight variations in prosthesis placement.
There are several limitations of this study. First, the in vitro nature can be questioned. However, measuring fracture strength in a patient is not possible and the quantification of fracture morphology would be very complicated, if possible at all. Additionally, advanced age of these patients, many with existing co-morbidities, will undoubtedly make it difficult to reach clear conclusions. The in vitro nature also excluded taking bone remodelling into account. Yet, to the best of our knowledge, there is no single clinical study indicating that bone-remodelling would be of greater concern in patients with small interprosthetic gaps. We hypothesize that bone remodelling will lead to weakening of the bone. Yet, based on the fact that bone fracture will occur close to the distal end of the hip stem, and considering that bone remodelling close to the tip will be limited (if at all), it is questionable whether bone remodelling would result in

reduced failure loads. Second, to construct the different gap distances, several THA sizes have been used. Even though larger revision THA stems seem to lead to a smaller deflection as compared to primary THA, the difference was not significant, neither was the difference in force at failure. Third, while IP gap fractures are prevalent in osteoporotic patients, Sawbones are not representative for osteoporotic bone quality, remodelled bone after prosthesis placement, or for hip fracture simulation (Soenen et al. 2011, Iesaka et al. 2005, Schroll 2003, Basso et al. 2014). Yet, as the inter-prosthetic gap is located at the femoral isthmus, which is less affected by osteoporosis than the metaphyseal regions, Sawbones can be used as a relevant model for human bone, especially since it was our goal to perform a comparative study where cadaveric-bone variability had to be avoided. Furthermore, validation studies have shown that Sawbones display stiffness and strains curves very similar to those of natural femurs but have a much lower variability thereby allowing them for utility in comparative tests (Zdero et al. 2008, Cristofolini et al. 1996, Heiner 2008, Gardner et al. 2010). In addition, the analogue cortical bone used in fourth generation sawbones also displays fracture toughness and tensile strength similar to human cortical bone (Chong et al. 2007). Fourth, we did not consider cortical thickness, even though it plays a dominant role in fracture load (Weiser et al. 2014). We believe that, even for bones with a thinner cortex, the findings of our comparative study still apply. Fifth, in this study we evaluated cemented prostheses. The use of bone cement will only slightly influence the bending rigidity as compared to uncemented specimens, since the cement is located close to the force-transmission line; hence, the findings of this study can be extrapolated to uncemented, press-fitted or ingrown prostheses. And sixth, only one loading condition was used. As we used a physiologically relevant load case along the mechanical axis of the femur (Cherian et al. 2014), and as we used the data in a comparative way only, we do not expect to find different conclusions when more complicated loading would have been applied. Furthermore, the measured failure load was substantially higher than the peak forces that arise in a variety of loading conditions (Bergmann et al. 2010). Torsional loads will be largely carried by the bone; hence, strong effects of the IP gap size were not expected and were not tested experimentally.

3.5 Conclusion

In summary, for the loading conditions used in this study, we conclude that this is the first study that experimentally evaluated the biomechanical influence of small (< 35 mm) inter-prosthetic gaps between the femoral components of hip and knee prostheses, using a relevant loading protocol. Our findings confirm earlier studies indicating that, during the immediate post-op situation,

inter-prosthetic gaps do not act as stress risers. In fact, small gaps require higher forces to fracture, thus do not have increased fracture risk. Due to the presence of the THA and TKA stems the typical failure will result in the creation of a medial butterfly fragment. Such fractures may warrant specific reconstruction techniques.

Acknowledgements

This study was partially funded by a grant of the BVOT - Belgische Vereniging voor Orthopedie en Traumatologie. This work was also supported by the Orthopaedic Surgery Department, University Hospital Leuven, Pellenberg, Belgium.

Chapter 4

Interprosthetic femoral fractures: effect of interprosthetic distance and anterior struts on the failure load of lateral plate reconstructions.

Thomas Quirynen[1], Kristoff Corten[3], Hans Feyen[2], Jean-Pierre Simon[2], Jos Vander Sloten[1], G. Harry van Lenthe[1]

[1] Biomechanics Section, Mechanical Engineering Department, KU Leuven, 3001 Heverlee, Belgium

[2] Orthopaedic Surgery Department, University Hospital Leuven, 3212 Pellenberg, Belgium

[3] Hip Unit, Orthopaedic Surgery Department, Hospital Oost-Limburg, 3600 Genk, Belgium

Submitted

Abstract

Objectives
The incidence of femoral fractures occurring between a total hip replacement and a total knee replacement are destined to rise. Yet, the biomechanics of these fractures and their reconstruction with bone fixation plates is not fully understood; i.e. it is unknown whether the distance between the two implants influences the failure load, and the use of additional bone struts is controversial. Therefore, the aim of this study was to quantify the effect of the interprosthetic gap and the addition of an anterior strut on the failure load of the fracture reconstruction performed with fixation plates.
Methods
Hip and knee implants were placed ipsilateral in artificial femora (Sawbones), resulting in interprosthetic gaps of 5, 10 and 15 cm respectively. Failure load of lateral plate reconstructions and lateral plate reconstructions with an additional anterior strut were evaluated through compressive loading along the mechanical axis of the femur.
Results & Conclusions
The failure load of the plate reconstructions and plate-strut reconstruction was not affected by gap size. The addition of a strut did not affect failure load, except in reconstructions of fractures where the plate reconstruction suffered from insufficient fracture reduction.

Keywords

Femur, interprosthetic fracture, biomechanics, implants, fracture reconstruction, strut

4.1 Introduction

The incidence of interprosthetic femoral fractures occurring between a total hip replacement (THR) and a total knee replacement (TKR) is low, around 1.25% in 320 limbs with ipsilateral prostheses (Kenny et al. 1998). Their incidence however is destined to rise (Mamczak et al. 2010, Michla et al. 2010, Ochs et al. 2013, Tsiridis et al. 2007) given that average age, life-expectancy and activity level of the population increases (Bryant et al. 2009, Della Rocca et al. 2011, Hou et al. 2011, Lehmann et al. 2010, Masri et al. 2004, Old et al. 2006, Platzer et al. 2011, Schroll 2003). It has been shown that the size of the interprosthetic (IP) gap can influence the femoral failure load, and that fractures mainly occur with a medial butterfly at the tip of the THA prosthesis (Quirynen et al. 2017). Peri- and inter-prosthetic fractures with stable prostheses are commonly reconstructed with fracture fixation plates and can be complemented with an additional strut; yet there is no defined treatment protocol (Bryant et al. 2009, Choi et al. 2010, Dennis et al. 2000, Ebraheim et al. 2014, Ebrahimi et al. 2012, Ehlinger et al. 2013, Lever et al. 2010, Masri et al. 2004, Perren 2002, Ricci et al. 2005, Solarino et al. 2014).
The aim of interprosthetic fracture reconstruction is to securely reduce the fracture fragments and to provide a stable fixation (Hoffmann et al. 2016, Solarino et al. 2014). The reconstruction of inter-prosthetic fractures and the influence of the interprosthetic gap size on failure load of these reconstructions have not yet been thoroughly investigated (Moazen et al. 2011) and clinical studies mostly consist of small patient groups (Solarino et al. 2014). Biomechanical testing of peri-prosthetic fracture reconstruction has shown that long plates fixed to the bone with screws are biomechanically superior compared to other fracture fixation constructs. Yet, in all these studies fractures have been greatly simplified; e.g. femurs have been commonly osteotomized with a saw in an oblique plane (45 degrees to the shaft axis) (Dennis et al. 2000, Dennis et al. 2001, Fulkerson et al. 2006, Moazen et al. 2011, Zdero et al. 2008).
Addition of a strut is a controversial treatment method. According to some studies, long locking plates provide adequate fixation strength and stability, and will result in optimal fracture healing (Hou et al. 2011, Lehmann et al. 2010, Mamczak et al. 2010, Platzer et al. 2011, Ricci et al. 2005, Sah et al. 2010). Similar studies see no need to add a allograft strut (Bryant et al. 2009, Hou et al. 2011) or only advice the use of a strut to improve the mechanical stability (Tomás Hernández & Holck 2015) or in case of osteoporosis, osteopenia or severe bone loss (Choi et al. 2010, Corten et al. 2009, Solarino et al. 2014). Patient cases with insufficient cortex reconstruction, insufficient fragment fixation, poor bone quality or short plate length might thus warrant an additional bone strut (Corten et al. 2009, Ebraheim et al. 2014, Masri et al. 2004, Moazen et al. 2011). Other studies however recommend routinely

adding a strut (Buttaro et al. 2007, Haddad et al. 2002) with the aim to increase fixation stability (Tomás Hernández & Holck 2015). Part of this controversy is due to the length of the fixation plate. We already identified this parameter as an important factor in fracture reconstruction in a preliminary study comparing different plate lengths and fixation types. Studies advocating routinely use of bone strut often combine the struts with short plates, which are on itself not suited to reconstruct the fractures (Buttaro et al. 2007, Talbot et al. 2008, Wilson et al. 2005, Zdero et al. 2008). The biomechanical contribution of these struts is thus unknown due to the large variety of fracture fixation constructs used in these studies. In fact, the range of fixation types and plate lengths influenced the reconstruction stability to a larger extent than did addition of a strut.

Therefore, the aims of this study were (1) to evaluate the effect of the interprosthetic gap on the failure load of femoral fractures reconstructed with a plate and (2) to quantify whether the addition of an anterior placed bone strut would increase the failure load.

4.2 Materials and methods

Eighteen medium sized (45.5 cm length) 4th generation artificial femora (Sawbones, Pacific Research Laboratories, Malmö, Sweden) were selected from a prior study which evaluated the biomechanical effect of different interprosthetic gap distances on femoral fracture strength and fracture morphology (Quirynen et al. 2017). In short, interprosthetic gaps were created by implanting a primary or revision hip prosthesis combined with a knee prosthesis stem of varying length, to obtain several interprosthetic gap sizes. The interprosthetic gap was measured between the distal tip of the hip and the proximal tip of the knee prosthesis. Both prostheses were cemented into the artificial femur. The specimens were mounted into a 250 kN mechanical testing machine (Instron, Norwood, Massachusetts) and loaded along the mechanical axis of the femur (Cherian et al. 2014). This axis has 7° of valgus inclination and a neutral position in the sagittal plane to simulate loading along the mechanical axis of the femur, which resulted in a combined compression and bending mode (Fig. 4.1). Distally, the specimens were placed in a V-shaped holder constraining the movement in the sagittal plane. Proximally, forces were applied to the femoral stem through a polyethylene socket that was potted in the Instron testing machine with neutral version relative to the stem. A compressive pre-load of 100 N was applied, followed by progressive compression displacement of 8 mm/minute until failure. The fracture pattern was documented with a high definition camera (Sony HDR-CX560VE) to allow for evaluation of the failure morphology.

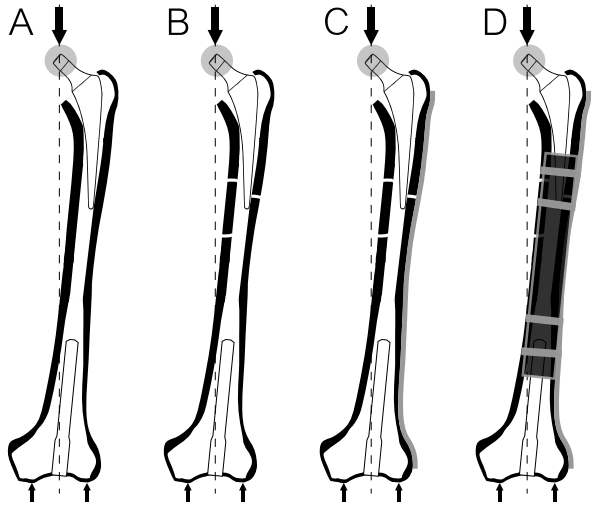

Figure 4.1: Schematic representation of test-setup with indicated load axis (dashed line) as described by the loading protocol. Arrows indicate load application (femoral prosthesis head) and the reaction forces in both knee condyles. Test sequence is shown from left to right: intact specimen (A), specimen fracture (B), plate reconstruction (C) and anterior addition of a strut (D).

The fractured specimen of gap sizes 5 cm, 10 cm and 15 cm (N=6 per group) were re-used in this study (Table 4.1). These specimens were reconstructed with a 43 cm non-contact bridging periprosthetic proximal femur plate (NCB, Zimmer, Winterthur, Switzerland). This plate was selected following a preliminary study which showed that, among the tested reconstruction devices, this construct achieved the highest failure load (see Appendix D).
The NCB plate bridged the fractured specimens from the condylar to the trochanteric region (Fig. 4.1). Apart from the screws to reduce and fixate the fracture fragments, four screws were locked distally and two screws were locked proximally in the greater trochanter to provide rotational stability (Borgeaud et al. 2000, Della Valle et al. 2003, Ricci et al. 2005) and to reach optimal fracture reconstruction (Hoffmann et al. 2016). Fracture reduction was assessed by a trained surgeon (H.F.). The same setup as described above was used, except that failure was defined as a 10% decrease in the measured force (Zdero et al. 2008).

	Gap Size [cm]		
	5	**10**	**15**
Number of specimens	6	6	6
THR length [cm]	20	14	14
TKR length [cm]	19	20	15
Interprosthetic gap [cm]	5	10	15

Table 4.1: Overview of the specimens used in this study. The different combinations of total hip revision (THR) and total knee revision (TKR) lengths are shown, together with the resulting interprosthetic gap.

Subsequently, an anterior Sawbone strut was added to the specimens. Specifically, a 23 cm long strut was cut from the anterior cortex of the diaphysis of a Sawbone specimen and fixed with four cables; two proximally and two distally of the fracture site. The additional fracture that occurred after the load to failure of the plate reconstruction was reduced and the specimen was loaded following the same loading protocol as described above. Failure load was measured as described above (Zdero et al. 2008).
One-way ANOVA was used to evaluate the effect of gap size on failure load. Correction for multiple testing was applied. Paired Student's T-test was used to evaluate the effect of adding a strut. All significance levels were set to 5%. All analyses were performed using Matlab 2014b's Statistics toolbox for Windows.

4.3 Results

Failure loads for the plate (p=0.559) and plate-strut (p=0.479) reconstructions of the 5 cm, 10 cm and 15 cm gap specimens were not affected by gap size (Table 4.2). Additional fracture after plate reconstruction occurred for seven specimens (e.g. calcar fracture, crack propagation, fragment fracture or fragment loss). Since the same specimens were used to test the plate and plate-strut reconstructions, this additional fracture influenced fracture morphology of the plate-strut reconstruction (Table 4.3). Throughout all tests, none of the prosthesis stems loosened, as assessed by a trained surgeon (H.F.). Fracture reduction was inadequate for specimen 10.6.
Failure load of all 18 plate-strut reconstructions did not differ from the failure load of the plate reconstructions (p=0.906, Table 4.2). In general, the addition of a strut did not increase failure load (less than 5% change in failure load for specimens without additional fracture).

	Gap Size [cm]			Overall
	5	10	15	
Plate	7305+/-1443	7106+/-2487	8234+/-1584	7548+/-1851
Plate & strut	6893+/-1428	7570+/-1839	8072+/-1656	7511+/-1627

Table 4.2: Failure loads (N) of the plate and plate-strut reconstructions. Gap size did not influence failure load of neither reconstruction technique. Comparison of the plate reconstruction with the plate-strut reconstruction showed that, in general, the addition of an anterior strut did not affect failure load.

Gap Size [cm]	Specimen	Initial interprosthetic fracture	Additional fracture after plate reconstruction
5	5.1	Lateral butterfly	/
	5.2	Multi-fragment	Multi-fragment
	5.3	Lateral butterfly	Calcar fracture
	5.4	Medial butterfly	/
	5.5	Medial butterfly	/
	5.6	Lateral butterfly	Trochanter crack propagation
10	10.1	Lateral butterfly	/
	10.2	Medial butterfly	Butterfly segment fracture
	10.3	Oblique fracture	/
	10.4	Anteromedial butterfly	/
	10.5	Medial butterfly	/
	10.6	Medial butterfly	/
15	15.1	Medial butterfly	/
	15.2	Lateral butterfly	/
	15.3	Medial butterfly	/
	15.4	Oblique fracture	Fragment loss
	15.5	Medial butterfly	Lateral crack propagation
	15.6	Medial butterfly	Lateral crack propagation

Table 4.3: Overview of the specimens used in this study. 'Initial interprosthetic fracture' indicates the morphology of the fracture reconstructed with a plate. For some specimen, the fracture propagated during the load to failure test of the plate reconstruction. 'Additional fracture after plate reconstruction' indicates the morphology of the fracture after plate-reconstruction and subsequently reconstructed with a plate-strut construct. Specimen names indicate gap size.

Four specimens (5.2, 5.3, 10.2 and 15.4) with additional fracture had lower failure loads when the strut was added (22%, 24%, 15% and 27% lower respectively). For four other specimens however (5.1, 10.4, 10.6 and 15.2), failure load of the plate-strut reconstruction was higher than that of the plate-reconstruction (13%, 11%, 104% and 15% higher respectively) (Fig. 4.2).

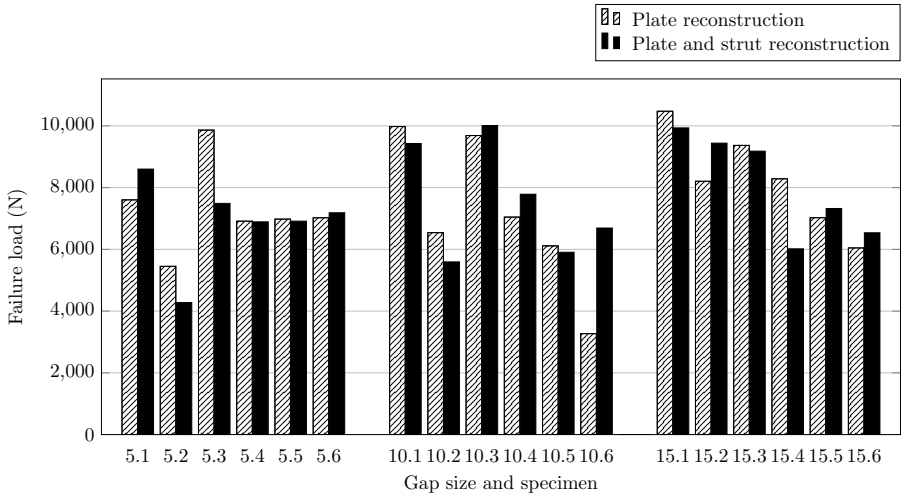

Figure 4.2: Specimen specific failure loads for all 18 specimens. Plate reconstructions are shown in hashed pattern, plate-strut reconstructions in black. Specimen names indicate gap distance and specimen number.

4.4 Discussion

The aims of this study were (1) to evaluate the effect of the distance between the tips of ipsilateral placed THR and TKR on the failure load of anatomically relevant femoral fractures reconstructed with a fixation plate and (2) to investigate if addition of an anterior placed bone strut to the plate reconstruction changes the failure load of the construct. The main result of our study is that, for fracture reconstruction with a long fixation plate, interprosthetic gap size does not affect failure load. In general, addition of a strut does not influence failure load either.

For ten specimens (55.6%), the plate provided adequate fracture reduction and addition of a strut did not influence failure load.

Four specimens (22.2%) showed increased failure load for the plate-strut reconstruction compared to the plate reconstruction (Table 4.2, Fig. 4.2).

E.g. specimen 10.6, a difficult to reconstruct medial butterfly fracture, had inadequate fracture reduction after plate reconstruction due to the inability to accurately reposition the fracture fragments. For this specimen addition of a strut provided additional construct stability. In other specimens (i.e. specimen 5.1, 10.4, 15.2), fracture fragments were partly located on the anterior side of the femur. Addition of the anterior strut restricted fragment movement, thereby improving reconstruction stability and failure load.
Four other specimens (22.2%) showed a decrease in failure load after the addition of a strut. This decrease is due to (extensive) additional fracture following plate reconstruction and prior to plate-strut reconstruction, impacting the reconstruction stability. As described above, the fracture fragment reduction plays a large role in construct stability. Multi-fragment fractures (specimen 5.2) or additional fracture; respectively calcar fracture, butterfly segment fracture or fragment loss for specimen 5.3, 10.2 and 15.4 all leads to suboptimal fracture reconstruction, and thus suboptimal stability and failure load.
All prostheses used in this study were cemented, as is the clinical approach for revision of THR and TKR. The bone cement in the intra-medullary canal will only slightly influence the bending rigidity of the specimen, since the cement is located close to the force-transmission line. Also, the effect of the fixation plate on bending rigidity, due to its larger E-modulus, will be two orders of magnitude higher than that of the bone cement. As such, the results of this study can also be used for press-fitted or ingrown prostheses.
There are several limitations to this study. First, we conducted this study in vitro since it is impossible to measure the failure load of a fracture reconstruction in vivo. Also, patient with ipsilateral prostheses are often of advanced age, and the additional co-morbidities will compromise the effort to reach clear conclusions. The in vitro nature excluded taking bone remodelling into account, hence the findings of this study are valid for the initial post-operative stability of the fracture reconstruction. Second, different THR lengths were used to create the interprosthetic gap sizes; yet prior research showed that THR length did not significantly influence failure load (Quirynen et al. 2017). Third, Sawbones do not represent osteoporotic bone (Basso et al. 2014, Soenen et al. 2011). Yet, validation studies have shown that stiffness and strains curves of natural femurs are very similar to those of sawbones, but the latter have a much lower variability thereby allowing them for utility in comparative tests (Gardner et al. 2010, Heiner 2008, Moazen et al. 2011, Zdero et al. 2008). In addition, the analogue cortical bone used in fourth generation sawbones also displays fracture toughness and tensile strength similar to human cortical bone (Chong et al. 2007). Fourth, the order of testing influenced the fracture morphology of some of the plate-strut reconstructions. As we were interested in the comparison of the plate and plate-strut reconstruction of the same fracture, all specimens were used twice, for plate and plate-strut reconstructions. As such, some

specimens had additional fracture which weakened the specimen. As a last limitation, only one loading condition was used. Application of the load along the mechanical axis of the femur (Cherian et al. 2014) is a physiologically relevant loading condition (Lever et al. 2010, Zdero et al. 2008) which has been used for evaluating peri-prosthetic fracture reconstructions before (Borgeaud et al. 2000, Choi et al. 2010, Dennis et al. 2000, Dennis et al. 2001, Ebrahimi et al. 2012, Fulkerson et al. 2006, Papini et al. 2007, Talbot et al. 2008, Wilson et al. 2005, Zdero et al. 2008). As we used the data in a comparative way only, we expect that similar conclusions will be reached when more complicated loading would have been applied.

4.5 Conclusion

In summary, we conclude that in lateral plate reconstructions of fractures between ipsilateral femoral prostheses, the size of the interprosthetic gap does not influence the failure load. The addition of an anterior strut is useful for specific fracture morphologies where the plate reconstruction does not offer adequate fracture reduction.

Acknowledgements

This study was supported by the Orthopaedic Surgery Department, University Hospital Leuven, Pellenberg, Belgium.

Chapter 5

Do small interprosthetic gaps increase bone fracture risk? A parametric study on gap size and location.

Thomas Quirynen[1], Jos Vander Sloten[1], Jean-Pierre Simon[2], G. Harry van Lenthe[1]

[1] Biomechanics Section, Mechanical Engineering Department, KU Leuven, 3001 Heverlee, Belgium

[2] Orthopaedic Surgery Department, University Hospital Leuven, 3212 Pellenberg, Belgium

Submitted

See appendix C for a short overview on finite element modelling.

Abstract

Objectives
The number of patients with ipsilateral hip and knee implants is increasing. The resulting interprosthetic gap has been hypothesized to act as a stress riser. The purpose of this work was to evaluate the effect of clinically relevant parameters such as gap size, gap location, cortical thickness and bone tissue modulus on bone strains.
Methods
We created a finite element model allowing for a parametric analysis of these factors. The model consisted of a cylindrical cortical bone, hip prosthesis and knee prosthesis stem. The length of the hip and knee stems were varied to change both gap size and gap location, as were the bone Young's modulus (E) and cortical thickness. A load along the mechanical axis of the femur was applied.
Results
We found that, for loading along the mechanical axis, large gaps and short hip prostheses caused the highest strains. These strains were lower than the strains in an intact femur. Thinner cortical thickness and reduced tissue modulus both increased bone strains, the former to a greater extent than the latter.
Conclusions
We conclude that interprosthetic gaps do not act as stress risers, and that not only gap size but also gap location influences the strains in the femur. Furthermore, bone strains are largely affected by cortical bone thickness.

Keywords

Femur, interprosthetic fracture, finite element analysis, biomechanics, implants

5.1 Introduction

Current demographic trends show a strongly aging population (Werner 2011, Kinsella & Velkoff 2001). Given the association between age and total joint replacement, the number of hip and knee replacements will increase, as will the number of ipsi-laterally placed hip and knee implants. Many orthopaedic surgeons intuitively fear that the resulting interprosthetic (IP) gap between the distal tip of the hip prosthesis and the proximal tip of the knee prosthesis influences the biomechanical response of the femur to mechanical load. It is known that interprosthetic gaps and especially the resulting fractures form a serious concern (Platzer et al. 2011, Mamczak et al. 2010, Sah et al. 2010, Solarino et al. 2014, Soenen et al. 2011, Ehlinger et al. 2013, Ochs et al. 2013, Kenny et al. 1998). The use of hip and knee prostheses with long stems, such as commonly used in revision surgery to obtain sufficient stability, have been hypothesized to act as stress risers (Soenen et al. 2011, Weiser et al. 2014), hence, may lead to increased fracture risk. This may form a substantial clinical problem, given that the number of revision prostheses is increasing (Iorio et al. 2008, Hou et al. 2011) However, it is not well understood how IP gaps, especially those smaller than 35 mm, affect local bone stresses and strains (Iesaka et al. 2005, Lehmann et al. 2010, Lehmann et al. 2012, Soenen et al. 2013, Weiser et al. 2014) and specific fracture management strategies are lacking (Platzer et al. 2011, Mamczak et al. 2010, Sah et al. 2010, Solarino et al. 2014, Ehlinger et al. 2013, Soenen et al. 2011). Furthermore, the role of bone size and bone tissue modulus upon femoral stains and stresses is unclear.
Some aspects of the IP gap have already been investigated (Weiser et al. 2014, Iesaka et al. 2005, Lehmann et al. 2010, Lehmann et al. 2012, Soenen et al. 2013). First, the influence of adding a knee prosthesis to an existing hip prosthesis was evaluated to see if a knee prosthesis acted as a stress riser. Two studies were conducted by the same group. The first study compared cadaveric human femora in which a total hip prosthesis (THA) had been placed to femora with both hip prosthesis and retrograde femoral nail (Lehmann et al. 2010). The second study included cadaveric femora with ipsi-lateral placed THA and TKA to the comparison (Lehmann et al. 2012). Four-point bending was selected to create a constant bending moment in between the two prostheses. Fracture strength of femora with ipsi-lateral placed THA and TKA was significantly higher than both other constructs. Another group used a finite element model to compare femoral strains of a healthy femur, loaded following a gait protocol, to those of a femur with an interprosthetic gap (Soenen et al. 2013). In none of the cases, loaded under gait, a stress riser effect was noted when an IP gap was created. TKA addition did not influence fracture strength (Lehmann et al. 2010, Lehmann et al. 2012), and the femoral strains of a femur with IP gap were lower than those of a healthy femur (Soenen et al. 2013).

Second, some studies already investigated an, albeit limited, variety of gap sizes (Weiser et al. 2014, Iesaka et al. 2005, Soenen et al. 2013). A simplified cylindrical model of a femur, loaded under cantilever bending, was used to model a range of mainly smaller interprosthetic gaps (1, 10, 35 and 85 mm) (Iesaka et al. 2005). Another, experimental biomechanical study investigated three different gap sizes (35, 80 and 160 mm), using cadaveric specimens and four-point bending (Weiser et al. 2014). Lastly, an anatomically relevant FE model was used to simulate a variety of IP gap sizes (50, 70, 90, 110, 130 and 150 mm), but small gaps were not included (Soenen et al. 2013). All three studies reached the same conclusion: the gap size did not influence peak femoral tensile stresses (Iesaka et al. 2005), fracture strength (Weiser et al. 2014), nor risk of fracture (Soenen et al. 2013).
Third, all three papers investigating IP gap size also modelled changes in bone tissue properties (e.g. to simulate the effect of osteoporotic bone). This was achieved by either adapting the cortical thickness (Iesaka et al. 2005), by using osteoporotic cadaveric specimen (Weiser et al. 2014), or by lowering the E-modulus of both cortical and trabecular bone, without adapting the cortical thickness (Soenen et al. 2013). Similar conclusions were reached: femoral stresses decreased when cortical thickness increased (Iesaka et al. 2005), fracture resistance significantly increased with increasing cortical thickness (Weiser et al. 2014) and osteoporotic specimens did have an increased risk of fracture (Soenen et al. 2013).
Still, some aspects of the IP gaps are unknown. First, the effect of the location of the gap (i.e., the length of the hip stem) has not yet been studied; still, this would be relevant information as hip stems with varying lengths are being used clinically. Second, no data exist covering a wide range of IP gaps (ranging from gaps smaller than 35 mm to gaps larger than 150 mm) while using a physiologically relevant loading condition.
Therefore, the aim of this study was to enhance our understanding of the factors that influence the strain in the interprosthetic gap. More specifically, the effect of gap size and gap location on strains in the femoral cortex was investigated and the impact of cortical thickness and bone tissue modulus was explored independently.

5.2 Materials and methods

A finite element model was created, representing a femur with implanted hip and knee prostheses (Figure 5.1). The bone was modelled as a cylinder, with inner and outer diameter of 10 mm and 20 mm, respectively; its length was set to 440 mm. The hip stem consisted of a cylindrical femoral stem with a diameter of 10 mm and a neck was added assuming a neck length of 45.5 mm,

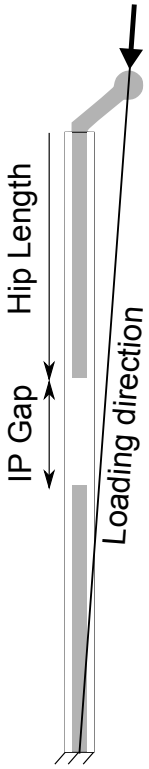

Figure 5.1: Schematic representation of the model, indicating the hip prosthesis, knee prosthesis and cortical bone. The arrow indicates the direction of the loading along the mechanical axis. The load was applied to the prosthesis head, and was oriented along a line connecting the centre of the prosthesis head and the intercondylar fossa of the femur. The length of the hip stem and the size of the interprosthetic gap were varied; all variations are indicated in table 1.

under a 40° angle with the prosthesis stem (Figure 5.1). This assembly mimics the basics of load transfer in the femoral component of a THA. The neck length was measured from the middle of the femoral head to the middle of the bone cylinder, along the neck axis. A prosthesis head with a diameter of 20 mm was added to ensure accurate load transfer. The length of the hip stem was varied from 50 to 400 mm. By including the stem of a knee prosthesis, gap sizes between 2 mm and 225 mm were created (Table 1). In order to evaluate the effect of the prostheses, a model without prostheses was created as well. For this intact case, the bone cylinder was extended with a neck length of 65 mm under a 40° angle with the bone cylinder axis. A 40 mm diameter sphere was

added to represent the femoral head. Linear elastic properties were assigned to all components of the model. Young's moduli were 220 GPa, 110 GPa and 17 GPa, for THA, TKA and bone, respectively. Poisson ratio was 0.3 for all components. These Young's moduli were selected to mimic material properties of specific prostheses used in preceding experimental tests.

		Interprosthetic gap (mm)											
		2	15	25	30	50	75	100	125	150	175	200	225
Hip prosthesis size (mm)	50	438	375	365	360	340	315	290	265	240	215	190	165
	75	363	350	340	335	315	290	265	240	215	190	165	140
	100	338	325	315	310	290	265	240	215	190	165	140	115
	125	313	300	290	285	265	240	215	190	165	140	115	90
	150	288	275	265	260	240	215	190	165	140	115	90	65
	175	263	250	240	235	215	190	165	140	115	90	65	40
	200	238	225	215	210	190	165	140	115	90	65	40	x
	225	213	200	190	185	165	140	115	90	65	40	x	x
	250	188	175	165	160	140	115	90	65	40	x	x	x
	275	163	150	140	135	115	90	65	40	x	x	x	x
	300	138	125	115	110	90	65	40	x	x	x	x	x
	325	113	100	90	85	65	40	x	x	x	x	x	x
	350	88	75	65	60	40	x	x	x	x	x	x	x
	375	63	50	40	x	x	x	x	x	x	x	x	x
	400	38	x	x	x	x	x	x	x	x	x	x	x

Table 5.1: Overview of all tested models. The columns represent different interprosthetic gaps which vary from 2 mm up to 225 mm. The rows indicate the length of the hip stem, which corresponds to the proximal distance of the interprosthetic gap. The numbers in the table represent the lengths of the knee stems. Crosses ('x') indicate configurations that are not feasible.

The tips of the hip and knee stems were modelled flat, opposed to their rounded physical appearance. Computational data (not shown) indicated that these modelling choices do not influence the stresses and strains that occur in the femoral shaft. The bone-prosthesis interface was modelled assuming complete bonding. This assumption resulted in accurate correspondence between experimental and numerical (FE) strains (Stolk et al. 2002) and is thus accepted in literature (Taylor & Prendergast 2015).
Finite element analyses were performed using Abaqus software (Abaqus 6.13, Dassault Systèmes Corp., Providence, RI, USA). The models were meshed using linear elastic hexahedral elements, type C3D8R. Convergence analysis (data not shown) showed that an element size of 1 mm was appropriate. Along the medial and lateral side of the femoral shaft the strains in the longitudinal direction were quantified (Table 5.1). Since the ultimate tensile strain for bone is lower than the ultimate compressive strain, regions with tensile strain are more prone

to fracture for all specimens modelled in this study, even when the compressive strain was higher (Bayraktar et al. 2004). This study thus focussed on tensile strain. Two specific parameters were defined to ease the evaluation of strain in the IP gap region. StrainH represents the maximal strain in the gap region; i.e., strainH is the maximum tensile strain, or compressive strain closest to zero when no tensile strains were present in the gap region). StrainL represents the minimal strain in the gap region; i.e. strainL is the maximum compressive strain, or the tensile strain closest to zero when no compressive strains were present in the gap region).
Boundary conditions representing loading along the mechanical axis, as described in Zdero et al (Zdero et al. 2008) and Speirs et al. (Speirs et al. 2007), were applied. The distal part of the model was modelled to resemble a knee, where translation and rotation were fully constrained. The proximal part of the model was constrained as well to obtain a physiological loading, as described by Speirs et al. (Speirs et al. 2007). Rotation of the prosthesis head was allowed while translation was only allowed along the line of force-direction, to mimic the restrictions of the acetabular cup on the femoral head (Figure 5.1). Loading was applied along the mechanical axis of the femur; specifically, a load of 7000 N was applied on the femoral head and was directed towards a point located in the middle of the intercondylar fossa, which resulted in compression in combination with a bending moment. A load of 7000 N was chosen since this was the highest load where none of the specimens fractured in the prior experimental tests (chapter 3). The length of the hip and knee stems were varied, as were the bone Young's modulus (E) and cortical thickness. The location and size of the interprosthetic gap were defined by the length of the hip stems and by the distance between the tips of the hip and knee stem. These incremental models were created through python coding (version 2.6.2, Python Software Foundation) starting from the model-code found in the Abaqus-model files. 132 variations of IP gap size (ranging from 2 mm to 225 mm) and location (hip prosthesis length of 50 to 400 mm) were tested (Table 1). Young's modulus and cortical thickness were varied for a model with a hip prosthesis of 150 mm and a 100 mm gap (190 mm TKA), which represents an anatomically relevant prosthesis placement. Starting from an initial tissue modulus of 17 GPa and a cortical thickness of 5 mm, 14 variations were tested independently. Specifically, a model with the initial tissue modulus was combined with variations of the (outer radius of the) cortical thickness identical to 85%, 90%, 95%, 100%, 105%, 110% and 115% of the initial thickness. Similarly, a model with the initial cortical thickness was combined with tissue moduli identical to 85%, 90%, 95%, 100%, 105%, 110% and 115% of the initial tissue modulus.

5.3 Results

All models were successfully meshed and solved. Larger gaps caused higher strains (Figure 5.2). A 100 mm hip stem with interprosthetic gaps of 25, 175 and 225 mm gaps had strainH values at the lateral side of the femur that were 13.8%, 22.5% and 23.0% higher than for the same stem with a 2 mm IP gap.

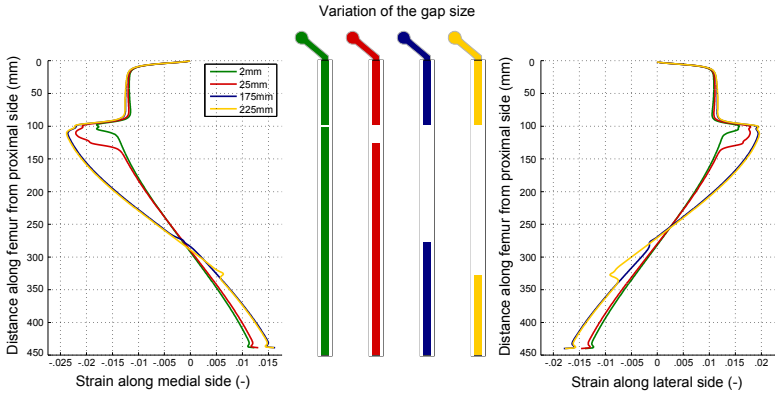

Figure 5.2: Influence of gap size on strain on the medial (left graph) and lateral (right graph) side of the femur. Larger gaps resulted in higher strains. Colours correspond to the models in the central panel, which show the varying configurations. Gaps of 2, 25, 175 and 225 mm starting at a proximal distance of 100 mm are shown. Stiffness-normalized strains can be found in appendix E.

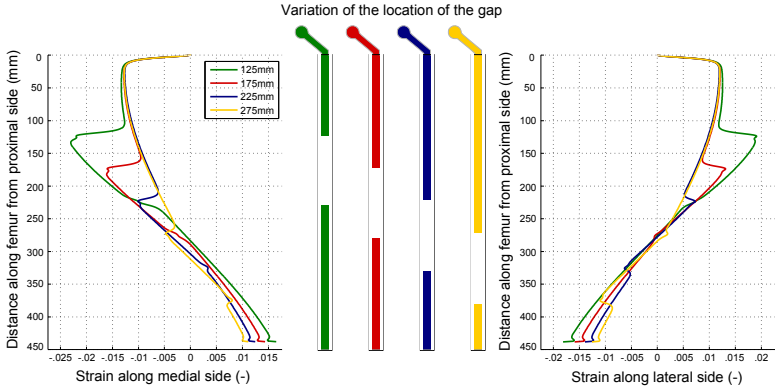

Figure 5.3: Influence of gap location on strain on the medial (left graph) and lateral (right graph) side of the femur. Smaller proximal distances, i.e. smaller hip stems, resulted in higher strains. Colours correspond to the models in the central panel, which show the varying configurations. A gap of 100 mm starting at proximal distances of 125, 175, 225 and 275 mm is shown. See appendix E.

For any hip stem, gaps larger than 50 mm had nearly identical strain patterns and peak tensile strains (strainH) in the gap region (Figure 5.2). Strain patterns at the medial side of the femur had identical shapes as those at the lateral side, but were compressive.
Consequently, the influence of gap size on peak compressive strains (strainL) at the medial side of the femur is equivalent to the description above. Strain patterns at the lateral side of the femur showed that strains in the gap region were either tensile (positive), compressive (negative) or both, dependent on the location and size of the gap (Figure 5.2 and 5.3). For most gap sizes and locations, strainH in the gap region was positive, thus tensile. These tensile strain maxima were lower when the gap was located more distally (Figure 5.3). E.g. for a gap of 100 mm, strainH in the lateral gap region was 0.0172, 0.0119, 0.0067 and 0.0020 when the proximal distance (hip stem) was 125, 175, 225 and 275 mm, respectively. Few gaps, located around the knee condyle, were subjected to only compressive (negative) strains. E.g. the entire gap region of all gap sizes with a 350 mm hip prosthesis (or larger) was subjected to compressive strains, as indicated by negative strainH and strain (Figure 5.4).

Along the femur, strains were highest in the interprosthetic gap region. The proximal part of the gap region experienced the highest strains. Yet, for all models with an IP gap, the maximum strains were lower than in the model representing the intact bone without prostheses (Figure 5.5).
Cortical thickness and bone tissue modulus both inversely correlated with the strains in the bone (Figure 5.6). Cortical thickness had a stronger effect on strain than the bone tissue modulus. E.g. a 10% decrease in E-modulus resulted in a 20% increase in the peak tensile strain (strainH), whereas a 10% decrease in cortical thickness more than doubled the peak tensile strain.

5.4 Discussion

It has been hypothesised that small interprosthetic (IP) gaps act as stress risers and may lead to increased fracture risk (Soenen et al. 2011, Weiser et al. 2014). Our study rejected these hypotheses. We found that, for the loading conditions used in this study, large IP gaps caused higher strains than smaller IP gaps, yet, in all configurations the strains were lower than those in the model without prostheses; hence, we did not find a stress riser effect.
Cortical thickness did have a clear influence on maximal strain, where a small decrease in cortical thickness greatly influenced peak strain and consequently, fracture risk. This finding is in agreement with previous work by Iesaka et al and Weiser et al.

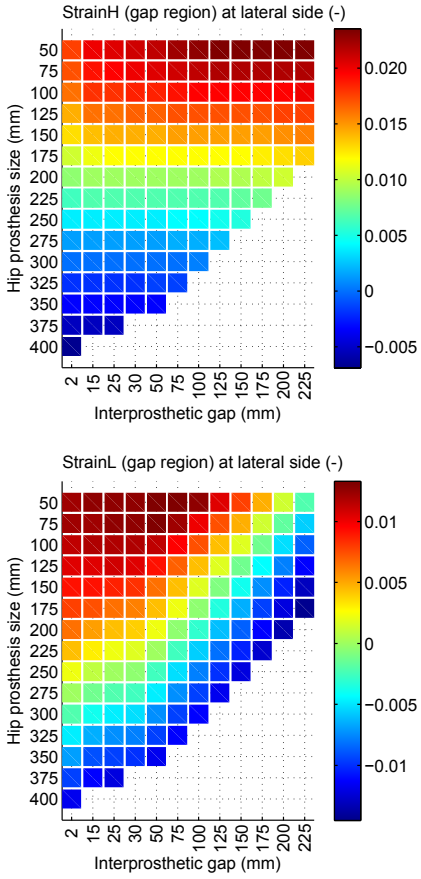

Figure 5.4: Influence of gap size and gap location on strains in the gap region of the bone. For each combination of prosthesis size and IP gap length, both StrainH (top graph) and StrainL (bottom graph) in the gap region are shown. StrainH represents the highest absolute value of the tensile strain, or lowest absolute value of the compressive strain. StrainL represents the opposite. Positive strains correspond to tensile strain, negative strains to compressive strains. Larger gaps resulted in higher peak tensile strains, as did smaller hip stems. Larger gaps and longer hip prostheses also influence the distal regions of the model (bottom graph).

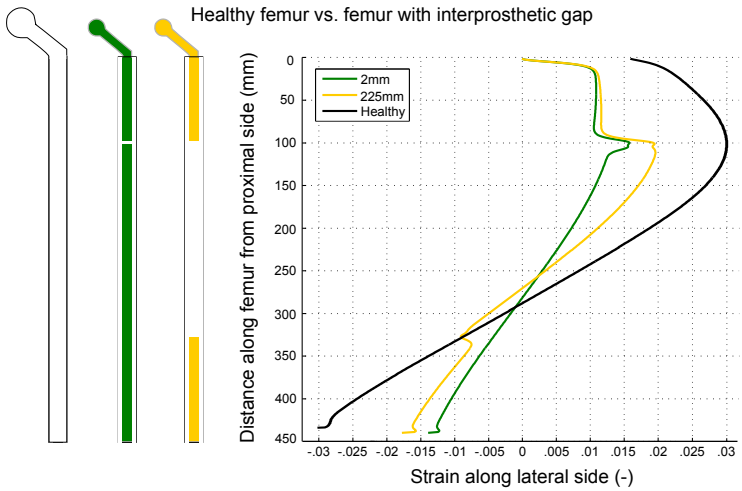

Figure 5.5: Comparison of a healthy femur to a femur with interprosthetic gap. Presence of ipsi-lateral hip and knee prosthesis lowers the femoral strains compared to the strain of a healthy femur. Colours correspond to the models in the central panel, which show the varying configurations. A healthy femur and an IP gap of 2 mm and 225 mm are shown.

The former used a simplified experimental model (cylindrical Sawbone material) and a simplified FE model (cylinder shape to represent the cortex) which were both loaded by cantilever bending (Iesaka et al. 2005). The latter conducted an experimental study with human femur specimens loaded under four-point bending (Weiser et al. 2014). Both studies showed that for well-fixated prostheses, interprosthetic distance did not influence fracture risk, and that cortical thickness was an important variable influencing femoral strain (Iesaka et al. 2005, Weiser et al. 2014).
The effects of gap size and location can be understood by evaluating the deformation of the model. The loading along the mechanical axis combined with the applied distal boundary conditions resulted in a bending moment with a maximum at the proximal end of the femur while linearly decreasing to zero at the distal end of the femur. In regions where a prosthetic stem is present the bending rigidity will be higher than in the gap region. As a consequence, the bending deformation and thus strains will be lower in these regions (Figure 5.2 and 5.3), matching the findings of the study by Soenen et al. (Soenen et al. 2013). The highest strains will be found in the gap region. The maximum value will be found at the location of the tip of the hip stem because the bending moment is larger here than at the tip of the knee stem. Hence, the

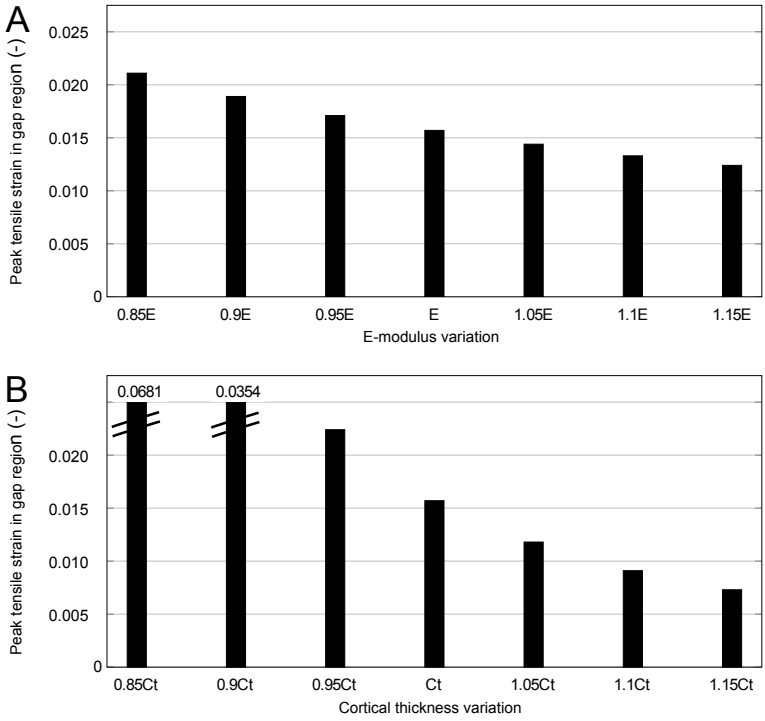

Figure 5.6: Peak tensile strain in the interprosthetic gap region as a function of (a) bone tissue modulus, and (b) cortical thickness. The model combined a hip stem of 150 mm with a knee stem of 190 mm, resulting in a 100 mm interprosthetic gap. This represents an anatomically relevant ipsilateral primary prosthesis placement. Strains are more sensitive to variation of cortical thickness than to variations of bone tissue modulus.

model indicates that fracture would always initiate at the tip of the hip stem, regardless of the IP gap. Indeed, this was found in our previous experimental study (Quirynen et al. 2017). The gap, as such, is the weakest section of the model.

Larger gaps resulted in a more pronounced bending deformation compared to smaller gaps. Notwithstanding the more pronounced bending deformation and resulting strain increase, peak tensile strains (strainH) reached a plateau for gaps larger than 50 mm. Thus, there is a similar risk of fracture for gaps larger than 50 mm. This is consistent with the findings of Soenen et al. (Soenen et al. 2013) who showed that, for a femur under gait loading, gaps varying from 50 to 150 mm did not influence the risk of fracture of the femur.

More distal gap locations (longer hip prosthesis stems) resulted in lower strainH values. This is due to the bending moment that decreases to zero towards the distal end of the femur (Figure 5.4). For gaps located in the distal half of the femur, negative strainL values indicated compressive strains. For small gaps, strainL values were tensile (positive), since the gap only spanned the proximal part of the femur. Larger gaps showed increasing peak compressive strains (negative strainL values increased), as the gaps spanned more distal regions of the femur.

Variation of the bone tissue modulus and of the cortex thickness provided insight in the fracture risk of interprosthetic gaps in a variety of bone types. In FE modelling to this date, osteoporotic bone was only modelled by a reduced E-modulus (Soenen et al. 2013), or by adapting the cortical thickness (Iesaka et al. 2005). This is the first study that evaluated variations in E-modulus and cortical thickness in one model. Our simulations showed that bone with a reduced Young's modulus (i.e. osteoporotic bone) experienced higher bending deformation, hence higher strains and higher fracture risk than bone with a normal Young's modulus. Variations of the cortical thickness had a much more pronounced influence on the strains in the femur than did the variations of bone tissue modulus. Hence, a small decrease in cortical thickness will lead to larger increase in strain than an identical (percentage-wise) decrease in bone tissue modulus (Figure 5.6), confirming earlier data (Iesaka et al. 2005, Soenen et al. 2013).

Although the simplified model allowed, for the first time, to test a large combination of gap sizes combined with different gap locations, there are some limitations to this study. First, the use of a simplified cylindrical model does not take the full anatomy into account. The growing cortical thickness from metaphysis to diaphysis for example is not modelled, even though, as described above, the cortical thickness played an important role in femoral strains. Yet, the interprosthetic gap is mostly located in the diaphysis, where cortical thickness is rather constant. Second, the cylindrical shape of the model, the lack of trabecular bone and the extreme loading condition of 7000 N lead to maximal stresses that exceeded the ultimate strain of healthy bone (Bayraktar et al. 2004). However, we were mainly interested in comparing different gap sizes, and we do not believe that lowering the load would change the outcome of this study. Third, we assumed perfect bonding between the stems and the bone. Since IP gaps mainly occur in revision surgeries, and revision surgery mainly uses cemented stems, we did not model loose stems.

A last limitation is that only one loading condition was used. As we used a physiologically relevant load case, combined with physiologically relevant boundary conditions, and as we used the data in a comparative way only, we do not expect to find different conclusions when more complicated loading would have been applied. Also, loading along the mechanical axis, or so-called

isometric loading (Moazen et al. 2011) was applied since it is a well-accepted testing protocol which represents the major compressive loading at the hip joint (Soenen et al. 2013, Zdero et al. 2008, Lever et al. 2010, Cristofolini et al. 2010, Schileo et al. 2014, Ali et al. 2014). We do acknowledge that addition of the abductor force, which is not included in our study, can change the bending moment at the interprosthetic gap, but do not believe that this would change the outcome of this comparative study.

5.5 Conclusion

In conclusion, we have shown that not only the gap size, but also the gap location influences the strains in the femur. The interprosthetic gap does not act as a stress riser, and smaller gaps are favourable. The size of the femoral cortex can greatly influence strains of the femur. The bone tissue modulus also affects bone strains, but only to a smaller extent. This study modelled osteoporotic bone properties which lead to an increase in the structural stiffness difference between the bone-prosthesis section and the gap section of the femur model. Since this further increased peak tensile strains in the gap region, IP gaps in osteoporotic bone are more prone to failure than IP gaps in healthy bone.

Chapter 6

Ipsilateral hip and knee implants do not increase bone fracture risk immediately after prosthesis placement.

Thomas Quirynen[1], Jean-Pierre Simon[2], Jos Vander Sloten[1], G. Harry van Lenthe[1]

[1] Biomechanics Section, Mechanical Engineering Department, KU Leuven, 3001 Heverlee, Belgium

[2] Orthopaedic Surgery Department, University Hospital Leuven, 3212 Pellenberg, Belgium

Submitted

See appendix C for a short overview on finite element modelling.

Abstract

Objectives
Current trends predict an increase in patients with both hip and knee prostheses. These ipsilateral prostheses create an interprosthetic gap which has been hypothesised to act as a stress riser. This work aimed to investigate the influence of clinically relevant parameters on bone strains, while using an anatomically relevant model and anatomical loading conditions. Parameters were hip prosthesis neck length, stem length and interprosthetic gap size.
Methods
We created an anatomically relevant finite element model. Several hip prostheses were digitally implanted and prosthesis neck length, gap size and gap location were varied. Three loading conditions were applied mimicking load along the mechanical axis of the femur, walking and stair climbing.
Results
We found that longer prosthesis neck lengths increased femoral strains, as did larger gaps. More distal gaps had lower strains. Of these parameters, gap size had the strongest effect. Bone strains in a model with a hip prosthesis only were always higher than the strains in models with an additional knee implant.
Conclusions
We conclude that the ipsilateral placement of a knee prosthesis does not act as a stress riser immediately post-surgery. Gap size, prosthesis neck and stem length all influenced femoral strains. Gap size had the largest influence, and small gaps did not act as a stress riser.

Keywords

Femur, interprosthetic fracture, finite element analysis, biomechanics, implants

6.1 Introduction

Projections of primary and revision hip (THA) and knee (TKA) arthroplasty surgeries predict a steady increase in number (Kurtz et al. 2007). Hence, the amount of patients with ipsilateral THA and TKA is destined to rise as well. Fractures in between ipsilateral THA and TKA form a serious clinical concern (Mamczak et al. 2010, Ochs et al. 2013, Platzer et al. 2011, Solarino et al. 2014). Revision surgeries often replace the affected prosthesis with a longer prosthesis, which may increase fracture risk further (Hou et al. 2011, Iorio et al. 2008).
In ipsilateral placement of THA and TKA the distance between the distal tip of the hip stem and the proximal tip of the knee stem is often referred to as the interprosthetic (IP) gap. There is ongoing debate on the influence of an IP gap on the risk for femoral fractures. On the one hand, IP gaps are considered to act as stress risers increasing fracture risk, especially for small gaps. This view is commonly found among orthopaedic surgeons (Soenen et al. 2011, Weiser et al. 2014). On the other hand, there is cumulating evidence that IP gaps do not pose a problem (Iesaka et al. 2005, Lehmann et al. 2012, Lehmann et al. 2010, Quirynen et al. 2017, Soenen et al. 2013, Weiser et al. 2014). More specifically, in an experimental study it was found that fracture strength in human cadaver femora with ipsilateral THA and TKA was significantly higher than in femora with THA only (Lehmann et al. 2012). In a study using synthetic femora, loaded along their mechanical axis, we also found that constructs with ipsilateral prostheses required higher loads to fracture (Quirynen et al. 2017). Yet, the clinical relevance of the applied four-point bending load in the first study is questionable, whereas the loading condition used in the latter study may be too simplified.
Some data on the influence of the size of the IP gap have been presented. In an experimental study using human cadaver femora three different gap sizes (35, 80, 160 mm) were compared. Little difference in fracture strength was noted between these three gap sizes (Weiser et al. 2014). In an experimental study using synthetic femora we found that small gaps (0 cm) had higher loads to failure than femora with larger IP gaps (15, 30, 50, 100, 150, 200 mm) (Quirynen et al. 2017). A computational study using a simplified cylindrical model of a femur demonstrated that gap size had no effect on peak femoral tensile strains (Iesaka et al. 2005). Yet, the loading conditions were four-point bending, loading along the mechanical axis of the femur, and cantilever bending for the first, second, and third study respectively; hence, the clinical relevance may be limited. A more comprehensive loading analysis, mimicking one instance of gait as well as fall loading and four-point bending, was simulated in a computational study (Soenen et al. 2013). It was found that gap size did not influence fracture risk; yet, gaps smaller than 50 mm were not included.

In summary, the available biomechanical and experimental data related to IP gaps are fragmented, such that clear conclusions on the role of the IP gap cannot be drawn. Therefore, the aim of this study was to enhance our understanding on how clinically relevant parameters affect strain in the IP gap. Specifically, we aimed at quantifying the effects of (1) neck length of a THA, (2) the size of the IP gap and (3) the location of the IP gap.

6.2 Materials and methods

The 'THA only' reference model
A 3D model of a synthetic bone (Left femur Sawbone #3403, Pacific Research Laboratories, Mälmo, Sweden) was obtained by computed tomography scanning (Fig. 6.1). The image data were segmented into cortical bone, trabecular bone and intramedullary space based on Hounsfield units and converted into a 3D model using dedicated software (Mimics Research 18.0, Materialise, Leuven, Belgium). The surface of a primary THA (14 cm C-stem, Depuy J&J, Warsaw, Indiana) and revision THA (20 cm Exeter, Stryker, Kalamazoo, Michigan) were captured by laser-scanning (GOM Atos II, GOM mbH, Braunschweig, Germany) and stored in STL-format. THA placement was simulated: femoral head and neck resection was performed virtually, and the hip prosthesis was placed following the AO guidelines (AO Foundation 2016). The centre of the THA head was matched to the centre of the healthy femoral head to ensure native anteversion. Prosthesis placement was verified by a trained orthopaedic surgeon.

		P1	**P2**	**P3**	**P4**
Mechanical axis	$\mathbf{F}_x$	-803.3	0	0	0
	$\mathbf{F}_y$	6953.7	0	0	0
	$\mathbf{F}_z$	0	0	0	0
Walking	$\mathbf{F}_x$	-451	540.9	-7.5	0
	$\mathbf{F}_y$	274	-127	-154.6	0
	$\mathbf{F}_z$	1916	-674.6	776.6	0
Stair climbing	$\mathbf{F}_x$	-502	703	-18.6	-74.5
	$\mathbf{F}_y$	513	-301.5	-189.7	-335.4
	$\mathbf{F}_z$	2001.5	-654.7	1144	2262.3

Table 6.1: Applied loads (in Newton) on the four load application points based on Heller et al. 2005 (Walking and Stair climbing). Direction of loading is consistent with the coordinate system of Figure 6.1.

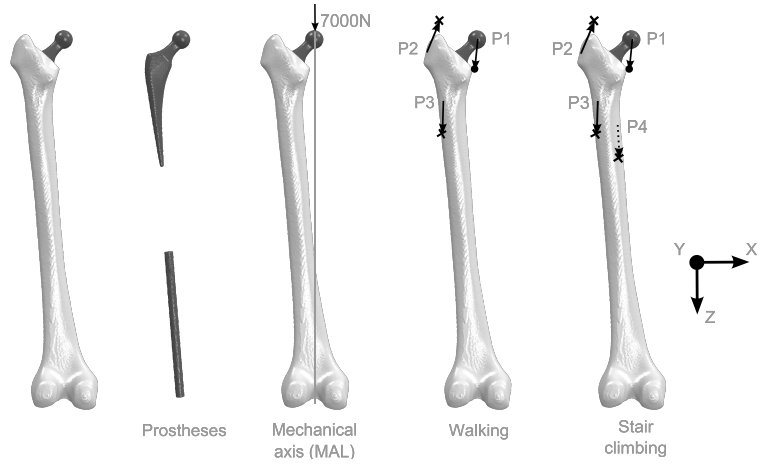

Figure 6.1: Representation of the model. Three load cases were applied; load along the mechanical axis of the femur, walking and stair climbing. Load application points for anatomical loading were according to Heller et al. 2005: hip prosthesis head (P1), abductor, tensor fascia latae and illio-tibial tract (P2), vastus lateralis (P3) and vastus medialis (P4). Load components along the axes of the coordinate system are shown in Table 6.1.

The models were meshed using quadratic tetrahedral elements, type C3D10. The novel Voronoi meshing algorithm provided a uniform mesh quality (3-matic Research 11.0.0.33 alpha test version, Materialise, Leuven, Belgium). Convergence analysis (data not shown) showed that an element size of 1.25 mm was appropriate. Material properties were assigned to all elements. Specifically, cortical bone was modelled transversely isotropic (Soenen et al. 2013): $E_1 = E_2 = 11.5$ GPa, $E_3 = 17$ GPa, $\nu_{12} = 0.51$, $\nu_{23} = \nu_{13} = 0.31$. The third axis was parallel to the anatomical axis of the femur (Cherian et al. 2014). Trabecular bone was considered linear isotropic (Soenen et al. 2013): $E = 2.13$ GPa, $\nu = 0.3$. Since cemented prostheses were modelled, the intramedullary space was assumed to be filled with cement: $E = 2.13$ GPa, $\nu = 0.3$ (Soenen et al. 2013). The THA used in this research was made from Cobalt Chrome and was considered linear isotropic: $E = 220$ GPa, $\nu = 0.3$. The prosthesis was modelled to be fully fixed to the bone to simulate the use of bone cement. Finite element analysis was performed using dedicated software (Abaqus 6.13, Dassault Systèmes Corp., Providence, RI, USA). Three different loading conditions were applied: Mechanical axis loading (MAL), walking (W) and stair climbing (SC) (Fig 1.). For MAL, boundary conditions as described in Zdero et al. (Zdero et al. 2008) and Speirs et al. (Speirs et al. 2007), were applied. In the distal part of the model translation and rotation were fully constrained. Rotation of

the prosthesis head was allowed while translation was only allowed along the line of force-direction. A load of 7000 N was applied on the femoral head and was directed towards a point located in the middle of the intercondylar fossa. This corresponds to loading along the mechanical axis of the femur (Cherian et al. 2014). A load of 7000 N was chosen since this was the highest load where none of the specimens fractured in the prior experimental tests (chapter 3). For both walking and stair climbing, boundary conditions and load application points as described in Heller et al. (Heller et al. 2005) were applied. The distal part of the model was modelled identical as described above while the proximal part was not constrained. Four load application points were defined (to model walking, only the first three points were needed). The first point represented the centre of the hip prosthesis head (P1). The three other points represented relevant muscle attachment regions: abductor, tensor fascia latae and illio-tibial tract (P2), vastus lateralis (P3) and vastus medialis (P4). Force components (Table 1) of all three loading conditions were orientented based the coordinate system shown in Figure 1. As outcome parameter the strains in the femoral cortex were quantified. Since the ultimate tensile strain for bone is 30% lower than the ultimate compressive strain (Bayraktar et al. 2004), regions with tensile strain are more prone to fracture (Bayraktar et al. 2004); hence, a strain-based criterion focussing on tensile strain was used (Schileo et al. 2008). Specifically, the mean of the 5% highest strains in the cortical bone was quantified and labelled ϵ_{95}.

Neck length
Load application points for the centre of the hip prosthesis head were moved for all three loading conditions to mimic change of neck length. For both primary and revision prosthesis STL models, the load application point was moved 5 mm in the medial and lateral direction along the neck axis, representing a 5 mm shorter and 5 mm longer neck length. The revision THA STL had a 22% longer neck length than the primary THA STL: 45 mm vs 55 mm for primary and revision THA respectively.

IP gap size
A TKA stem (Profix, Smith&Nephew, Memphis, Tennessee) was modelled as a cylinder and placed into the femur model to create an IP gap. Prior research showed that the stem features (notches and slit at the stem tip) did not influence femoral strains (Quirynen et al. 2014). TKA stem length was varied to create gaps of 15, 30, 50, 100 and 150 mm in combination with the 140 mm primary THA and the 200 mm revision THA. A 0 mm gap in combination with a revision THA and a 200 mm gap in combination with a primary THA were added to span all relevant gap sizes. The size of the interprosthetic gap was defined by the distance between the distal tip of the hip stem and the proximal tip of the knee stem. These IP gap models were prepared for FE analysis identically as

described above. Linear-elastic and isotropic material properties were assumed for the TKA (E = 110 GPa, $\nu = 0.3$), representing titanium. The TKA was modelled to be fully fixed to the bone.

IP gap location
To quantify the influence of the location of the IP gap on femoral strains the THA revision stem was digitally lengthened using dedicated software (3-matic Research 10.0, Materialise, Leuven, Belgium). This software allowed cutting of the stem of the prosthesis model to adapt its length. The revision THA stem length (original length of 200 mm) was elongated to obtain THA lengths of 220, 240 and 260 mm which were the stem lengths used in our previous experimental study (Quirynen et al. 2017). Gaps of 0, 15 and 30 mm were created in combination with the standard 200 mm revision THA and the lengthened revision THAs.

6.3 Results

All models were successfully meshed and solved. Strain patterns changed when comparing MAL to the two anatomical loads W and SC. Strain patterns for stair climbing shifted towards the frontal side of the femur, compared to the strain patterns for MAL which were located at the lateral side of the femur.
Qualitative analyses showed that THA neck length influenced femoral strains (Fig. 6.2). For a model with a 100 mm gap, shorter neck lengths (-5 mm) showed lower strains in the IP gap ranging from a reduction of 35 to 42% for MAL and 13% for W and SC, respectively. Longer neck lengths (+5 mm) showed higher strains in the IP gap ranging from a increase of 10% to 14% for MAL and 11% for W and SC, respectively (Table 6.2). Similar findings were found for all other gap sizes.

	Mechanical axis			**Walking**			**Stair Climbing**		
Neck length	**-5 mm**	**ref**	**+5 mm**	**-5 mm**	**ref**	**+5 mm**	**-5 mm**	**ref**	**+5 mm**
Primary THA	5.49	9.46	10.82	2.83	3.24	3.64	4.63	5.31	5.89
Revision THA	7.55	11.66	12.84	3.28	3.74	4.15	5.33	6.04	6.66

Table 6.2: Strain parameter ϵ_{95} (10^{-3}), as the mean of the highest 5% strains in the cortical bone. A 100 mm gap was modelled. Initial neck lengths were 45 mm vs 55 mm for primary and revision THA respectively. For both primary and revision THA, shorter prosthesis neck length showed lower ϵ_{95} and longer neck length showed higher ϵ_{95}.

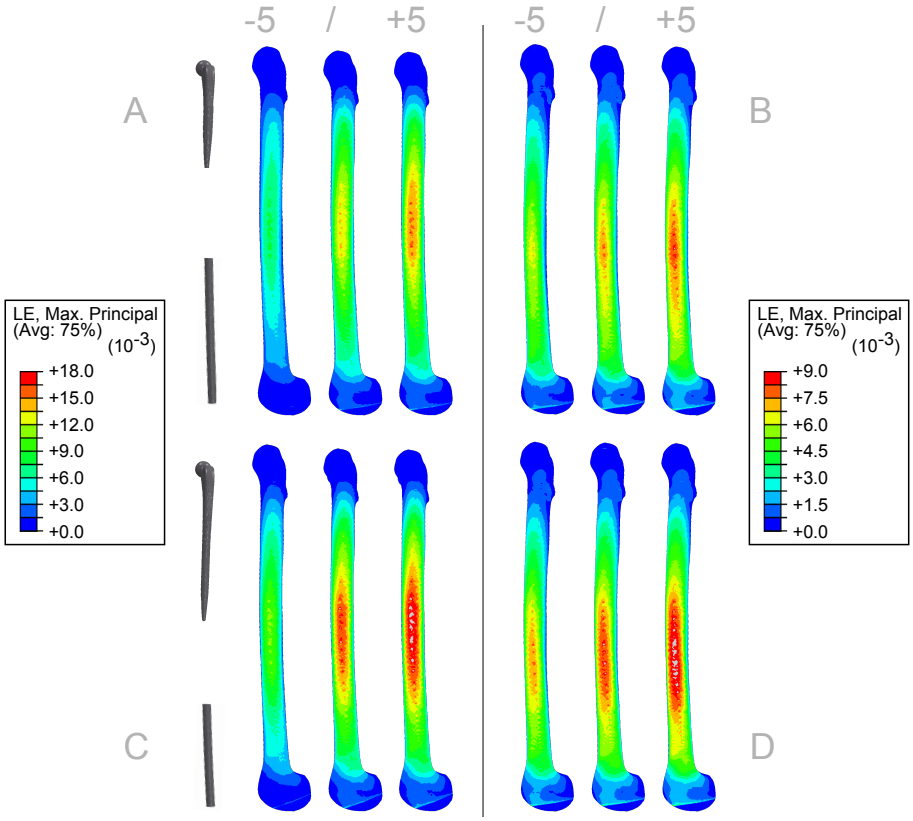

Figure 6.2: Surface strains at the lateral side of the femur with a 100 mm gap. Model with a primary THA loaded under (A) MAL and (B) SC. Identically, model with a revision THA loaded under (C) MAL and (D) SC. For both prostheses types, shorter prosthesis neck length (-5 mm) showed lower strains in the IP gap and longer neck length (+5 mm) showed higher strains. Initial neck lengths (/) were 45 mm vs 55 mm for primary and revision THA respectively. Findings similar to the SC load were found for the load case mimicking walking.

For models with an interprosthetic gap, strains were highest in the gap region. Maximal strains were located in the proximal region of the gap for MAL loading and were located more distally in the gap for the anatomical loading conditions W and SC. For all models with THA and TKA, ϵ_{95} was lower than for a THA only model (Table 6.3). Larger IP gaps caused higher strains in the gap region for both hip prostheses and all loading conditions (Fig. 6.3).

	Gap size [mm]	0	15	30	50	100	150	200	THA Only
Primary THA	Mechanical axis	/	8.15	8.42	8.65	9.46	10.11	10.52	10.62
	Walking	/	3.10	3.13	3.16	3.24	3.32	3.42	3.46
	Stair climbing	/	5.08	5.13	5.15	5.31	5.45	5.57	5.60
Revision THA	Mechanical axis	10.06	10.29	10.47	10.91	11.66	12.03	/	12.04
	Walking	3.52	3.54	3.56	3.62	3.74	3.84	/	3.85
	Stair climbing	5.69	5.72	5.73	5.85	6.04	6.17	/	6.18

Table 6.3: Strain parameter ϵ_{95} (10^{-3}), as the mean of the highest 5% strains in the cortical bone for models with an interprosthetic gap. Stem length of the primary and the revision THA was 140 mm and 200 mm respectively. Larger gaps resulted in higher ϵ_{95} than smaller gaps. ϵ_{95} in the 'hip only' model was higher than in all 'hip and knee' models.

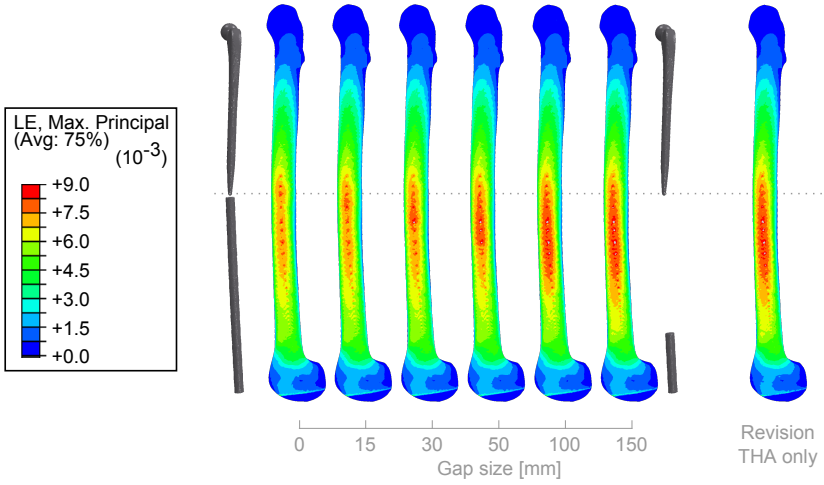

Figure 6.3: Surface strains at the lateral side of the femur, loaded mimicking stair climbing. Larger gaps resulted in higher strains than smaller gaps. Maximal strains were located in the gap region. Strains in the 'hip only' model were higher than in all 'hip and knee' models. Similar findings were found for models with a primary THA and for the load cases mimicking loading along the mechanical axis and walking.

More distal gaps showed lower ϵ_{95}. Gap sizes of 0, 15 and 30 mm modelled with the elongated revision prostheses had lower ϵ_{95} than the same gaps modelled with the 200 mm revision prosthesis (Fig. 6.4, Table 6.4). Similar findings were found for the load cases mimicking walking and stair climbing.

		ϵ_{95} **(200 mm THA)**	ϵ_{95} **(more distal gap)**
Change in gap	20 mm	10.29	10.21
location (more distal)	40 mm	10.06	9.58
compared to 200 mm THA	60 mm	10.47	9.63

Table 6.4: Strain parameter ϵ_{95} (10^{-3}), as the mean of the highest 5% strains in the cortical bone for models with an interprosthetic gap loaded along the mechanical axis. For three gap sizes, a change in gap location was modelled. Gaps were modelled with a 200 mm revision THA and a lengthened revision THA respectively. More distal gaps had lower ϵ_{95}. Similar findings were found for the load case mimicking walking and stair climbing.

6.4 Discussion

Small interprosthetic gaps have been hypothesised to increase fracture risk, due to their stress riser effect (Soenen et al. 2011, Weiser et al. 2014). This study rejects this hypothesis. The results of this study showed that smaller gaps had lower strains than large gaps, and that a model with ipsilateral hip and knee prostheses had lower strains than a model with a hip prosthesis only. Hence, ipsilateral prosthesis placement does not act as a stress riser, nor increases fracture risk. In regions where a prosthetic stem is present the stiffness was higher, thus bending deformation was lower than in the gap region. As a consequence, strains in the prosthetic regions were lower than in the gap region, similar as described by Soenen et al. (Soenen et al. 2013). Hence, fracture is expected to occur in the gap region, just below the THA tip where strains were highest; indeed, this was the location where we found fracture initiation in an experimental study (Quirynen et al. 2017). For both anatomical loading conditions, strain maxima were located more distally in the gap due to a change in resulting moment compared to MAL load. A longer neck length created a larger lever arm and consequently increased the resulting moment leading to larger ϵ_{95}. Vice versa shorter neck lengths had lower ϵ_{95}. This effect is also noticeable when comparing the primary THA to the revision THA. Since the neck length of the revision THA is 10 mm longer than the primary THA neck length, ϵ_{95} for a bone with revision THA will always be higher than that of

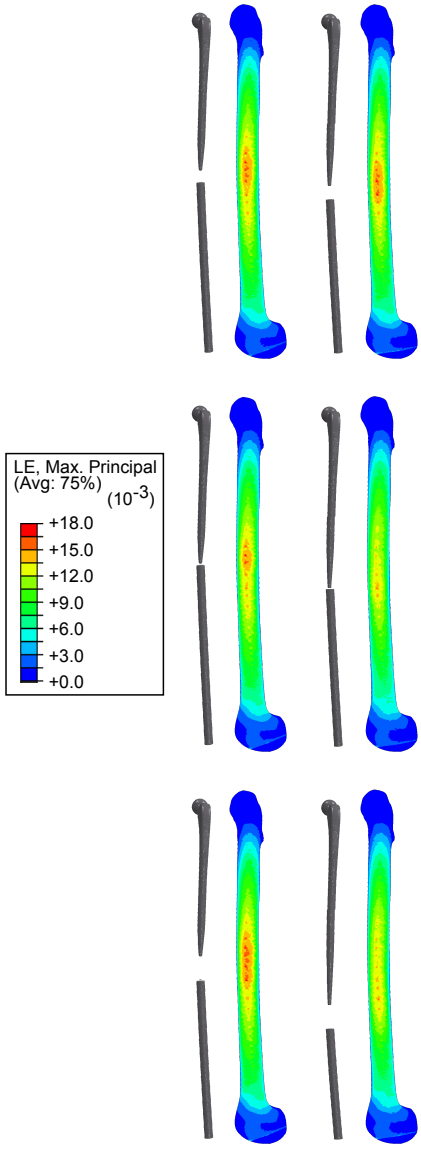

Figure 6.4: Surface strains at the lateral side of the femur, loaded along the mechanical axis. Gaps were modelled with a 200 mm THA (left) and a lengthened THA respectively, increasing the distal location with 20, 40 and 60 mm (right). Distal gaps showed lower strains in the IP gap. Similar findings were found for the load case mimicking walking and stair climbing.

same bone with a primary THA. For IP gaps, larger gaps led to larger zones of low stiffness compared to the regions where a prosthesis was present. These low stiffness regions had higher deformations thus higher ϵ_{95}, and strain patterns showed an increased region that was affected by high strains (Fig. 6.3). Hence, small IP gaps do not increase fracture risk, which matches the findings of our earlier studies (Quirynen et al. 2017, Quirynen et al. 2014) and those of Soenen and al (Soenen et al. 2013). Since more distal gaps were created with a longer hip prosthesis stem, and Young's modulus of the hip prosthesis stem is twice as high as the knee prosthesis stem, the overall stiffness of the model increased for more distal gaps. A stiffer model, as discussed above, led to lower strains. Anatomical loading caused torsion and bending in the sagittal plane, while MAL caused bending only. The addition of a torsion moment towards the frontal side of the femur caused the strain pattern for SC to shift accordingly (Fig. 6.2).

This anatomical model allowed for modelling of three important clinical parameters (neck length, IP gap size and location) and quantified their effect on femoral strains. As such, it offers a clear conclusion on the role of the IP gap. Still, there are some limitations to this study. First, we did not perform cadaver specimen experiments neither conducted an in vivo follow-up study but decided to use a finite element model instead. Finite element analysis is commonly used to replace experimental set-ups (Schileo et al. 2014, Soenen et al. 2013). It allowed for detailed adaptation of the bone and prosthesis properties (length, material, etc) and gave detailed insight in the strain patterns and location of the maximal strains, without high specimen cost connected to experimental research. Cadaver specimens have the downside of bone variability, and strain measurement in vivo is not possible. Also, the IP gap is mainly prevalent in elderly patients. Their advanced age and the existing co-morbidities will undoubtedly make it difficult to reach clear conclusions based on an in vivo study. Second, bone remodelling is not taken into account in this FE model; hence, this study addresses the immediate post-operative situation only. Third, we did not quantify the role of the cortical wall thickness. Yet, in our previous work we found that the differences in strain between gap sizes and location remains the same irrespectively of the cortical wall thickness (Quirynen et al. 2014). Fourth, we filled the intramedullary space with cement to simulate placement of cemented prostheses. Since the intramedullary space is located close to the neutral line of the model, the bending rigidity and resulting strains are only slightly influenced. The findings of this study can thus be expanded to uncemented press-fitted or ingrown prostheses. Fifth, our prostheses were modelled as fully fixed to the bone, as interprosthetic gaps often are the result of revision surgeries where cemented stems are used.

6.5 Conclusion

We conclude that, in an immediate post-surgery situation, longer neck length increased femoral strains. Furthermore, larger gaps resulted in higher femoral strains than smaller gaps, whereas gaps located more distally resulted in lower strains. Gap size had a stronger effect than gap location. For all models with a hip and knee prostheses the femoral strains were lower than for a model with a hip prosthesis only, hence, the placement of a TKA did not act as a stress riser. We hypothesize that in patients a bone adaptive response could occur, leading to decreased bone quality and an increased risk for fracture; this may explain the clinical fear for introducing small interprosthetic gaps. Addition of bone remodelling simulations to the FE model could offer insight in the long-term behaviour of the IP gap size and location hence should be investigated in a follow-up study.

Chapter 7

General discussion

This chapter offers an overview of all previous chapters, followed by a discussion of the research aims posed in chapter 1. A global conclusion subsequently summarizes this thesis. Finally, directions for future work are suggested.

7.1 Chapter summary

Chapter 2 introduced the concept of the interprosthetic (IP) gap between a hip and knee prosthesis. Based on current and future trends in orthopaedic surgery, an exponential increase in amount of patients with an interprosthetic gap was predicted and the challenging procedure of IP fracture reconstruction was defined. Next, an overview was given of the main causes leading to prosthesis placement. Commonly used prosthesis types were explained and existing fracture reconstruction constructs and guidelines for fracture treatment were outlined. The clinical hypothesis and intuitive fear amongst surgeons concerning (small) interprosthetic gaps were mentioned. The state of the art in biomechanical testing concerning the interprosthetic gap was discussed as well as its limitations. The state of the art was discussed for both existing experimental and finite element literature. The most common limitation was that only part of the clinically relevant range of interprosthetic gap sizes was modelled, and often a non-anatomical loading protocol of limited clinical relevance was selected. Other clinically relevant parameters such as IP gap location or prosthesis shape have not yet been explored. This thesis aimed to overcome these limitations by modelling the full range of IP gap sizes, while focusing on gaps below 50 mm, since the clinical hypothesis is that (especially small) IP gaps increase femoral fracture risk. IP gap location, bone mechanical properties and prosthesis shape were varied as well. Finite element modelling, combined with experimental testing, allowed to investigate the clinical relevant parameters stated above.

Chapter 3 discussed the results of an experimental set-up identifying the influence of the interprosthetic gap size on femoral fracture load. The clinical hypothesis that small IP gaps increase fracture risk was investigated. Three parameters were selected to identify sub-optimal gap sizes: fracture load, work to failure and deflection at failure. Fracture morphology was monitored as well to better understand fracture mechanics of interprosthetic gaps. A validated synthetic bone specimen was preferred over the use of cadaver bone. Cadaver bone can only be compared contralaterally (left and right femur of the same cadaver), as the variability of femur properties can be large. The benefit of the synthetic bones (Sawbones) is that they offer a stable base-line for comparative research, have low variability and approximate the properties of healthy cadaver bone (Papini et al. 2007, Chong et al. 2007, Heiner 2008, Cristofolini et al. 2010). Additionally, notwithstanding the lack of visco-elasticity, synthetic bones perform within the range of healthy human bone for fracture morphology in the diaphysis of the femur (Gardner et al. 2010). These specimen were implanted with a cemented primary or revision hip prosthesis only to create 12 control specimens. Consequently, 51 specimens with gaps of 0, 15, 30, 50, 100, 150 and 200 mm were created by implanting both a cemented hip and

knee prosthesis. Specimens were loaded to failure mimicking loading along the mechanical axis (MAL) which consisted of both compressive loading and bending along the mechanical axis of the femur. The abductor force was not modelled, as is common in experimental studies (Table 2.1). Some studies have emphasized that the abductor force should be modelled (Stolk et al. 2001). Yet, the boundary conditions implemented in our study (movement along the mechanical axis only (Speirs et al. 2007)) countered the bending due to the lack of the abductor force and resulted in physiological bending as well. Additionally, the results of chapter 6 showed that the inclusion of the abductor force (Heller et al. 2005) did not influence the outcome of our comparative study. These results indicated that, for the loading conditions used in this study, small gaps required higher fracture load. Creation of an IP gap did not increase fracture risk. The most prevalent fracture morphology was that of a medial butterfly. Even though non-cemented prostheses might change the load transmission to the femur and might create local stress risers, we do not expect a different outcome when the influence of gap size is compared with these non-cemented prostheses.

Chapter 4 outlined the results of an experimental study that focused on the reconstruction of fractured specimens with an interprosthetic gap. A fracture reconstruction protocol was drafted based upon experimental studies on peri-prosthetic fractures and clinical studies on interprosthetic fractures. A previous study identified a long fracture fixation plate, connected with screws, as the optimal fracture fixation method (see Appendix D). Progressing from the results of chapter 3, 18 fractured specimens (of sub-optimal gap sizes 5, 10 and 15 mm) were reconstructed following the drafted protocol. All studies up to date have evaluated precisely defined 'hand-made' fractures (see table 2.1) (Moazen et al. 2011). The benefit of using physiological fractures is that they more closely represent the factures that occur in clinic. The limitation however is that there is a quite large spread in the results (see table 4.2). Specimens were loaded to failure following an identical loading protocol as described above and failure load was recorded. Consequently, as we were interested in the comparison of the plate and plate-strut reconstruction of the same fracture, the same specimens were reconstructed and an anterior bone strut was added. Specimens were once again loaded to failure. Fracture propagation did occur for some specimens (see table 4.3), which did influence the failure load of some of the plate-and-strut reconstructions. Results showed that gap size did not influence construct failure load. Addition of a strut was only useful with certain fracture types or when adequate fracture reduction could not be achieved.

Chapter 5 conducted a parametric study on the effect of the interprosthetic gap on femoral strains through finite element modelling. Since we were interested

in the strains in the IP gap and in the strain maxima around the hip prosthesis tip, application of the beam theory is insufficient (see Appendix A.3). As such, simplified parametric model was created consisting of cortical bone and a knee prosthesis, both modelled as a cylinder. The hip prosthesis was modelled as a cylinder as well, but did feature an angled prosthesis neck. As a control a model without prostheses was created. 132 models were simulated in which both hip and knee prosthesis stem length were varied to represent change in IP gap size and IP gap location. E-modulus and cortical thickness of the bone were altered as well to study the influence of inter-patient variability of bone mechanical properties. All models were loaded and constrained similar to the experimental loading described above. A load of 7000 N was applied along the mechanical axis of the femur model from the middle of the prosthesis head to the middle of the intercondylar fossa. The abductor force was not modelled, as described in the summary of chapter 3. Strain patterns and strain maxima were registered. Nalla et al. described that fracture in bone is strain dependent (Nalla et al. 2003). As the ultimate strain is lower for tensile strain than for compressive strain, fracture would occur due to tensile stain for all specimens, even when the maximal compressive strains were higher (Bayraktar et al. 2004). Results demonstrated that, for the loading conditions used in this study, not only IP gap size but also IP gap location influenced femoral strains in the IP gap. A model with ipsilateral prostheses always had lower strains than the control without prostheses. Small IP gaps led to lower strains thus lower fracture risk, consistent with the experimental tests of chapter 3. Longer hip prosthesis stems, i.e. more distal gaps, lowered strains as well. Both bone E-modulus and cortical thickness inversely influenced strains, the latter to the biggest extent.

Chapter 6 expanded on chapter 3 and 5. A physiologically relevant model was created based upon a CT-scan of a synthetic bone specimen combined with scanned 3D-models of the prostheses used in chapter 3. Both primary and revision hip prosthesis were scanned. These models were used to examine the influence of prosthesis neck length. The revision prosthesis stem was virtually lengthened to investigate the influence of stem length and to include all stem lengths used in the experimental part of this thesis. Control models were made with only a hip prosthesis, and all gap sizes from chapter 3 were modelled with both primary and revision hip prostheses. Three loads were applied; loading along the mechanical axis identical as described above, a load mimicking walking (W) and a load mimicking stair climbing (SC). These loads were selected since they are close to physiological loading (Heller et al. 2005). Moreover, application of pure bending (four-point bending), pure torsion or pure compression would not offer a more relevant load. Furthermore, it was our aim to conduct a comparative study, and as such we did not focus on the absolute values of the tensile strain in the IP gap. Results revealed that, in an immediate post-op

situation, long neck lengths increased femoral strains. Distally located gaps and small gaps both resulted in lower strains, consistent with chapter 5. Gap size did have the largest effect on strains. The consistent finding that IP gap creation did not act as a stress riser was confirmed here as well, since the control models had the highest strains.

7.2 Evaluation of research questions

A first contribution of this thesis is that it is the first study that models the full range of **interprosthetic gap sizes** and evaluates its effect on femoral fracture load and femoral strains. Gap sizes of 0, 15, 30, 50, 100, 150 and 200 mm were tested during the experimental part of this thesis (Chapter 3) and were modelled within an anatomically relevant FE model (Chapter 6). The simplified FE model of chapter 5 simulated an even larger amount of gap sizes in between 0 and 225 mm. Smaller gaps were investigated in greater detail since the clinical hypothesis was that (especially small) interprosthetic gaps increase the fracture risk of the femur. Both experimental tests and finite element models reached the same results and contradicted this clinical hypothesis. Creation of an interprosthetic gap by implanting an ipsilateral knee prosthesis did not increase fracture risk, but on contrary, lowered strains and increased load needed for fracture compared to femurs with only a hip prosthesis. Furthermore, small gaps required higher fracture loads and displayed lower strains than large gaps, which leads us to the conclusion that small gaps are favourable over large gaps. These conclusion were due to the fact that the prostheses are significantly stiffer than the bone, thus prosthesis implantation increased the overall stiffness of the femur (see Appendix A for the underlying theory). Since strains were connected to the deflection of the femur, a stiffer specimen with ipsilateral prostheses showed a smaller deflection and lower strain compared to a specimen with a hip prosthesis only. This also explained why the strain in the IP gap was higher than the strain in the bone where a prosthesis was present. Larger gaps, or specimens with a larger region of low stiffness, consequently displayed higher deflection and strains. We can thus conclude that, for an immediate post-op situation, small gaps are the preferred treatment option.

Investigation of the influence of **interprosthetic gap location** indicated that IP gap location did influence femoral strains. Variation of IP gap location and the influence on femoral strains has not yet been examined in literature. Chapter 5 simulated 132 combinations of interprosthetic gap size and location. Even though some of these gap locations were not clinically relevant or feasible, they did still contribute to clarify the changes in strain with varying gap location. Chapter 6 modelled gap sizes of 0, 15 and 30 mm with the 200 mm revision

prosthesis and with a longer revision prosthesis which led to more distal gaps. Both chapters concluded that more distal gaps had lower strains hence lower fracture risk. Lower strains in the model could again be attributed to the increase in stiffness caused by a longer THA stem combined with a shorter TKA stem. As a matter of fact, the THA had a twice as high E-modulus (thus stiffness) than the TKA. As the strain differences were more pronounced for MAL loading than for both anatomical loads, influence of gap location seemed to be also related to the load and the resulting moment applied on the model. For MAL loads, the resulting moment decreased to zero when moving from the proximal to the distal part of the femur. Hence more distal gaps were subjected to a lower resulting moment. For the anatomical W and SC loads, resulting moment increased when moving from the proximal to the distal part of the femur. Thus, for the latter two anatomical loads, distal gaps were subjected to a higher resulting moment. The decrease in strain (ϵ_{95}, chapter 6) due to the longer THA stems was smaller than under MAL loading due to the higher resulting moment for the anatomical loads (see Appendix A). We can however still conclude that, for an immediate post-op situation, distal gaps are less susceptible to fracture.

As a third aim, influence of **other parameters** that might influence femoral strains were examined. Until now, variation of cortical thickness and bone E-modulus within the same model has not yet been performed. Also, the influence of prosthesis neck length and prosthesis stem length on femoral strain has not yet been investigated. Chapter 5 and 6 respectively eliminated these shortcomings. Strains in the femur were largely affected by cortical bone thickness, and to a lesser extent by bone E-modulus (See Appendix A.4). Osteoporotic bone properties led to an increase in the difference of structural stiffness between the bone-prosthesis section and the gap section of the femur model. Since this further increased peak tensile strains in the gap region, IP gaps in osteoporotic bone are more prone to failure than IP gaps in healthy bone. The longer prosthesis neck length in models with a revision prosthesis increased the cantilever arm for the loads on the prosthesis head. As such the moment of the prosthesis head load increased. Longer THA stem length, as discussed above, increased model stiffness and thus lowered strains. Even though neck and stem length influenced femoral strains, IP gap size still had the most significant influence. Prosthesis stem diameter (or E-modulus) also played a significant role in strains in the IP gap (see Appendix B). Smaller stem diameter or lower E-modulus led to higher strains in the entire model, and especially in the IP gap. Prosthesis properties should thus be carefully selected, to ensure the lowest possible strain in the IP gap without compromising on minimal strains needed to avoid bone remodelling (section 7.3 and 7.4). Results indicate that long prosthesis necks should be avoided as they increase femoral strains. Long prosthesis stems on

the other hand can be beneficial, as they lower femoral strains and thus fracture risk. Gaps in osteoporotic bone should be treated with great care.

A first aspect of fracture treatment is the characterisation of the most prevalent **fracture morphology**. Presence of ipsilateral prostheses in the bone led to typical failure that resulted in the creation of a medial butterfly fragment in 67% of all recorded fractures. When a specimen was loaded along the mechanical axis, the largest strain or deformation in the bone was located at the tip of the THA stem. Since the ultimate tensile strain is lower than the ultimate compressive strain (Bayraktar et al. 2004), the fracture will originate at the lateral side of the IP gap, where high tensile stresses occurred that co-located with the low strength of the IP gap. When the crack grew in the transverse direction, the failure mode switched to compressive failure, which caused an oblique (shear) fracture line. As a consequence, a butterfly-shaped bone fragment was created (Fig. 7.1). These butterfly fractures may warrant specific reconstruction techniques.

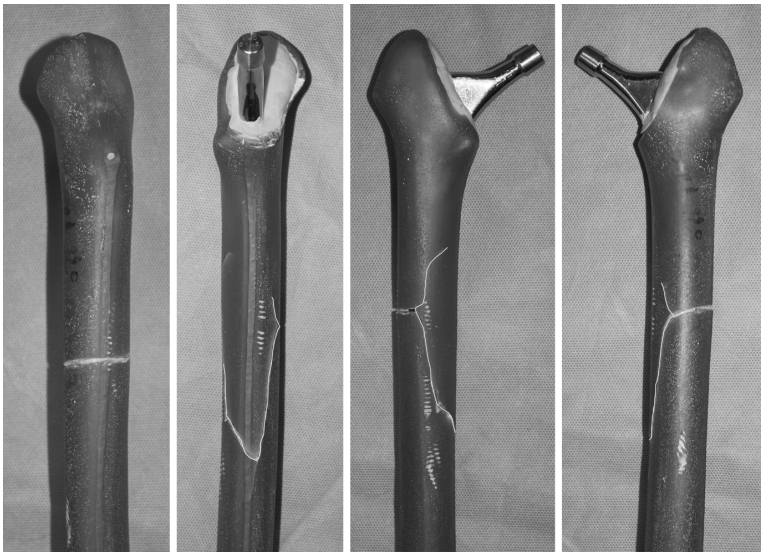

Figure 7.1: Fracture lines of a butterfly fracture failed under MAL loading. From left to right: lateral, medial, caudal and ventral view.

A fifth and last contribution of this thesis is to define a protocol for interprosthetic **fracture reconstruction**. Even though fracture morphology showed a fracture type that might warrant specific treatment strategy, the fracture treatment protocol shows similarities with the treatment of peri-

prosthetic fractures. The important features of fracture reconstruction were that a good reconstruction or reduction of the fracture is a prerequisite to achieve stability. Also, the plate length and fixation type (cables, screws or mixed) should be chosen carefully, as defined in chapter 4. Both chapter 4 and clinical studies indicate that long locking plates connected with screws are mechanically and biologically favourable, since they overlapped the fracture area and would not damage the periosteal blood supply (See section 2.2.2). Cable fixation was, opposed to screw fixation, sensitive to slippage when loaded leading to a loss of fracture segment reduction. As struts did not contribute to overall stiffness of the construct, and as strut placement damages blood supply on the anterior face of the femur, it is only advisable to use struts in cases where the plate fails to offer sufficient initial stability or when a optimal fracture reduction cannot be achieved. As such, the proposed fixation method is a long locking plate with screw fixations that spanned the entire femur.
The weakest point of the plate and reconstructed femur construct, loaded under MAL loads, is the location of the reconstructed fracture just below the THA tip (chapter 4). All construct failures initiated here, hence IP gap did not influence fracture risk of the reconstructed femur.

7.3 Global conclusion

Fracture treatment confirmed the advice from literature that peri-prosthetic fracture treatment protocols were transferable to interprosthetic fracture. An optimal reduction of the fracture segments held in place with a long locking plate proved to be both mechanically and biologically advantageous and made additional strut fixation redundant for most fracture types.
In vitro experimentation and *in silico* modelling, provided models and methods are validated, solved the shortcomings of *in vivo* testing (comorbidities, bone variability, ...) and allowed for a detailed investigation of one specific change to the models parameters. Starting from the same initial situation by using identical synthetic specimens and one 3D model based on a CT-scanned synthetic specimen, we were able to test and compare a wide range clinical relevant parameters (cortical thickness, bone E-modulus, gap size, gap location, prosthesis neck length) and evaluate their effect on fracture risk or strains.
Experiments and FE modelling reached similar results, as both concluded that small IP gaps were favourable and implantation of the ipsilateral prosthesis did not negatively influence femoral fracture risk. Also, the most prevalent medial butterfly fracture morphology could be verified based on the FE strain patterns, as the maximal tensile strains in the IP gap correctly identified the location where fracture initiated experimentally. Finite element modelling further expanded on the experimental tests and offered a more detailed insight

in strain patterns and maxima. The simplified and anatomical relevant models were both compatible and complementary. Both models concluded that gaps of 50 mm and larger had similar maximal strains, which could be validated through literature (Soenen et al. 2013). Irrespectively of the applied load and resulting moment, distal gaps were proven to be favourable. The simplified model pointed out the significant influence of cortical thickness on femoral strains and the critical care of osteoporotic patients arising thereof. The anatomically relevant model demonstrated the impact of THA neck length on femoral strains. The strain pattern further clarified that there was an higher strain in the gap region of the femur compared to the lower strains in the region where a prosthesis was implanted.
The interprosthetic gap had not yet been studied into detail before this thesis, since its occurrence is quite rare. Current trends and predictions indicate that the IP gap will more sooner than later become a major clinical concern. In conclusion, this thesis investigates the effect of several clinically relevant parameters on the immediate post-op characteristics of the IP gap. Influence of IP gap size, IP gap location, bone mechanical properties and THA neck and stem length on femoral fracture load and femoral strains, for an immediate post-surgery situation, were quantified. Interprosthetic fracture morphology and fracture reconstruction were studied as well. Addition of bone remodelling simulations to the finite element model could offer insights in the long-term behaviour of the IP gap size and location. This could be investigated in a future study.

7.4 Future work

Bone remodelling

Bone is a living tissue with an adaptive capability which means that both geometry and material properties can change in response to mechanical load. Bone remodelling initiates following bone fracture or following noticeable changes to the sensed load (Bartel et al. 2006). One might thus argue that ipsilateral prosthesis placement, especially for the smaller gaps with low strains in the IP gap, will induce bone remodelling. The IP gap, regardless of gap size, lowers femoral strains compared to a femur with only a THA or compared to a femur with no prostheses. As the load of an ipsilateral implanted femur is divided between bone and prostheses, the bone will carry a smaller part of the load and bone remodelling will cause the apparent bone modulus to decrease due to decrease in cortical bone density. This will then lead to an

even larger discrepancy in stiffness between prosthesis and bone, whereby the bone will carry an even smaller part of the load causing a downward spiral of bone remodelling. As we demonstrated in chapter 5, decrease in cortical radius and E-modulus will lead to an increase in fracture risk. Too small femoral strains should thus be avoided. Addition of a bone remodelling routine to our model could thus offer a more detailed insight in the long-term behaviour of the different IP gap sizes and locations.

Addition of impact loads

The loads applied in this thesis represented daily activities. These loads; loading along the mechanical axis, walking and stair climbing, were described in detail in literature and are commonly used in biomechanical testing (Heller et al. 2005, Zdero et al. 2008). As noticed in clinical practice, falling is a common injury leading to femoral fracture. Inclusion a loading protocol mimicking falling could thus expand our insight into the biomechanics of the IP gap. There are two ways to model falling mentioned in literature. A first set-up uses four-point bending to simulate falling on an object. A second set-up mimics sideways falling. This set-up leads to a more physiological relevant load protocol where load is applied on the femoral head and boundary conditions are applied on the trochanter major and the distal condyle. The strain patterns resulting from loading under four point bending appear to depend on the distances between the four holds that serve as loading points (Cristofolini et al. 1996). As such, sideways falling seems to be the most robust loading protocol that could be added to the existing loads in a future study (Courtney et al. 1995).

7.5 Clinical implications

Extraction of clinically relevant data from finite element simulations or experimental tests is not straightforward. Still, this manuscript reaches some useful conclusions that could be used to inform surgeons concerning the post-op behaviour of the IP gap. First, a small gap does not seem to negatively influence the fracture risk of the femur, contrary to the hypothesis and intuitive fear amongst surgeons. As such, a prosthesis with a long revision stem can be used to replace a primary prosthesis in a patient with a ipsilateral knee prosthesis, without concern of increased fracture risk. Second, gap size and location are rarely fully customizable since the patient will often have either hip or knee prosthesis implanted in a prior surgery to the placement of the ipsilateral prosthesis. Still, if possible, the surgeon should aim for a distal and small IP gap. Third, long plates connected to the bone with screws is the preferred

fracture fixation method, even though it is an invasive surgery, as the fixation of the bone fragments is essential for reconstruction stability. Fourth, a strut does not seem to offer a consistent mechanical benefit to the fracture reconstruction of an IP fracture. Due to the infection risk encountered in strut placement surgeries, the additional periosteal stripping and the disruption of the blood supply around the fracture site needed to place the strut, strut placement is not encouraged. A limitation is that fracture reconstruction in clinic is more difficult than in vitro, possibly yielding a lower reduction quality in clinical practice. As our results do indicate that strut placement is useful in fracture reconstructions with low reduction quality, this could be investigated in a clinical follow-up study. Fifth, as mentioned above, the conclusions of this manuscript can be applied to non-cemented prostheses and prostheses of similar shapes as well.

Appendix A

Mechanical model & Beam theory

This appendix further explains the results of this thesis through the use of *beam theory*. This theory offers calculation of the load-bearing and deflection characteristics of beams. Section A.1 explains the formulas behind beam theory. Section A.2 applies this theory to the three different loading protocols to explain the differences in strain pattern. The loads applied in this appendix are identical to those applied on the FE models in chapter 5 and 6.

A.1 Beam theory

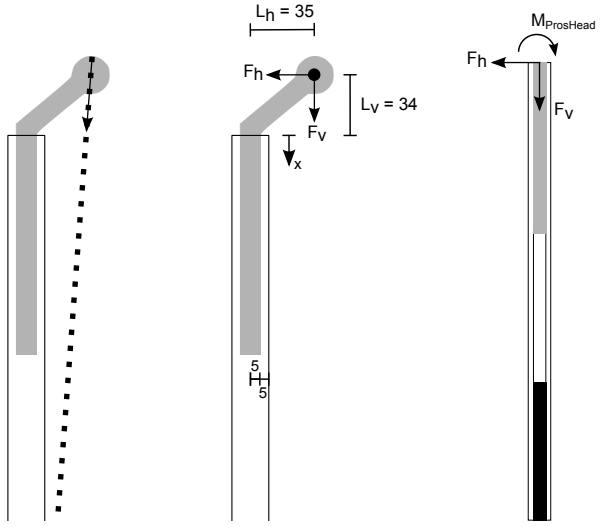

Figure A.1: MAL loading, force resolution and resulting forces.

Stress (σ) and strain (ϵ) result from compression (vertical force component F_v), constant moment and variable moment (horizontal force component F_h) (Fig. A.1).
For the compression and moment respectively stresses can be expressed as:

$$\sigma = \frac{F_v}{A} \qquad \text{with} \begin{cases} F_v &= \text{vertical force component} \\ A &= \text{cross-section surface} \end{cases} \tag{A.1}$$

$$\sigma = \frac{My}{I} \qquad \text{with} \begin{cases} M &= \text{Moment along bone axis} \\ y &= \text{distance to the neutral axis} \\ I &= \text{second moment of area} \end{cases} \tag{A.2}$$

$$A = \pi(r_0^2 - r_i^2), \;\; I = \frac{\pi(r_0^4 - r_i^4)}{4} \qquad \text{with} \begin{cases} r_0 &= \text{Outer radius} \\ r_i &= \text{Inner radius} \end{cases} \tag{A.3}$$

$$M = F_v L_h - F_h(L_v + x) \qquad \text{see figure A.1} \tag{A.4}$$

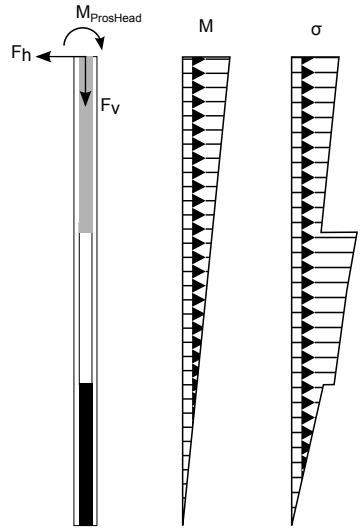

Figure A.2: Moment (M) and Stress (σ) from MAL loading.

Since the construct consists out of multiple materials, composite beam theory is used:

$$\sigma_j = \frac{E_j M t}{E_b I_b + E_p I_p}$$

$$\text{with} \begin{cases} M & = \text{Moment along bone axis} \\ t & = \text{distance to the neutral axis of entire beam} \\ I_b \ \ or \ \ I_p & = \text{second moment of area of bone or prosthesis} \\ E_b \ \ or \ \ E_p & = \text{Young's modulus of bone or prosthesis} \end{cases} \tag{A.5}$$

We can thus write the stress in the bone as the following function (Fig. A.2):

$$\sigma_b = \begin{cases} \dfrac{E_b M(x) t}{E_b I_b + E_{hip} I_{hip}} & \text{for } \ x \leq \mathrm{l}_{hip} \\ \dfrac{E_b M(x) t}{E_b I_b} & \text{for } \ \mathrm{l}_{hip} \leq x \leq \mathrm{l}_{hip} + \mathrm{l}_{Ip} \\ \dfrac{E_b M(x) t}{E_b I_b + E_{knee} I_{knee}} & \text{for } \ \mathrm{l}_{hip} + \mathrm{l}_{Ip} \leq x \leq \mathrm{l}_{hip} + \mathrm{l}_{Ip} + \mathrm{l}_{knee} \end{cases} \tag{A.6}$$

A.2 Loading protocol comparison

This section applies the formulas of *beam theory* to the three applied loading protocols. The force directions and moment arms used in the calculation of the moments below can be found in figure A.3. Resulting moments are shown in figure A.4. A moment is defined as positive when the lateral or dorsal femoral cortex is loaded under tensile strains. Loads for MAL are located in point P_0, for walking in points $P_0 \rightarrow P_2$ & for stair climbing in points $P_0 \rightarrow P_3$ (chapter 6).

Constant moment due to the load in the Z-direction

$$M = 0.048 * P_{0z} + 0.012 * P_{1z} - 0.0115 * P_{2z} + 0.0115 * P_{3z} \tag{A.7}$$

Moment due to the load in the X-direction

$$M = -(0.0175 + x) * P_{0x} + (0.01 + x) * P_{1x} - (x - 0.04) * P_{2x} - (x - 0.07) * P_{3x} \tag{A.8}$$

Torsion due to the load in the Y-direction and in the X-direction for loads in points P_2 & P_3

$$\begin{aligned} T = {} & 0.048 * P_{0y} + 0.012 * P_{1y} + 0.0115 * P_{2y} - 0.0115 * P_{3y} \\ & + 0.0115 * P_{2x} - 0.0115 * P_{3x} \end{aligned} \tag{A.9}$$

Moment due to the load in the Y-direction and in the Z-direction for loads in points P_2 & P_3

$$\begin{aligned} M_{\otimes} = {} & -(0.0175 + x) * P_{0y} + (0.01 + x) * P_{1y} + (x - 0.04) * P_{2y} + (x - 0.07) * P_{3y} \\ & - 0.0115 * P_{2z} + 0.0115 * P_{3z} \end{aligned} \tag{A.10}$$

For MAL loading (6.59° angle with Z-axis), this results in:

$$\begin{aligned} M &= 0.048 * 6953.7 - (0.0175 + x) * 803.3 \\ &= \textbf{319.7 - 803.3x} \end{aligned} \tag{A.11}$$

$$\text{If } x = 0.2 \text{ m} \quad \longrightarrow \quad \boxed{M = 159 \text{ Nm}}$$

For Walking, this results in:

$$\begin{aligned} M &= 0.048 * 1916 + 0.012 * 674.6 - 0.0115 * 776.6 \\ &\quad - (0.0175 + x) * 451 + (0.01 + x) * 540.9 - (x - 0.04) * 7.5 \\ &= \mathbf{88.9 + 82.4x} \end{aligned} \tag{A.12}$$

$$\begin{aligned} T &= 0.048 * 274 + 0.012 * 127 + 0.0115 * 154.6 + 0.0115 * 7.5 \\ &= \mathbf{16.5} \end{aligned} \tag{A.13}$$

$$\begin{aligned} M_{\otimes} &= -(0.0175 + x) * 274 + (0.01 + x) * 127 + (x - 0.04) * 154.6 - 0.0115 * 776.6 \\ &= \mathbf{-18.6+7.6x} \end{aligned} \tag{A.14}$$

If $x = 0.2$ m $\longrightarrow$ $\boxed{M = 105.4 \text{ Nm} \quad T = 16.5 \text{ Nm} \quad M_{\otimes} = -17 \text{ Nm}}$

For Stair climbing, this results in:

$$\begin{aligned} M &= 0.048 * 2001.5 + 0.012 * 654.7 - 0.0115 * 1144 + 0.0115 * 2262.3 \\ &\quad - (0.0175 + x) * 502 + (0.01 + x) * 703 - (x - 0.04) * 18.6 - (x - 0.07) * 74.5 \\ &= \mathbf{121+107.9x} \end{aligned} \tag{A.15}$$

$$\begin{aligned} T &= 0.048 * 513 + 0.012 * 301.5 + 0.0115 * 189.7 - 0.0115 * 335.4 \\ &\quad + 0.0115 * 18.6 - 0.0115 * 74.5 \\ &= \mathbf{25.9} \end{aligned} \tag{A.16}$$

$$\begin{aligned} M_{\otimes} &= -(0.0175 + x) * 513 + (0.01 + x) * 301.5 + (x - 0.04) * 189.7 \\ &\quad + (x - 0.07) * 335.4 - 0.0115 * 1144 + 0.0115 * 2262.3 \\ &= \mathbf{-24.2+313.6x} \end{aligned} \tag{A.17}$$

If $x = 0.2$ m $\longrightarrow$ $\boxed{M = 142.6 \text{ Nm} \quad T = 25.9 \text{ Nm} \quad M_{\otimes} = 38.5 \text{ Nm}}$

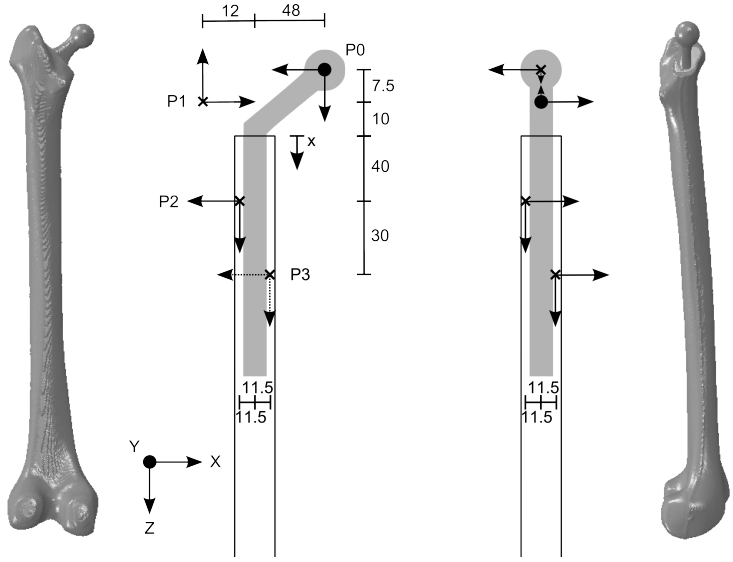

Figure A.3: Posterior and medial view of the femur with forces and points of application.

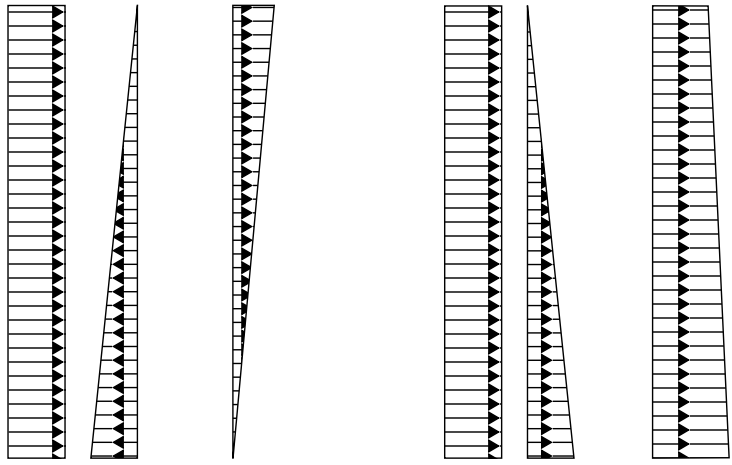

(a) Moment MAL load (b) Moment anatomical load

Figure A.4: Constant, variable and resulting moment due to bending.

For all three loading cases, a moment was defined as positive when the lateral or dorsal femoral cortex was loaded under tensile strains. For all loads, the lateral cortex was subjected to tensile strains. However, loading along the mechanical axis gave rise to a different resulting moment compared to both anatomical loading conditions. The resulting moment for loading along the mechanical axis was maximal at the hip prosthesis head and zero at the knee condyle (Fig. A.4, Formula A.11). For both anatomical loading conditions, there was no location where the resulting moment was zero. Also, the resulting moment slightly increased when moving distally, away from the hip prosthesis head (Formula A.12 and A.15).
Fracture location was defined by both resulting moment and stiffness. As discussed in Chapter 3 to 6, higher strains increased fracture risk. In regions where a prosthetic stem was present the stiffness was higher, thus bending deformation was lower than in the gap region. As a consequence, strains were lower in the prosthesis regions, similar to the study of (Soenen et al. 2013). Maximal strains could thus be found in the gap region, and fracture initiated where the resulting moment was maximal. As concluded in chapter 3, MAL loading led to fracture near the THA tip. For the anatomical loading conditions, strain maxima thus fracture location moved closer towards the TKA tip (Fig. A.6).
The difference in resulting moment also further explains some of the results of chapter 6. We concluded that longer revision THA stems lowered the strains in the model. Still, while strains for MAL loading changed by around 8% for each elongation of the THA stem (200, 220, 240 and 260 mm, Fig. A.5) a significant smaller change was noted for both models loaded with either walking or stair climbing loads (Table A.1). As such, we see that the increase in resulting moment partially counteracted the decrease in strain due to a longer stem.

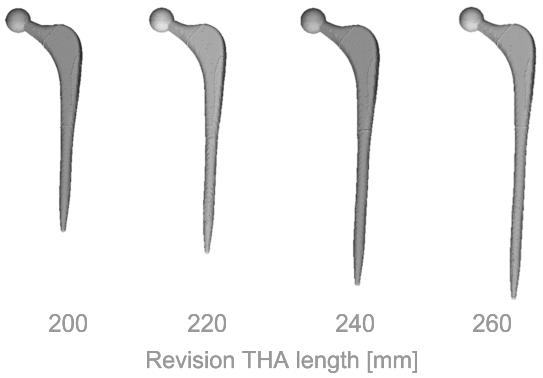

Figure A.5: Change in revision THA length.

	Revision THA			
THA stem length [mm]	**200**	**220**	**240**	**260**
MAL	12.03	11.64	10.70	9.99
W	3.85	3.79	3.79	3.74
SC	6.17	6.08	6.01	5.89

Table A.1: Strain parameter ϵ_{95} (10^{-3}), as the mean of the highest 5% strains in the cortical bone for models with revision THA only, loaded along the mechanical axis (MAL), mimicking walking (W) and Stair climbing (SC). Longer THA's had lower ϵ_{95}.

This counteraction could be noted as well when the gaps created with a 200 mm THA were compared to the same gaps created with a 220, 240 and 260 mm THA respectively. While we expected a decrease in strain for the more distal gaps, the strains (ϵ_{95}) for the anatomical loads were only slightly smaller or equal then those of the gaps with the 200 mm THA. For MAL loading, a more distally located gap was subjected to lower strains, due to the lower resulting moment. This amplified the effect of the longer THA stem. On contrary, for anatomical loading, the resulting moment thus load increased for more distal gaps, counteracting the effect of the longer THA stem (See table A.2, which expands on table 6.4).
Besides bending in the coronal plane, anatomical loading caused torsion and bending in the sagittal plane. While for both walking and stair climbing, torsion was oriented in the same direction, bending in the sagittal plane was oriented in a opposed direction. For walking, the ventral femoral cortex was loaded under tensile strains (Formula A.14). Contrary, for stair climbing, the dorsal femoral cortex was loaded under tensile strains (Formula A.17). This explains why the stain patterns for walking and stair climbing shifted towards the ventral respectively dorsal side of the femur (Fig. A.7).

			ϵ_{95} **(200 mm THA)**	ϵ_{95} **(more distal gap)**
Change in gap location (more distal) compared to 200 mm THA	**MAL**	20 mm	10.29	10.21
		40 mm	10.06	9.58
		60 mm	10.47	9.63
	W	20 mm	3.54	3.54
		40 mm	3.52	3.51
		60 mm	3.56	3.56
	SC	20 mm	5.72	5.69
		40 mm	5.69	5.67
		60 mm	5.73	5.71

Table A.2: Strain parameter ϵ_{95} (10^{-3}), as the mean of the highest 5% strains in the cortical bone for models with an interprosthetic gap, loaded along the mechanical axis (MAL), mimicking walking (W) and Stair climbing (SC). For three gap sizes, a change in gap location was modelled. Gaps were modelled with a 200 mm revision THA and a lengthened revision THA respectively. More distal gaps had lower ϵ_{95}.

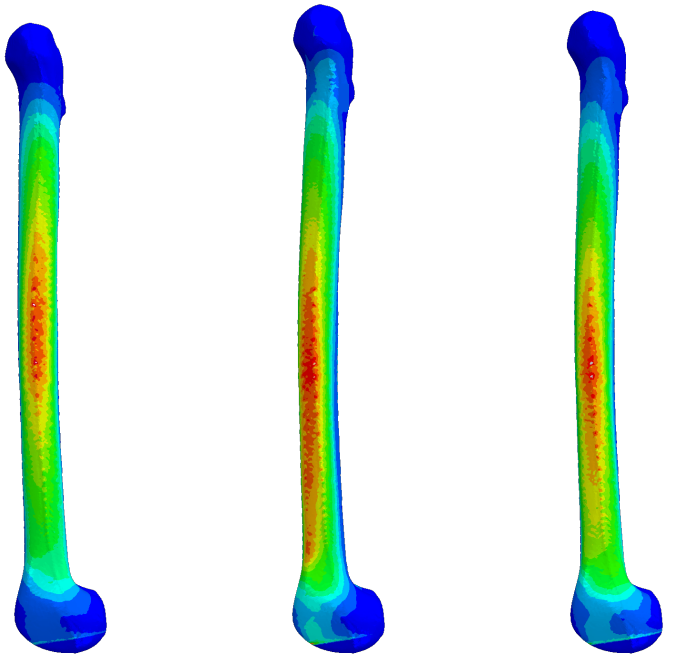

(a) Mechanical axis (b) Walking (c) Stair climbing

Figure A.6: Variations in strain pattern due to variation in resulting moments. Decreasing resulting moment leads to strain maxima at THA tip for MAL, while increasing resulting moment (walking and stair climbing) shifts strain maxima towards TKA stem tip.

(a) Walking (b) Stair climbing

Figure A.7: Variations in strain pattern due to variation in torque. Change in direction of torque for walking and stair climbing shifts the strain pattern ventral for walking and dorsal for stair climbing.

A.3 Limitations of Beam theory

The beam theory can be used as a comparative tool to investigate the change in strain in the IP gap compared to the region where a prosthesis is present. However, it fails to include some important effects such as the distal boundary condition as described by Speirs et al. (Speirs et al. 2007) and the behaviour of the region of the IP gap where the prosthesis stems end. These effects are included in the simplified parametric model (as shown in figure A.8 & A.9), preferring it over the beam theory.

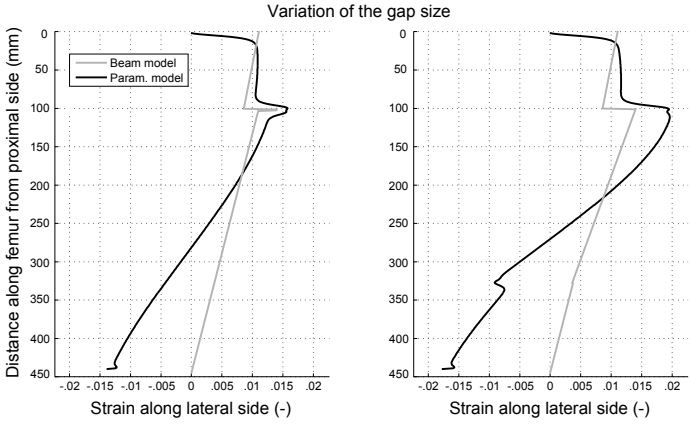

Figure A.8: Comparison of the beam model to the parametric model, for change in gap size. 2 mm gap (left) and 225 mm gap (right) at 100 mm proximal distance.

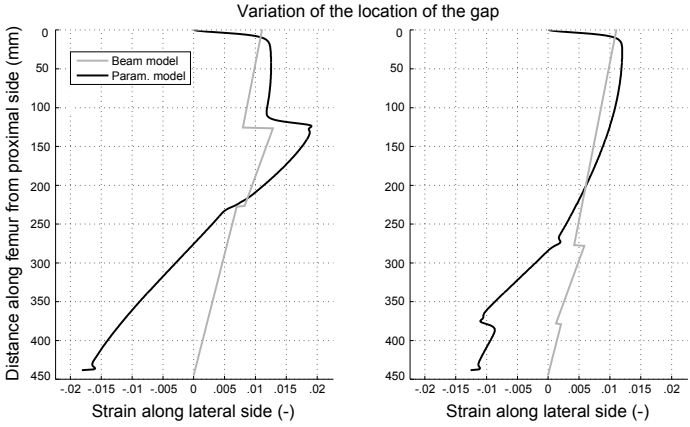

Figure A.9: Comparison of the beam model to the parametric model, for change in gap location. 100 mm gap at 125 mm proximal distance (left) and 275 mm proximal distance (right).

A.4 Mechanical parameters of the bone

In chapter 5 (Fig. A.10), we concluded that the cortical E-modulus had a linear influence on strain in the IP gap, while the cortical thickness had a exponential influence. This can be explained using formula A.6. The part of this formula that describes the stress in the gap region is copied and expanded on below:

$$\begin{aligned}
\sigma &= \frac{E_b M(x) t}{E_b I_b} = \frac{M(x) t}{I_b} \\
I &= \frac{\pi(r_0^4 - r_i^4)}{4} \\
\epsilon &= \frac{\sigma}{E} = \frac{M(x) t}{E_b I_b} \\
&= \frac{4 M(x) t}{E_b \pi (r_0^4 - r_i^4)}
\end{aligned} \tag{A.18}$$

Beam theory confirms these conclusions. E-modulus and radius can both be found in the denominator of the strain formula A.18. Changes in radius, due to the fourth order, will have a larger influence than the linear influence of E-modulus.

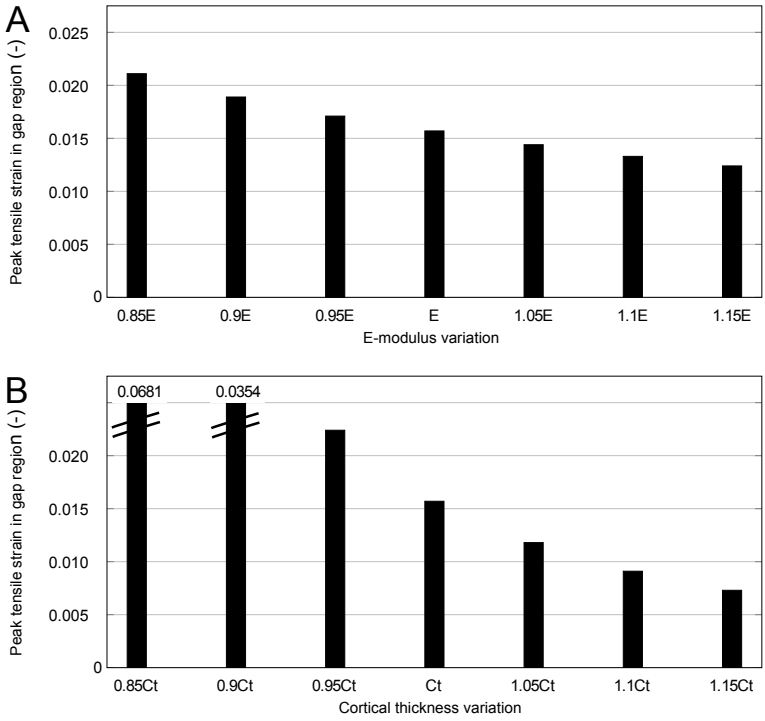

Figure A.10: Peak tensile strain in the interprosthetic gap region as a function of (a) bone tissue modulus, and (b) cortical thickness. The model combined a hip stem of 150 mm with a knee stem of 190 mm, resulting in a 100 mm interprosthetic gap. This represents an anatomically relevant ipsilateral primary prosthesis placement. Strains are more sensitive to variation of cortical thickness than to variations of bone tissue modulus.

Appendix B

Prosthesis E-modulus influence

This appendix investigates the influence of prosthesis E-modulus or prosthesis stem thickness on cortical strains (both at the prosthesis location and at the gap location). *Beam theory* from Appendix A is utilized to explain the differences shown in FEA results.

Since a large variety of prosthesis shapes exists, we were interested to examine the effect of prosthesis E-modulus on cortical strains. This effect could also be used to investigate the change in prosthesis stem diameter.
For a model with a 140 mm THA and a 100 mm gap (Fig. B.1a), E-modulus of THA and both THA and TKA were doubled (Fig. B.1b and B.1c respectively) and halved (Fig. B.1d and B.1e respectively).

Stiffer prostheses lead to a stiffer overall construct, which will be subjected to less severe bending deformations. This explains the lower strains in the IP gap for the model with a stiffer THA, and the even lower strains for the model with stiffer THA and TKA (Fig. B.1b and B.1c). Vice versa for the lower stiffness prostheses (Fig. B.1d and B.1e).
Formula A.6 shows both E-modulus and second moment of area in the denominator of the stress formula. For the strain in the femoral cortex at the height if the hip prosthesis, the formula becomes (see formula A.3 & A.5):

$$\epsilon = \frac{4M(x)t}{E_b\pi(r_{b0}^4 - r_{bi}^4) + E_{hip}\pi(r_{hip0}^4)} \tag{B.1}$$

It shows that both stem radius increase and E-modulus increase of the hip prosthesis decrease cortical strains.

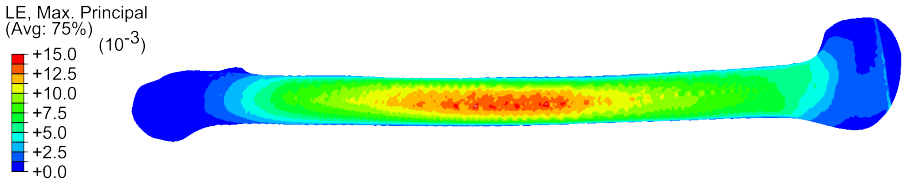

(a) 100 mm Gap, 140 mm THA

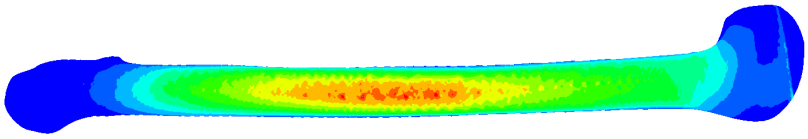

(b) THA E-modulus * 2

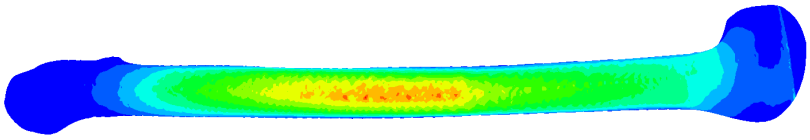

(c) THA & TKA E-modulus * 2

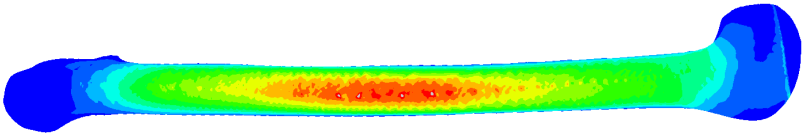

(d) THA E-modulus / 2

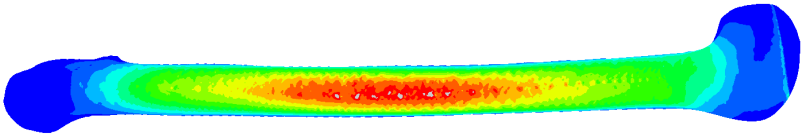

(e) THA & TKA E-modulus / 2

Figure B.1: Influence of prosthesis E-modulus on cortical strains. Stiffer prostheses decrease cortical strains in both the prosthesis area and the IP gap.

Appendix C

Finite element modelling

This appendix explains the concept of finite element simulations and shows the different element types used in this thesis to create the finite element models used in chapter 5 and 6.

In this thesis, a synthetic bone analogue was digitized through CT-scanning and converted into a 3D model using specified software (Mimics Research 18.0, Materialise, Leuven, Belgium). Based on Hounsfield values, the 3D model was segmented into prostheses, trabecular bone, intramedullary space and cortical bone (Fig. C.1). Physiologically correct material properties were added to all model parts. Following this segmentation, the model was converted into a FE model using specified software (Fig. C.2, Voronoi meshing algorithm, 3-Matic Research 11.0 *alpha version*, Materialise, Leuven, Belgium). This model was subsequently imported in dedicated FE software (Abaqus 6.13, Dassault Systèmes Corp., Providence, RI, USA) and analysed to investigate strain patterns on the bone.

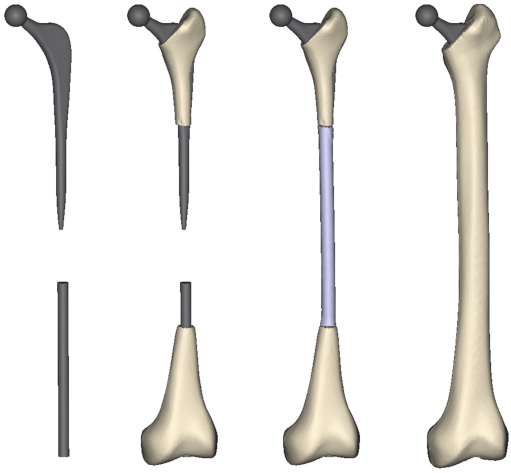

Figure C.1: A 3D-model of a synthetic bone with ipsilateral prosthesis, segmented in line with material region.

Hex and Tet elements

Several element types can be used in finite element analysis, depending on the shape and complexity of the model. Reduced integration hexahedral elements (*C3D8R* Fig. C.3a, used in chapter 5) are the most cost-efficient choice of elements, featuring both low calculation times and accurate results. The downside is that the 3D model has to be quite simple and symmetric to successfully *mesh* (convert to a FE model) with hexahedral elements. Linear tetrahedral elements (*C3D4* Fig. C.3b) are less calculation intensive as quadratic tetrahedral elements (*C3D10* Fig. C.3c, used in chapter 6), since they only contain one integration point instead of four. However, they are not suited for simulation unless element size is small (*Abaqus 6.13 Online Documentation* 2013).

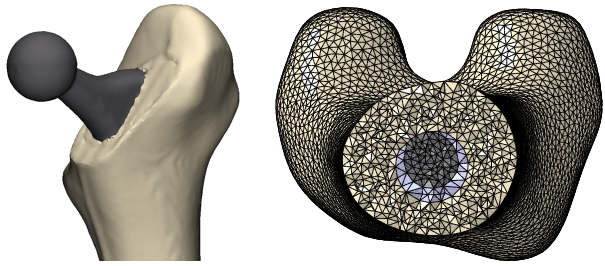

Figure C.2: Choice of FE element type (C3D10) and material distribution.

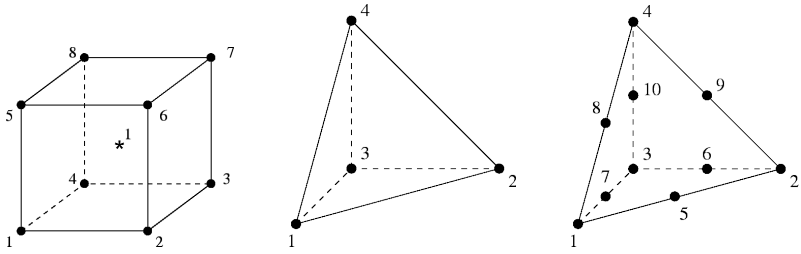

(a) C3D8R (b) C3D4 (c) C3D10

Figure C.3: Finite element types used in this thesis. From (Dhondt 2012).

Another consideration that should be made is the size of the elements. Small element sizes strongly increase calculation time, since there is an exponential relationship between element size and calculation time (Fig. C.4). Accordingly, element size should be maximized. However, too large elements result in inaccurate simulation results. To determine the biggest element still resulting in accurate results, convergence analysis can be conducted by gradually decreasing element size until results (e.g. strain) converge (Fig. C.4).

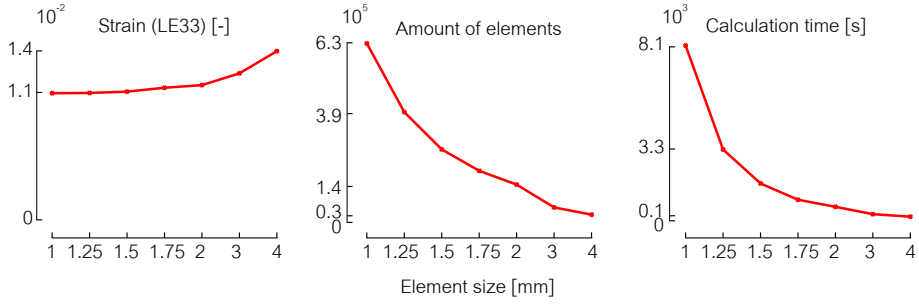

Figure C.4: Convergence analysis indicates that 1.25 mm is the largest element size that reaches accurate strain results (<1% difference with smaller elements).

Appendix D

Fracture fixation plates

This appendix compares three different fracture fixation plates, used in the prior study mentioned in chapter 4.

Before the specimens in chapter 4 were reconstructed with plate and plate-strut, three different fracture fixation plates were compared:

- the Accord plate (Smith&Nephew, 20 cm, Fig. D.1a)
- the LCP plate (Synthes, 39 cm, Fig. D.1b)
- the NCB plate (Zimmer, 43 cm, Fig. D.1c)

These plates were fixed to the bone with cables, screws and cables or screws respectively. The longest plate, connected to the specimen with screws only (NCB), reached the highest relative fracture loads, and as such was the preferred plate to reconstruct interprosthetic fractures (Fig. D.2). This was also mentioned in literature; see chapter 2 (section 2.1 & 2.2.2).

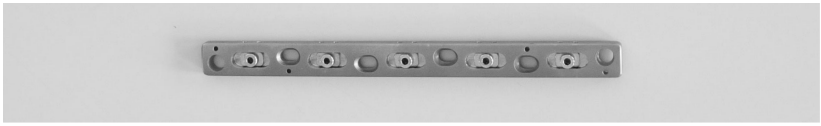

(a) Accord plate

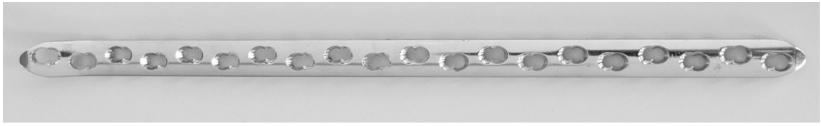

(b) LCP plate

(c) NCB plate

Figure D.1: Three different types of fracture fixation plates which are commonly used in clinical practice.

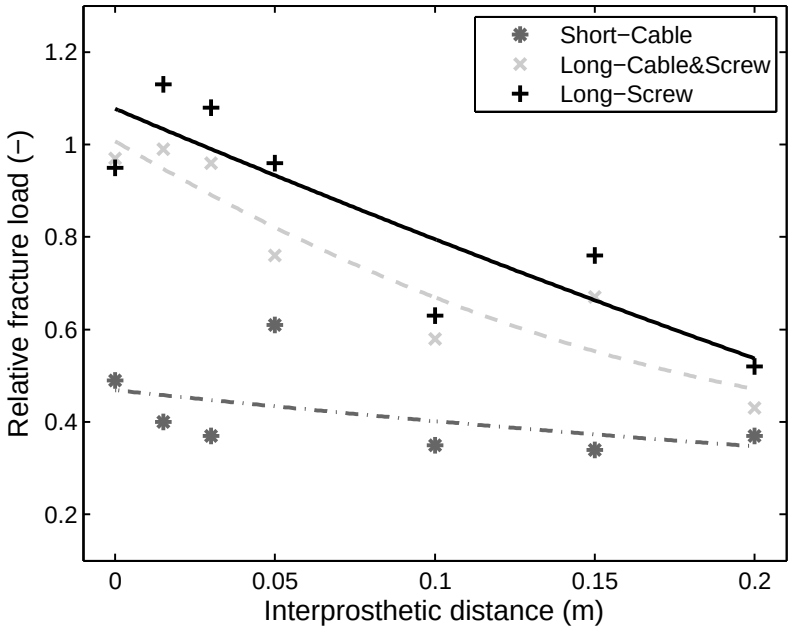

Figure D.2: Comparison of relative fracture load of three fracture fixation plates: the short cable-plate (Accord), the long cable&screw-plate (LCP) and the long screw-plate (NCB). The NCB plate offered optimal fracture load.

Appendix E

Stiffness normalized strains

This appendix shows the strains for the parametric model (See chapter 5). Strains were normalized by the initial stiffness of the model.

The variation in gap size also caused a change in initial stiffness of the model. Smaller gaps, or longer prosthetic stems, increased the initial stiffness. To investigate the variation of the gap size, the strains (ϵ) shown in chapter 5 were normalized by their initial stiffness.

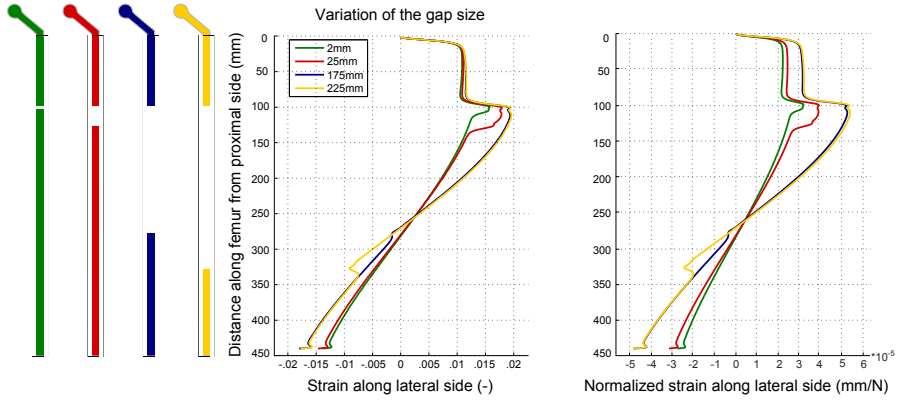

Figure E.1: Influence of gap size on strain (normalized by stiffness) on the medial (left graph) and lateral (right graph) side of the femur. Larger gaps resulted in higher strains. Colours correspond to the models in the central panel, which show the varying configurations. Gaps of 2, 25, 175 and 225 mm starting at a proximal distance of 100 mm are shown.

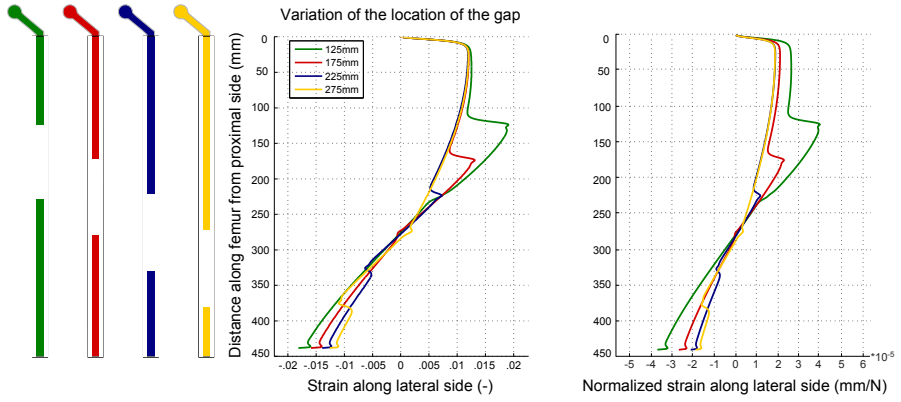

Figure E.2: Influence of gap location on strain (normalized by stiffness) on the medial (left graph) and lateral (right graph) side of the femur. Smaller proximal distances, i.e. smaller hip stems, resulted in higher strains. Colours correspond to the models in the central panel, which show the varying configurations. A gap of 100 mm starting at proximal distances of 125, 175, 225 and 275 mm is shown.

All strains were divided by their respective stiffness, based on the formula for springs:

$$F = kx \qquad \text{with} \begin{cases} F &= \text{the applied force} \\ k &= \text{the stiffness of the model} \\ x &= \text{the deflection of the model} \end{cases}$$

$$k = \frac{F}{x}$$

$$\epsilon_{normalized} = \frac{\epsilon}{k}$$

There was no change in outcome of our comparative study when the strains were normalized. Larger gaps still had higher strains, as did more proximal gaps.

Bibliography

AAOS - American academy of orthopaedic surgeons (2016). Inflammatory Arthritis of the Hip, `http://orthoinfo.aaos.org/topic.cfm?topic=A00396`. [Online; accessed 02-February-2016].

Abaqus 6.13 Online Documentation (2013).

Abendschein, W. (2003). Periprosthetic femur fractures–a growing epidemic., *American journal of orthopedics (Belle Mead, N.J.)* **32**(9 Suppl): 34–6.

Ali, A. a., Cristofolini, L., Schileo, E., Hu, H., Taddei, F., Kim, R. H., Rullkoetter, P. J. & Laz, P. J. (2014). Specimen-specific modeling of hip fracture pattern and repair, *Journal of Biomechanics* **47**(2): 536–543.

AO Foundation (2016). Fixation plate types, `https://www2.aofoundation.org/wps/portal/surgery`. [Online; accessed 02-February-2016].

Bartel, D. L., Davy, D. T. & Keaveny, T. M. (2006). *Orthopaedic Biomechanics. Mechanics and Design in Musculoskeletal Systems*, Pearson Prentice Hall Bioengineering - Pearson education, Inc.

Basso, T., Klaksvik, J., Syversen, U. & Foss, O. a. (2014). A biomechanical comparison of composite femurs and cadaver femurs used in experiments on operated hip fractures., *Journal of biomechanics* **47**(16): 3898–902.

Bayraktar, H. H., Morgan, E. F., Niebur, G. L., Morris, G. E., Wong, E. K. & Keaveny, T. M. (2004). Comparison of the elastic and yield properties of human femoral trabecular and cortical bone tissue., *Journal of biomechanics* **37**(1): 27–35.

Bergmann, G., Graichen, F., Rohlmann, a., Bender, a., Heinlein, B., Duda, G. N., Heller, M. O. & Morlock, M. M. (2010). Realistic loads for testing hip implants., *Bio-medical materials and engineering* **20**(2): 65–75.

Berry, D. J. (1999). Epidemiology: Hip and knee, *Orthopedic Clinics of North America* **30**(2): 183–190.

Borgeaud, M., Cordey, J., Leyvraz, P. & Perren, S. (2000). Mechanical analysis of the bone to plate interface of the LC-DCP and of the PC-FIX on human femora, *Injury* **31**: 29–92.

Bryant, G. K., Morshed, S., Agel, J., Henley, M. B., Barei, D. P., Taitsman, L. a. & Nork, S. E. (2009). Isolated locked compression plating for Vancouver Type B1 periprosthetic femoral fractures., *Injury* **40**(11): 1180–6.

Buttaro, M. A., Farfalli, G., Paredes Núñez, M., Comba, F. & Piccaluga, F. (2007). Locking compression plate fixation of Vancouver type-B1 periprosthetic femoral fractures., *The Journal of bone and joint surgery. American volume* **89**(9): 1964–9.

Cherian, J. J., Kapadia, B. H., Banerjee, S., Jauregui, J. J., Issa, K. & Mont, M. A. (2014). Mechanical, Anatomical, and Kinematic Axis in TKA: Concepts and Practical Applications., *Current reviews in musculoskeletal medicine* **7**(2): 89–95.

Choi, J. K., Gardner, T. R., Yoon, E., Morrison, T. a., Macaulay, W. B. & Geller, J. a. (2010). The effect of fixation technique on the stiffness of comminuted Vancouver B1 periprosthetic femur fractures., *The Journal of arthroplasty* **25**(6 Suppl): 124–8.

Chong, A. C. M., Miller, F., Buxton, M. & Friis, E. a. (2007). Fracture toughness and fatigue crack propagation rate of short fiber reinforced epoxy composites for analogue cortical bone., *Journal of biomechanical engineering* **129**(4): 487–493.

Corten, K., Vanrykel, F., Bellemans, J., Frederix, P. R., Simon, J.-P. & Broos, P. L. O. (2009). An algorithm for the surgical treatment of periprosthetic fractures of the femur around a well-fixed femoral component., *The Journal of bone and joint surgery. British volume* **91**(11): 1424–30.

Courtney, A. C., Wachtel, E. F., Myers, E. R. & Hayes, W. C. (1995). Age-related reductions in the strength of the femur tested in a fall-loading configuration., *The Journal of bone and joint surgery. American volume* **77**(3): 387–95.

Cristofolini, L., Schileo, E., Juszczyk, M., Taddei, F., Martelli, S. & Viceconti, M. (2010). Mechanical testing of bones: the positive synergy of finite-element models and in vitro experiments., *Philosophical transactions. Series A, Mathematical, physical, and engineering sciences* **368**(1920): 2725–63.

Cristofolini, L., Viceconti, M., Cappello, A. & Toni, A. (1996). Mechanical validation of whole bone composite femur models., *Journal of biomechanics* **29**(4): 525–35.

Culliford, D., Maskell, J., Judge, A., Cooper, C., Prieto-Alhambra, D. & Arden, N. K. (2015). Future projections of total hip and knee arthroplasty in the UK: results from the UK Clinical Practice Research Datalink., *Osteoarthritis and cartilage / OARS, Osteoarthritis Research Society* **23**(4): 594–600.

Della Rocca, G. J., Leung, K. S. & Pape, H.-C. (2011). Periprosthetic fractures: epidemiology and future projections., *Journal of orthopaedic trauma* **25 Suppl 2**(6 supplement): S66–S70.

Della Valle, C. J., Tejwani, N. & Koval, K. J. (2003). Interprosthetic fracture of the femoral shaft treated with a percutaneously inserted dynamic condylar screw: case report., *The Journal of trauma* **54**(3): 602–5.

Dennis, M. G., Simon, J. a., Kummer, F. J., Koval, K. J. & Di Cesare, P. E. (2001). Fixation of Periprosthetic Femoral Shaft Fractures: A Biomechanical Comparison of Two Techniques, *Journal of Orthopaedic Trauma* **15**(3): 177–180.

Dennis, M. G., Simon, J. a., Kummer, F. J., Koval, K. J. & DiCesare, P. E. (2000). Fixation of periprosthetic femoral shaft fractures occurring at the tip of the stem: a biomechanical study of 5 techniques., *The Journal of arthroplasty* **15**(4): 523–8.

Dhondt, G. (2012). Element types, `http://bconverged.com/calculix/doc/ccx/html/node20.html`. [Online; accessed 03-February-2016].

Drake, R. L., Vogl, A. W. & Mitchell, A. W. (2015). *Gray's anatomy for students third ed.*, Churchill Livingstone, Elsevier.

Ebraheim, N., Carroll, T., Moral, M. Z., Lea, J., Hirschfeld, A. & Liu, J. (2014). Interprosthetic femoral fractures treated with locking plate., *International orthopaedics* **38**(10): 2183–9.

Ebrahimi, H., Rabinovich, M., Vuleta, V., Zalcman, D., Shah, S., Dubov, A., Roy, K., Siddiqui, F. S., Schemitsch, E. H., Bougherara, H. & Zdero, R. (2012). Biomechanical properties of an intact, injured, repaired, and healed femur: An experimental and computational study, *Journal of the Mechanical Behavior of Biomedical Materials* **16**(1): 121–135.

Ehlinger, M., Czekaj, J., Adam, P., Brinkert, D., Ducrot, G. & Bonnomet, F. (2013). Minimally invasive fixation of type B and C interprosthetic

femoral fractures., *Orthopaedics & traumatology, surgery & research : OTSR* **99**(5): 563–9.

Fiedler, M. & Fenton, B. (2011). *Staying Mobile: A guide to mobility management in ageing societies*, The Regional Environmental Center for Central and Eastern Europe.

Franklin, J. & Malchau, H. (2007). Risk factors for periprosthetic femoral fracture., *Injury* **38**(6): 655–60.

Fulkerson, E., Egol, K. a., Kubiak, E. N., Liporace, F., Kummer, F. J. & Koval, K. J. (2006). Fixation of diaphyseal fractures with a segmental defect: a biomechanical comparison of locked and conventional plating techniques., *The Journal of trauma* **60**(4): 830–5.

Fulkerson, E., Tejwani, N., Stuchin, S. & Egol, K. (2007). Management of periprosthetic femur fractures with a first generation locking plate., *Injury* **38**(8): 965–72.

Gardner, M. P., Chong, A. C. M., Pollock, A. G. & Wooley, P. H. (2010). Mechanical evaluation of large-size fourth-generation composite femur and tibia models, *Annals of Biomedical Engineering* **38**(3): 613–620.

Graham, S. M., Mak, J. H., Moazen, M., Leonidou, A., Jones, A. C., Wilcox, R. K. & Tsiridis, E. (2015). Periprosthetic femoral fracture fixation: a biomechanical comparison between proximal locking screws and cables., *Journal of orthopaedic science : official journal of the Japanese Orthopaedic Association* **20**(5): 875–80.

Haddad, F. S., Duncan, C. P., Berry, D. J., Lewallen, D. G., Gross, A. E. & Chandler, H. P. (2002). Periprosthetic femoral fractures around well-fixed implants: use of cortical onlay allografts with or without a plate., *The Journal of bone and joint surgery. American volume* **84-A**(6): 945–50.

Haddad, F. S., Masri, B. A., Garbuz, D. S. & Duncan, C. P. (1999). The prevention of periprosthetic fractures in total hip and knee arthroplasty., *The Orthopedic clinics of North America* **30**(2): 191–207.

Heiner, A. D. (2008). Structural properties of fourth-generation composite femurs and tibias., *Journal of biomechanics* **41**(15): 3282–4.

Heller, M. O., Bergmann, G., Kassi, J.-P., Claes, L., Haas, N. P. & Duda, G. N. (2005). Determination of muscle loading at the hip joint for use in pre-clinical testing., *Journal of biomechanics* **38**(5): 1155–63.

Hoffmann, M., Lotzien, S. & Schildhauer, T. (2016). Clinical outcome of interprosthetic femoral fractures treated with polyaxial locking plates, *Injury* **47**(4): 934–38.

Hou, Z., Moore, B., Bowen, T. R., Irgit, K., Matzko, M. E., Strohecker, K. a. & Smith, W. R. (2011). Treatment of interprosthetic fractures of the femur., *The Journal of trauma* **71**(6): 1715–9.

Iesaka, K., Kummer, F. J. & Di Cesare, P. E. (2005). Stress Risers Between Two Ipsilateral Intramedullary Stems, *The Journal of Arthroplasty* **20**(3): 386–391.

Iorio, R., Robb, W. J., Healy, W. L., Berry, D. J., Hozack, W. J., Kyle, R. F., Lewallen, D. G., Trousdale, R. T., Jiranek, W. a., Stamos, V. P. & Parsley, B. S. (2008). Orthopaedic surgeon workforce and volume assessment for total hip and knee replacement in the United States: preparing for an epidemic., *The Journal of bone and joint surgery. American volume* **90**(7): 1598–605.

Kane, R., Saleh, K., Wilt, T., Bershadsky, B., Cross, W. I., MacDonald, R. & Rutks, I. (2003). Total Knee Replacement. Evidence Report/Technology Assessment No. 86, *Technical report*, AHRQ Publication No. 04-E006-1. Rockville, MD: Agency for Healthcare Research and Quality.

Kenny, P., Rice, J. & Quinlan, W. (1998). Interprosthetic fracture of the femoral shaft, *The Journal of Arthroplasty* **13**(3): 361–364.

Kinsella, K. & Velkoff, V. (2001). *An aging world: 2001 - http://www.census.gov/prod/2001pubs/p95-01-1.pdf*, U.S. Department of Health and Human Services.

Kurtz, S., Mowat, F., Ong, K., Chan, N., Lau, E. & Halpern, M. (2005). Prevalence of primary and revision total hip and knee arthroplasty in the United States from 1990 through 2002., *The Journal of bone and joint surgery. American volume* **87**(7): 1487–97.

Kurtz, S., Ong, K., Lau, E., Mowat, F. & Halpern, M. (2007). Projections of primary and revision hip and knee arthroplasty in the United States from 2005 to 2030., *The Journal of bone and joint surgery. American volume* **89**(4): 780–5.

Learmonth, I. D., Young, C. & Rorabeck, C. (2007). The operation of the century: total hip replacement., *Lancet (London, England)* **370**(9597): 1508–19.

Lehmann, W., Rupprecht, M., Hellmers, N., Sellenschloh, K., Briem, D., Püschel, K., Amling, M., Morlock, M. & Rueger, J. M. (2010). Biomechanical

evaluation of peri- and interprosthetic fractures of the femur., *The Journal of trauma* **68**(6): 1459–63.

Lehmann, W., Rupprecht, M., Nuechtern, J., Melzner, D., Sellenschloh, K., Kolb, J., Fensky, F., Hoffmann, M., Püschel, K., Morlock, M. & Rueger, J. M. (2012). What is the risk of stress risers for interprosthetic fractures of the femur? A biomechanical analysis., *International orthopaedics* **36**(12): 2441–6.

Lever, J. P., Zdero, R., Nousiainen, M. T., Waddell, J. P. & Schemitsch, E. H. (2010). The biomechanical analysis of three plating fixation systems for periprosthetic femoral fracture near the tip of a total hip arthroplasty., *Journal of orthopaedic surgery and research* **5**: 45.

Lewallen, D. G. & Berry, D. J. (1998). Periprosthetic fracture of the femur after total hip arthroplasty: treatment and results to date., *Instructional course lectures* **47**: 243–249.

Lindahl, H., Malchau, H., Herberts, P. & Garellick, G. (2005). Periprosthetic femoral fractures classification and demographics of 1049 periprosthetic femoral fractures from the Swedish National Hip Arthroplasty Register., *The Journal of arthroplasty* **20**(7): 857–65.

Mäkelä, K. T., Eskelinen, A., Pulkkinen, P., Paavolainen, P. & Remes, V. (2008). Total hip arthroplasty for primary osteoarthritis in patients fifty-five years of age or older. An analysis of the Finnish arthroplasty registry., *The Journal of bone and joint surgery. American volume* **90**(10): 2160–70.

Mamczak, C. N., Gardner, M. J., Bolhofner, B., Borrelli, J., Streubel, P. N. & Ricci, W. M. (2010). Interprosthetic femoral fractures., *Journal of orthopaedic trauma* **24**(12): 740–4.

Masri, B. A., Meek, R. M. D. & Duncan, C. P. (2004). Periprosthetic fractures evaluation and treatment., *Clinical orthopaedics and related research* **1**(420): 80–95.

Michla, Y., Spalding, L., Holland, J. P. & Deehan, D. J. (2010). The complex problem of the interprosthetic femoral fracture in the elderly patient., *Acta orthopaedica Belgica* **76**(5): 636–43.

Moazen, M., Jones, A. C., Jin, Z., Wilcox, R. K. & Tsiridis, E. (2011). Periprosthetic fracture fixation of the femur following total hip arthroplasty: a review of biomechanical testing., *Clinical biomechanics (Bristol, Avon)* **26**(1): 13–22.

Nalla, R. K., Kinney, J. H. & Ritchie, R. O. (2003). Mechanistic fracture criteria for the failure of human cortical bone., *Nature materials* **2**(3): 164–8.

Nork, S. E. (2006). Biomechanics of Fixation and Fractures, *in* R. W. Bucholz, J. D. Heckman & C. Court-Brown (eds), *Rockwood and Green's Fractures in Adults, Volume 1*, 6 edn, Lippincott Williams & Wilkins, pp. 1846–1910.

Ochs, B. G., Stöckle, U. & Gebhard, F. (2013). Interprosthetic fractures—a challenge of treatment, *European Orthopaedics and Traumatology* **4**(2): 103–109.

Old, A. B., McGrory, B. J., White, R. R. & Babikian, G. M. (2006). Fixation of Vancouver B1 peri-prosthetic fractures by broad metal plates without the application of strut allografts., *The Journal of bone and joint surgery. British volume* **88**(11): 1425–9.

Pabinger, C. & Geissler, A. (2014). Utilization rates of hip arthroplasty in OECD countries., *Osteoarthritis and cartilage / OARS, Osteoarthritis Research Society* **22**(6): 734–41.

Pabinger, C., Lothaller, H. & Geissler, A. (2015). Utilization rates of knee-arthroplasty in OECD countries., *Osteoarthritis and cartilage / OARS, Osteoarthritis Research Society* **23**(10): 1664–73.

Papini, M., Zdero, R., Schemitsch, E. H. & Zalzal, P. (2007). The biomechanics of human femurs in axial and torsional loading: comparison of finite element analysis, human cadaveric femurs, and synthetic femurs., *Journal of biomechanical engineering* **129**(1): 12–9.

Perren, S. M. (2002). Evolution of the internal fixation of long bone fractures. The scientific basis of biological internal fixation: choosing a new balance between stability and biology., *The Journal of bone and joint surgery. British volume* **84**(8): 1093–110.

Pires, R. E. S., de Toledo Lourenço, P. R. B., Labronici, P. J., da Rocha, L. R., Balbachevsky, D., Cavalcante, F. R. & de Andrade, M. A. P. (2014). Interprosthetic femoral fractures: proposed new classification system and treatment algorithm., *Injury* **45 Suppl 5**: S2–6.

Pivec, R., Johnson, A. J., Mears, S. C. & Mont, M. A. (2012). Hip arthroplasty., *Lancet (London, England)* **380**(9855): 1768–77.

Platzer, P., Schuster, R., Luxl, M., Widhalm, H. K., Eipeldauer, S., Krusche-Mandl, I., Ostermann, R., Blutsch, B. & Vécsei, V. (2011). Management and outcome of interprosthetic femoral fractures., *Injury* **42**(11): 1219–25.

Quirynen, T., Corten, K., Segal, O., Bellemans, J., Vander Sloten, J., Simon, J.-P. & van Lenthe, G. H. (2017). Small interprosthetic gaps do not increase femoral peri-prosthetic fracture risk. An in vitro biomechanical analysis., *Acta orthopaedica Belgica* **83**(2).

Quirynen, T., van Lenthe, G. H. & Vander Sloten, J. (2014). Do small interprosthetic gaps increase bone fracture risk?, *Abstracts 13th National Day on Biomedical Engineering*, p. 35.

Ravi, B., Croxford, R., Reichmann, W. M., Losina, E., Katz, J. N. & Hawker, G. A. (2012). The changing demographics of total joint arthroplasty recipients in the United States and Ontario from 2001 to 2007, *Best Practice & Research Clinical Rheumatology* **26**(5): 637–647.

Ricci, W. M., Bolhofner, B. R., Loftus, T., Cox, C., Mitchell, S. & Borrelli, J. (2005). Indirect reduction and plate fixation, without grafting, for periprosthetic femoral shaft fractures about a stable intramedullary implant., *The Journal of bone and joint surgery. American volume* **87**(10): 2240–5.

Rorabeck, C. H., Angliss, R. D. & Lewis, P. L. (1998). Fractures of the femur, tibia, and patella after total knee arthroplasty: decision making and principles of management., *Instructional course lectures* **47**: 449–458.

Sah, A. P., Marshall, A., Virkus, W. V., Estok, D. M. & Della Valle, C. J. (2010). Interprosthetic fractures of the femur: treatment with a single-locked plate., *The Journal of arthroplasty* **25**(2): 280–6.

Savela, S., Komulainen, P., Sipilä, S. & Strandberg, T. (2015). [Physical activity of the elderly - what kind of and what for?]., *Duodecim; lääketieteellinen aikakauskirja* **131**(18): 1719–25.

Schileo, E., Balistreri, L., Grassi, L., Cristofolini, L. & Taddei, F. (2014). To what extent can linear finite element models of human femora predict failure under stance and fall loading configurations?, *Journal of biomechanics* **47**(14): 3531–8.

Schileo, E., Taddei, F., Cristofolini, L. & Viceconti, M. (2008). Subject-specific finite element models implementing a maximum principal strain criterion are able to estimate failure risk and fracture location on human femurs tested in vitro., *Journal of biomechanics* **41**(2): 356–67.

Schroll, M. (2003). Physical activity in an ageing population, *Scandinavian Journal of Medicine and Science in Sports* **13**(1): 63–69.

Sing, D. C., Feeley, B. T., Tay, B., Vail, T. P. & Zhang, A. L. (2015). Age-Related Trends in Hip Arthroscopy: A Large Cross-Sectional Analysis., *Arthroscopy : the journal of arthroscopic & related surgery : official publication of the Arthroscopy Association of North America and the International Arthroscopy Association* **31**(12): 2307–2313.e2.

Skyttä, E. T., Jarkko, L., Antti, E., Huhtala, H. & Ville, R. (2011). Increasing incidence of hip arthroplasty for primary osteoarthritis in 30- to 59-year-old patients., *Acta orthopaedica* **82**(1): 1–5.

Soenen, M., Baracchi, M., De Corte, R., Labey, L. & Innocenti, B. (2013). Stemmed TKA in a femur with a total hip arthroplasty: is there a safe distance between the stem tips?, *The Journal of arthroplasty* **28**(8): 1437–45.

Soenen, M., Migaud, H., Bonnomet, F., Girard, J., Mathevon, H. & Ehlinger, M. (2011). Interprosthetic femoral fractures: analysis of 14 cases. Proposal for an additional grade in the Vancouver and SoFCOT classifications., *Orthopaedics & traumatology, surgery & research : OTSR* **97**(7): 693–8.

Solarino, G., Vicenti, G., Moretti, L., Abate, A., Spinarelli, A. & Moretti, B. (2014). Interprosthetic femoral fractures-A challenge of treatment. A systematic review of the literature., *Injury* **45**(2): 362–8.

Speirs, A. D., Heller, M. O., Duda, G. N. & Taylor, W. R. (2007). Physiologically based boundary conditions in finite element modelling, *Journal of Biomechanics* **40**(10): 2318–2323.

Stoffel, K., Sommer, C., Kalampoki, V., Blumenthal, A. & Joeris, A. (2016). The influence of the operation technique and implant used in the treatment of periprosthetic hip and interprosthetic femur fractures: a systematic literature review of 1571 cases., *Archives of orthopaedic and trauma surgery* **136**(4): 553–61.

Stolk, J., Verdonschot, N., Cristofolini, L., Toni, A. & Huiskes, R. (2002). Finite element and experimental models of cemented hip joint reconstructions can produce similar bone and cement strains in pre-clinical tests., *Journal of biomechanics* **35**(4): 499–510.

Stolk, J., Verdonschot, N. & Huiskes, R. (2001). Hip-joint and abductor-muscle forces adequately represent in vivo loading of a cemented total hip reconstruction., *Journal of biomechanics* **34**(7): 917–26.

Talbot, M., Zdero, R. & Schemitsch, E. H. (2008). Cyclic loading of periprosthetic fracture fixation constructs., *The Journal of trauma* **64**(5): 1308–12.

Taylor, M. & Prendergast, P. J. (2015). Four decades of finite element analysis of orthopaedic devices: where are we now and what are the opportunities?, *Journal of biomechanics* **48**(5): 767–78.

Tencer, A. F. (2006). Biomechanics of Fixation and Fractures, *in* R. W. Bucholz, J. D. Heckman & C. Court-Brown (eds), *Rockwood and Green's Fractures in Adults, Volume 1*, 6 edn, Lippincott Williams & Wilkins, pp. 4–39.

Tomás Hernández, J. & Holck, K. (2015). Periprosthetic femoral fractures: When I use strut grafts and why?, *Injury* **46 Suppl 5**: S43–6.

Tsiridis, E., Haddad, F. S. & Gie, G. a. (2003). The management of periprosthetic femoral fractures around hip replacements, *Injury* **34**(2): 95–105.

Tsiridis, E., Spence, G., Gamie, Z., El Masry, M. a. & Giannoudis, P. V. (2007). Grafting for periprosthetic femoral fractures: strut, impaction or femoral replacement., *Injury* **38**(6): 688–97.

United Nations (2013). *World Population Ageing*, United Nations publication.

Weiser, L., Korecki, M. a., Sellenschloh, K., Fensky, F., Püschel, K., Morlock, M. M., Rueger, J. M. & Lehmann, W. (2014). The role of inter-prosthetic distance, cortical thickness and bone mineral density in the development of inter-prosthetic fractures of the femur: a biomechanical cadaver study., *The bone & joint journal* **96-B**(10): 1378–84.

Werner, C. A. (2011). *The older population: 2010 - http://www.census.gov/prod/cen2010/briefs/c2010br-09.pdf*, U.S. Department of Commerce.

Wilson, D., Frei, H., Masri, B. a., Oxland, T. R. & Duncan, C. P. (2005). A biomechanical study comparing cortical onlay allograft struts and plates in the treatment of periprosthetic femoral fractures., *Clinical biomechanics (Bristol, Avon)* **20**(1): 70–6.

World Health Organization (2011). *Global Health and Aging*, WHO Press.

World Health Organization (2015). *World Report on Ageing and Health*, WHO Press.

Zdero, R., Walker, R., Waddell, J. P. & Schemitsch, E. H. (2008). Biomechanical evaluation of periprosthetic femoral fracture fixation., *The Journal of bone and joint surgery. American volume* **90**(5): 1068–77.

Curriculum vitae

Personalia

Name:	Thomas Quirynen
Date of birth:	November 6, 1987
Place of birth:	Leuven, Belgium

Contact information

Biomechanics section
Department of Mechanical Engineering, KU Leuven
Celestijnenlaan 300C, B-3001 Heverlee, Belgium

Tel: +32 472 90 29 15
Email: thomas.quirynen@kuleuven.be or thomasquirynen@gmail.com

Work experience

2010 - 2016

PhD student - Biomechanics Section, KU Leuven, Belgium
Keywords: Biomechanics, Finite element modelling, Abaqus, Mimics, 3-matic

Summer 2015

Short project - Dentsply Implants, Hasselt, Belgium
Keywords: Biomechanics, Finite element modelling, dentistry, oral implants
Projects: Investigation of a design modification to the shape of an dental implant-carried suprastructure (ATLANTIS^{TM} ISUS) for prosthetic fixation. The aim was to determine the predicted improved fracture behaviour.

2010 - 2013

Research Engineer - Institute of Orthopaedic Research and Training (IORT) UZ Leuven, Belgium
Keywords: Interdisciplinary research, orthopaedics
Projects: Metacarpal drill tunnel placement during LRTI surgery, Influence of tackle impacts on soccer shin guards

Summer 2009

Summer Job - Mobelife NV, Leuven, Belgium
Keywords: Patient specific modelling, MATLAB
Projects: Design of a patient-specific muscle model for patient-specific shoulder-implants

Summer 2008

Summer Job - Materialise Dental, Leuven, Belgium
Keywords: Access, dentistry
Projects: Design of a database to investigate inaccuracies comparing planned vs post-operative dental implant location and orientation

Education

2008 - 2010

Master of Engineering: Biomedical Technology: Biomechanics & biomaterials KU Leuven, Belgium

2005 - 2008

Bachelor of Engineering: Mechanical Engineering (major) & Chemical Technology (minor)
KU Leuven, Belgium

Publications

Articles in internationally reviewed academic journals

Quirynen, T., Corten, K., Segal, O., Simon, J-P., Vander Sloten, J., van Lenthe, G.H. (2017) Small interprosthetic gaps do not increase femoral peri-prosthetic fracture risk. An in vitro biomechanical analysis. Accepted in *Acta Orthopaedica Belgica* **83**(2)

Quirynen, T., Corten, K., Simon, J-P., Vander Sloten, J., Feyen, H., van Lenthe, G.H. (2016) Interprosthetic femoral fractures: effect of interprosthetic distance and anterior struts on the failure load of lateral plate reconstructions. *Submitted*

Quirynen, T., Simon, J-P., Vander Sloten, J., van Lenthe, G.H. (2016) Ipsilateral hip and knee implants do not increase bone fracture risk immediately after prosthesis placement. *Submitted*

Quirynen, T., Vander Sloten, J., Simon, J-P., van Lenthe, G.H. (2016) Do small interprosthetic gaps increase bone fracture risk? A parametric study on gap size and location. *Submitted*

Quirynen, T., Quirynen, M., Duyck, J. (2015) Prevention of distal extension cantilever fracture in mandibular overdentures. *Journal of Dentistry* 43(9):1140-7

Abstracts presented at international scientific conferences

Quirynen, T., Segal, O., Feyen, H., Bellemans, J., Vander Sloten, J., Vanaudekercke, R., Simon, J-P., Corten, K. The interprosthetic gap as a risk factor for peri-prosthetic femoral fractures: A biomechanical evaluation. (Poster) *Program book EORS 2012* European Orthopaedic Research Society (EORS). Amsterdam, Netherlands, 26-28 September 2012.

Quirynen, T., Segal, O., Feyen, H., Bellemans, J., Vander Sloten, J., Vanaudekercke, R., Simon, J-P., Corten, K. The influence of interprosthetic gap on single-plate fracture reconstruction with or without anterior strut allograft: A biomechanical evaluation. (Poster) *Program book EORS 2012* European Orthopaedic Research Society (EORS). Amsterdam, Netherlands, 26-28 September 2012.

Quirynen, T., Segal, O., Feyen, H., Bellemans, J., Vander Sloten, J., Vanaudekercke, R., Simon, J-P., Corten, K. The interprosthetic gap as a risk factor for peri-prosthetic fractures of the femur. A bio-mechanical evaluation.

(Presentation) *Abstracts from the 10th Congress of the European Hip Society, Hip International (2012); 22(4): 403 - 485* European Hip Society (EHS). Milano, Italy, 20-22 September 2012.

Quirynen, T., Segal, O., Feyen, H., Bellemans, J., Vander Sloten, J., Vanaudekercke, R., Simon, J-P., Corten, K. The influence of interprosthetic gap on single-plate fracture reconstruction with or without anterior strut : A biomechanical evaluation. (Presentation) *Abstracts from the 10th Congress of the European Hip Society, Hip International (2012); 22(4): 403 - 485* European Hip Society (EHS). Milano, Italy, 20-22 September 2012.

Abstracts presented at other scientific conferences

Quirynen, T., Vander Sloten, J., van Lenthe, G.H. Ipsilateral hip and knee implants do not increase bone fracture risk: a computational study. *Program book of the 14th Belgian Day on Biomedical Engineering.* Belgian Day on Biomedical Engineering. Brussels, Belgium, 4 March 2016.

Quirynen, T., van Lenthe, G.H., Vander Sloten, J. Do small interprosthetic gaps increase bone fracture risk? *Program book of the 13th Belgian Day on Biomedical Engineering.* Belgian Day on Biomedical Engineering. Brussels, Belgium, 28 November 2014.

FACULTY OF ENGINEERING SCIENCE
DEPARTMENT OF MECHANICAL ENGINEERING
BIOMECHANICS SECTION
Celestijnenlaan 300C - bus 2419
B-3001 Heverlee
thomas.quirynen@kuleuven.be or thomasquirynen@gmail.com
http://www.mech.kuleuven.be/en/bme